An Approach for Classifying ECG Arrhythmia Based on Features Extracted from EMD and Wavelet Packet Domains

by

Raju Sinha

MASTER OF SCIENCE IN ELECTRICAL AND ELECTRONIC ENGINEERING

Department of Electrical and Electronic Engineering
BANGLADESH UNIVERSITY OF ENGINEERING AND TECHNOLOGY

July 2012

The thesis entitled **"An Approach for Classifying ECG Arrhythmia Based on Features Extracted from EMD and Wavelet Packet Domains"** submitted by Raju Sinha, Student No.: 1009062081F, Session: October, 2009 has been accepted as satisfactory in partial fulfillment of the requirement for the degree of MASTER OF SCIENCE IN ELECTRICAL AND ELECTRONIC ENGINEERING on July 12, 2012.

BOARD OF EXAMINERS

1. ____

(Dr. Celia Shahnaz) *Assistant Professor* Department of Electrical and Electronic Engineering Bangladesh University of Engineering and Technology Dhaka - 1000, Bangladesh.	**Chairman** (Supervisor)

2. ____

(Dr. Pran Kanai Saha) *Professor and Head* Department of Electrical and Electronic Engineering Bangladesh University of Engineering and Technology Dhaka - 1000, Bangladesh.	**Member** (Ex-officio)

3. ____

(Dr. Mohammed Imamul Hassan Bhuiyan) *Associate Professor* Department of Electrical and Electronic Engineering Bangladesh University of Engineering and Technology Dhaka - 1000, Bangladesh.	**Member**

4. ____

(Dr. Mohammad Rakibul Islam) *Professor* Department of Electrical and Electronic Engineering Islamic University of Technology (IUT) Board Bazar, Gazipur-1704.	**Member** (External)

CANDIDATE'S DECLARATION

I, do, hereby declare that neither this thesis nor any part of it has been submitted elsewhere for the award of any degree or diploma.

Signature of the Candidate

Raju Sinha

Dedication

To my ever caring elder brother and parents
whose inspirations are behind my every success.

Acknowledgment

I would like to mention some people who I owe a great gratitude for the moral and technical support they provided me during my thesis progress. First of all, I would like to give my greatest gratitude to my supervisor Dr. Celia Shahnaz for all her support, encouragement, guidance and useful suggestions throughout this research work. The discussions we had and her ideas not only helped me with the completion of my thesis but also gave me a different perspective and vision for my life and my future career. Thank you for your constructive comments on my work, for being friendly and tolerant to extra meetings.

I would also like to thank the rest of the members of my thesis committee: Prof. Dr. Pran Kanai Saha, Dr. Mohammed Imamul Hassan Bhuiyan, and Prof. Dr. Mohammad Rakibul Islam, for their encouragement and insightful comments. I would like to thank the head of the department of Electrical and Electronic Engineering for allowing me to use the lab facilities, which contributed greatly in completing the work in time. I wish to express note of thanks to Dr. Shaikh Anowarul Fattah, for providing inspiration and thoughtful comments.

Special note of thanks goes to my elder brother Mr. Rajib Sinha for his continuous moral support and friendly cooperation. I am greatly indebted to him, for his constant inspiration and effective suggestions. My acknowledgments will be incomplete without the final word of gratitude to those persons who have been the wind beneath my wings - all the way. Thanks to my parents. Without them I would never have come so far in pursuing my dream. Last but not the least, I would like to thank my friends Rajib Goswami and Partha Pratim Acharjee for their suggestions, support and inspirations all along.

Abstract

Any disturbance in the activity of heart can cause irregular heart rhythm known as cardiac arrhythmia. Electrocardiogram (ECG) is one of the most promising tools for classification of different types of arrhythmia, which is necessary until it goes fatal and causes loss of life. For ECG arrhythmia classification, a wide range of signal processing techniques extracting features from time, frequency and time frequency domains have been reported in the literature. Since, ECG is a non-stationary signal, time frequency analysis can perform better than the conventional time or frequency analysis methods. But, development of a multi-class arrhythmia classification method, which is simple yet effective in handling practical conditions such as lack of enough training dataset and random selection of training and testing dataset, is still a challenging task. ECG signals can be well modeled as self-affined fractal sets which vary under different arrhythmia. Thus local fractal dimension (LFD) can be employed as a feature in classifying different ECG arrhythmia. In the empirical mode decomposition (EMD) domain, the basic functions are directly derived from the original signal without the knowledge of any previous value of the signal. Therefore, the Hurst exponent (HE) required for deriving a set of LFD features is calculated from the intrinsic mode functions (IMFs) obtained via EMD of ECG signals. Since, for better approximation of LFD, at least three IMFs are to be determined which is dependent on the length of the ECG signal, time-frequency analysis in the wavelet packet decomposition (WPD) domain is performed for calculating the HE as well as deriving a set of more effective LFD features. Considering the complexity and ease of implementation as an important criterion, a feature set based on energy and entropy of only the 4th level detail WPD coefficients is found to be simple yet the highest capable of solving a multi-class ECG arrhythmia problem. Each of the proposed sets of feature when fed to Euclidean distance based classifier can classify different arrhythmia even with reduced training dataset as well as randomly selected training and testing dataset. Simulations are carried out to evaluate the performance of the proposed method in terms of sensitivity, specificity and accuracy. It is shown that the proposed method outperforms some of the state-of-the-art methods with superior efficacy.

Contents

Dedication **iii**

Acknowledgement **iv**

Abstract **v**

1 Introduction **1**

1.1 The Heart Anatomy 2

1.2 Electrocardiogram 4

1.3 Leads in ECG 5

1.3.1 Einthoven Leads 5

1.3.2 Unipolar Limb leads 6

1.3.3 Chest (precordial) leads 6

1.4 ECG Waves and Interval 7

1.4.1 P Wave 7

1.4.2 PR Segment 7

1.4.3 PR Interval 8

1.4.4 QRS complex 8

1.4.5 T wave 8

1.4.6 ST Segment 8

1.4.7 ST Interval 9

1.4.8 QT Interval 9

1.4.9 U wave 9

1.5 Arrhythmias in ECG Signal 9

1.5.1 Sinus Node Arrhythmias 11

1.5.2 Atrial Arrhythmias 11

1.5.3 Junctional Arrhythmias 13

1.5.4 Ventricular arrhythmias 14
1.5.5 Atrioventricular Blocks 16
1.5.6 Bundle Branch Blocks 17
1.6 Problem Definition 19
1.7 Objective of the Thesis 20
1.8 Organization of the Thesis 20

2 Literature Review 21
2.1 Introduction 21
2.2 Time Domain Approaches 22
2.3 Frequency Domain Approaches 23
2.4 Time-Frequency Domain Approaches 24
2.5 Other Approaches 27
2.6 Conclusion 30

3 An Empirical Mode Decomposition Based Fractal Dimension Feature for ECG Arrhythmia Classification 31
3.1 Introduction 31
3.2 Preliminaries 32
3.2.1 Fractals and Fractal Dimension 32
3.2.2 Recent Methods for Computing Fractal Dimension 33
3.3 Proposed Method 37
3.3.1 Empirical Mode Decomposition 37
3.3.2 Computation of Fractal Dimension Feature 38
3.3.3 Selection of Window Length 40
3.3.4 Classification 41
3.4 Conclusion 44

4 A Wavelet Packet Based Fractal Dimension Feature for ECG Arrhythmia Classification 45
4.1 Introduction 45
4.2 Proposed Method 45
4.2.1 Wavelet Transform 46
4.2.2 Wavelet Packet Transform 47

4.2.3 Selection of Mother Wavelet 47
4.2.4 Rationale behind Selection of Detail Coefficients 49
4.2.5 Computation of Fractal Dimension Feature and Classification 50
4.3 Conclusion 53

5 An Approach for ECG Arrhythmia Classification Based on Energy and Entropy of the 4th Level Detail Wavelet Packet Coefficients 55
5.1 Introduction 55
5.2 Proposed Method 56
5.2.1 Rationale behind Taking 4th Level Detail WPD Coefficients . 56
5.2.2 Feature Extraction and Classification 59
5.3 Conclusion 60

6 Simulation Results and Performance Evaluation 61
6.1 Introduction 61
6.2 Simulation Results 61
6.2.1 Database 61
6.2.2 Simulation Conditions 62
6.2.3 Performance Evaluation Criteria 63
6.3 Performance Comparison using LFD Estimation Method in EMD Domain 68
6.3.1 Clustering Analysis 68
6.3.2 Performance Comparison using Confusion Matrix 70
6.3.3 Performance Comparison using ROC Curves 72
6.3.4 Performance Comparison using Reduced Training Dataset . . 74
6.3.5 Performance Comparison using Error-bar Calculation 75
6.4 Performance Comparison using LFD Estimation Method in WPD Domain 75
6.4.1 Clustering Analysis 76
6.4.2 Performance Comparison using Confusion Matrix 78
6.4.3 Performance Comparison using ROC Curves 80
6.4.4 Performance Comparison using Reduced Training Dataset . . 81
6.4.5 Performance Comparison using Error-bar Calculation 82

6.5 Performance Comparison using Energy and Entropy of Detail WPD Coefficients 83
6.5.1 Clustering Analysis 83
6.5.2 Performance Comparison using Confusion Matrix 85
6.5.3 Performance Comparison using ROC Curves 86
6.5.4 Performance Comparison using Reduced Training Dataset . . 88
6.5.5 Performance Comparison using Error-bar Calculation 88
6.6 Conclusion 91

7 Conclusion 92

7.1 Concluding Remarks 92
7.2 Contribution of the Thesis 93
7.3 Scopes for Future Work 93

List of Tables

1.1 Types of leads used in ECG monitoring 5
1.2 Amplitude and duration of waves, intervals and segments of ECG signal 10

5.1 Average value of cross-correlation coefficients 59

6.1 The MIT-BIH database file number and the number of QRS complexes used in this study 62
6.2 The GSI index obtained using the proposed method of LFD estimation in EMD domain for each pair of arrhythmia classes 69
6.3 Confusion matrix for PSDFE method using Euclidean distance classifier 71
6.4 Confusion matrix for VFE method using Euclidean distance classifier 71
6.5 Confusion matrix for proposed method based on LFD estimation in EMD domain using Euclidean distance classifier 71
6.6 Comparison of average sensitivity obtained by using the PSDFE, VFE methods and the proposed method based on LFD estimation in EMD domain 72
6.7 Comparison of average specificity obtained by using the PSDFE, VFE methods and the proposed method based on LFD estimation in EMD domain 73
6.8 Comparison of average accuracy obtained by using the PSDFE, VFE methods and the proposed method based on LFD estimation in EMD domain 73
6.9 The GSI index obtained using the proposed method of LFD estimation in WPD domain for each pair of arrhythmia classes 77
6.10 Confusion matrix for proposed method based on LFD estimation in WPD domain using Euclidean distance classifier 78

6.11 Comparison of average sensitivity obtained by using the PSDFE, VFE methods and the proposed method based on LFD estimation in WPD domain 79
6.12 Comparison of average specificity obtained by using the PSDFE, VFE methods and the proposed method based on LFD estimation in WPD domain 80
6.13 Comparison of average accuracy obtained by using the PSDFE, VFE methods and the proposed method based on LFD estimation in WPD domain 80
6.14 The GSI index between each arrhythmia for the proposed method based on energy and entropy of detail WPD coefficients 84
6.15 Confusion matrix for proposed method based on energy and entropy of detail WPD coefficients using Euclidean distance classifier 86
6.16 Comparison of average sensitivity obtained by using the PSDFE, VFE methods and the proposed method based on energy and entropy of detail WPD coefficients 87
6.17 Comparison of average specificity obtained by using the PSDFE, VFE methods and the proposed method based on energy and entropy of detail WPD coefficients 87
6.18 Comparison of average accuracy obtained by using the PSDFE, VFE methods and the proposed method based on energy and entropy of detail WPD coefficients 88

List of Figures

1.1 A diagrammatic structure of human heart [1]. 3

1.2 Heart conduction system [1]. 3

1.3 All leads' position on the body [1]. 5

1.4 Schematic representation of normal ECG waveform. 7

1.5 Sinus arrhythmias [1]. 12

1.6 Atrial arrhythmias [1]. 14

1.7 Junctional arrhythmias [1]. 15

1.8 Ventricular arrhythmias [1]. 16

1.9 Atrioventricular blocks [1]. 18

1.10 A ventricular pacemaker generates a normal heart rate but with a bizarre-shaped QRS-complex. The pacemaker spike precedes each QRS-complex [1]. 18

1.11 Bundle branch blocks [1]. 19

3.1 Fractal dimensions of (a) normal ECG (b) upward baseline shifted ECG (c) downward baseline shifted ECG and (d) scaled ECG 34

3.2 Fractal dimension of normal ECG and five classes of ECG arrhythmia. 35

3.3 Mean Fractal dimension with standard deviation (SD) error bars for different ECG arrhythmias. 36

3.4 Empirical mode decomposition to ECG signal. 39

3.5 Average no. of IMF per window with the increase in window length for a) class N, b) class L and c) class PB ECG arrhythmia. 42

3.6 Percentage of window involving single or double or multiple IMFs with respect to varying window length for a) class N b) class L and c) class PB ECG arrhythmia. 43

4.1 Wavelet packet decomposition. 47

4.2 Different mother wavelets along with ECG beat: a) Mexican hat wavelet b) Morlet wavelet c) Meyer wavelet d) Daubechies (db4) wavelet e) Daubechies (db6) wavelet and f) Symlets (sym11) wavelet. 48
4.3 Detail and approximate coefficients of different classes of arrhythmias a) class N (detail), b)class N (approximate) c) class L (detail) d) class L (approximate) e) class R (detail) f) class R (approximate) g) class PB (detail) h) class PB (approximate) i) class V (detail) j) class V (approximate) k) class A (detail) l) class A (approximate). 51
4.4 Mean value of detail coefficients with SD in errorbars for different ECG arrhythmias. 52
4.5 Mean value of approximate coefficients with SD in errorbars for different ECG arrhythmias. 52

5.1 Normalized energy of sum of detail coefficients at different levels of WPD for a) Class N b) Class R and c) Class A. 57
5.2 Frequency contents of ECG signal and that of sum of detail WPD coefficients at different levels for N type ECG signal. 58

6.1 Confusion matrix. 65
6.2 Average inter-patient Bhattacharya distances obtained using PSDFE, VFE and the proposed method of LFD estimation in EMD domain for each class of arrhythmia. 70
6.3 Performance comparison in terms of ROC curves for the PSDFE, VFE methods and the proposed method based on LFD estimation in EMD domain. 74
6.4 Performance comparison in terms of average sensitivity vs reduction factor for the PSDFE, VFE methods and the proposed method based on LFD estimation in EMD domain. 75
6.5 Performance comparison in terms of Error-bar for the PSDFE, VFE methods and the proposed method based on LFD estimation in EMD domain. 76

6.6 Average inter-patient Bhattacharya distances obtained using the PS-DFE, VFE methods and the proposed menthod of LFD estimation in WPD domain. 77
6.7 Performance comparison in terms of ROC curves for the PSDFE, VFE methods and the proposed method based on LFD estimation in WPD domain. 81
6.8 Performance comparison in terms of average sensitivity vs reduction factor for the PSDFE, VFE methods and the proposed method based on LFD estimation in WPD domain. 82
6.9 Performance comparison in terms of Error-bar for the PSDFE, VFE methods and the proposed method based on LFD estimation in WPD domain. 83
6.10 Average inter-patient Bhattacharya distances obtained using the PS-DFE, VFE methods and the proposed method based on energy and entropy of detail WPD coefficients. 85
6.11 Performance comparison in terms of ROC curves for the PSDFE, VFE methods and the proposed method based on energy and entropy of detail WPD coefficients. 89
6.12 Performance comparison in terms of average sensitivity vs reduction factor for the PSDFE, VFE methods and the proposed method based on energy and entropy of detail WPD coefficients. 90
6.13 Performance comparison in terms of Error-bar for the PSDFE, VFE methods and the proposed method based on energy and entropy of detail WPD coefficients. 90

List of abbreviations

ECG	Electrocardiogram
LFD	Local Fractal Dimension
EMD	Empirical Mode Decomposition
IMF	Intrinsic Mode Function
WPD	Wavelet Packet Decomposition
VFE	Variance Based Fractal Dimension Estimator
PSDFE	Power Spectrum Density Based Fractal Dimension Estimator
ROC	Receiver Operating Characteristics
GSI	Geometric Separability Index
BD	Bhattacharya Distance

Chapter 1

Introduction

The term arrhythmia suggests abnormalities in the heart rate, although it is commonly used to refer to changes in the shape of the heart wave. The electrocardiogram (ECG) is the most important bio-signal used by cardiologists for diagnostic purposes. The ECG signal, if properly analyzed, provides key information about the electrical activity of the heart. Life threatening situations, signalled by the occurrence of premature ventricular contractions (PVC), ventricular fibrillation (VF) or other serious arrhythmias, can often be reversed if detected in time for proper treatment. However, ECG being a non-stationary signal, the irregularities may not be periodic and may not show up all the time, but would manifest at certain irregular intervals during the day. So continuous ECG monitoring permits observation of cardiac variations over an extended period of time, either at the bedside or when patients are ambulatory, providing more information to physicians. Thus, continuous monitoring increases the understanding of patients' circumstances and allows more reliable diagnosis of cardiac abnormalities. Detection of abnormal ECG signals is a critical step in administering aid to patients. Often, patients are hooked up to cardiac monitors in hospital continuously. This requires continuous monitoring by the physicians. Since clinical observation of ECG can take long hours and can be very tedious, the cardiac intensive care unit has been incorporated into hospitals in order to improve the chances of survival of and to treat patients suffering traumatic episodes of heart diseases. Modern era of medical science is facilitated by computer aided feature extraction and disease diagnostics in which various signal processing techniques have been utilized in extracting different kinds of features from the ECG signals. The objective of computer aided digital signal processing of ECG signal is to reduce the time taken by the cardiologists in interpreting the results. Due to the large number of patients in intensive care units, the need for continuous observation of them and the high possibility of the analyst missing the vital information by visual analysis, over the years researchers have developed a variety of relatively effective signal processing techniques in time or frequency or time-frequency domain in order to classify ECG arrhythmia accurately. However, the problem of classifying different types of ECG arrhythmia still poses a challenge to the area of signal processing. In a particular arrhythmia condition, morphological changes occur in different sections of a normal ECG beat and such changes vary from beat to beat under the same arrhythmia. Thus extracting the very detail characteristics of each arrhythmia through signal processing techniques into a feature vector capable of correctly classifying among different types of ECG arrhythmia is a difficult task. Complexity and ease of implementation of the cardiac arrhythmia classification methods is also of concern in real life applications. The overall goal of arrhythmia classification technique is to find a simple yet effective method capable of performing the classification task with greater sensitivity, specificity and accuracy.

1.1 The Heart Anatomy

The heart contains four chambers that is right atrium, left atrium, right ventricle, left ventricle and several atrioventricular and sinoatrial node as shown in the Fig. 1.1 [1]. The two upper chambers are called the left and right atria, while the lower two chambers are called the left and right ventricles. The atria are attached to the ventricles by fibrous, non-conductive tissue that keeps the ventricles electrically isolated from the atria. The heart conduction system is shown in Fig. 1.2 [1]. The right atrium and the right ventricle together form a pump to the circulate blood to the lungs. Oxygen-poor blood is received through large veins called the superior and inferior vena cava and flows into the right atrium. The right ventricle then pumps the blood to the lungs where the blood is oxygenated. Similarly, the left atrium and the left ventricle together form a pump to circulate oxygen-enriched blood received from the lungs (via the pulmonary veins) to the rest of the body [2].

In heart Sino-atrial (S-A) node spontaneously generates regular electrical impulses, which then spread through the conduction system of the heart and initiate

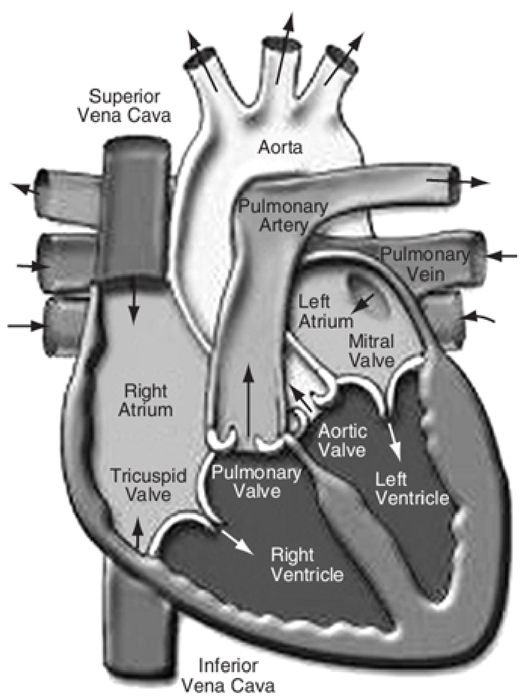

Fig. 1.1: A diagrammatic structure of human heart [1].

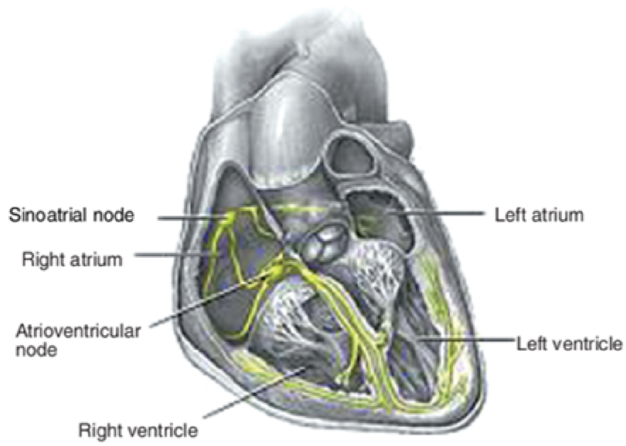

Fig. 1.2: Heart conduction system [1].

contraction of the myocardium. Propagation of an electrical impulse through excitable tissue is achieved through a process called depolarization. Depolarization of the heart muscles collectively generates a strong ionic current [1]. This current flows through the resistive body tissue generating a voltage drop. The magnitude of the voltage drop is sufficiently large to be detected by electrodes attached to the skin. ECGs are thus recordings of voltage drops across the skin caused by ionic current flow generated from myocardial depolarization [3]. Atrial depolarization results in the spreading of the electrical impulse through the atrial myocardium and appears as the P-wave. Similarly, ventricular depolarization results in the spreading of the electrical impulse throughout the ventricular myocardium.

1.2 Electrocardiogram

Electrocardiogram (ECG) is a diagnosis tool that reported the electrical activity of heart recorded by skin electrode. The morphology and heart rate reflects the cardiac health of human heart beat [1]. It is a noninvasive technique that means this signal is measured on the surface of human body, which is used in identification of the heart diseases [4]. Any disorder of heart rate or rhythm, or change in the morphological pattern, is an indication of cardiac arrhythmia, which could be detected by analysis of the recorded ECG waveform. The amplitude and duration of the P-QRS-T wave contains useful information about the nature of disease afflicting the heart. The electrical wave is due to depolarization and repolarization of Na^+ and K^+ ions in the blood [4]. The ECG signal provides the following information of a human heart [5]:

- heart position and its relative chamber size
- impulse origin and propagation
- heart rhythm and conduction disturbances
- extent and location of myocardial ischemia
- changes in electrolyte concentrations
- drug-effects on the heart.

ECG does not afford data on cardiac contraction or pumping function.

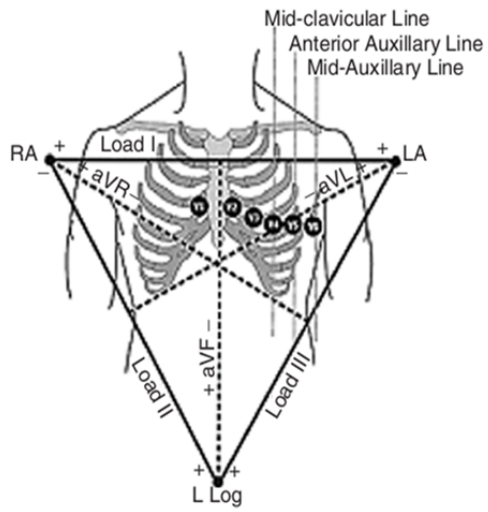

Fig. 1.3: All leads' position on the body [1].

1.3 Leads in ECG

The standard ECG has 12 leads which include 3 bipolar leads, 3 augmented unipolar leads and 6 chest (precordial) leads. In Fig. 1.3 all leads' position are shown in human body. A lead is a pair of electrodes (+ve & -ve) placed on the body in designated anatomical locations & connected to an ECG record [5]. Bipolar leads record the potential difference between two points (+ve & -ve poles), whereas unipolar leads record the electrical potential at a particular point by means of a single exploring electrode.

Table 1.1: Types of leads used in ECG monitoring

Einthoven Leads	Limb Leads	Chest Leads
Bipolar leads	Unipolar leads	Unipolar leads
		V1
Lead I	aVR	V2
Lead II	aVL	V3
Lead III	aVF	V4
		V5
		V6

1.3.1 Einthoven Leads

- Lead I: records potentials between the left and right arm,

- Lead II: between the right arm and left leg, and
- Lead III: those between the left arm and left leg.

1.3.2 Unipolar Limb leads

- aVR: when the +ve terminal is on the right arm,
- aVL: when the +ve terminal is on the left arm and
- aVF: when the +ve terminal is on the left leg.

One lead connected to +ve terminal acts as the different electrode, while the other two limbs are connected to the -ve terminal serve as the indifferent (reference) electrode [3]. Wilson leads (V1-V6) are unipolar chest leads positioned on the left side of the thorax in a nearly horizontal plane. The indifferent electrode is obtained by connecting the 3 standard limb leads. When used in combination with the unipolar limb leads in the frontal plane, they provide a three-dimensional view of the integral vector.

1.3.3 Chest (precordial) leads

- V1: 4th intercostal space, right sternal edge.
- V2: 4th intercostal space, left sternal edge.
- V3: between the 2nd and 4th electrodes.
- V4: 5th intercostal space in the midclavicular line.
- V5: on 5th rib, anterior axillary line.
- V6: in the midaxillary line.

To make recordings with the chest leads (different electrode), the three limb leads are connected to form an indifferent electrode with high resistances. The chest leads mainly detect potential vectors directed towards the back. These vectors are hardly detectable in the frontal plane [1]. Since the mean QRS vector is usually directed downwards and towards the left back region, the QRS vectors recorded by leads V1-V3 are usually negative, while those detected by V5 and V6 are positive [3]. In

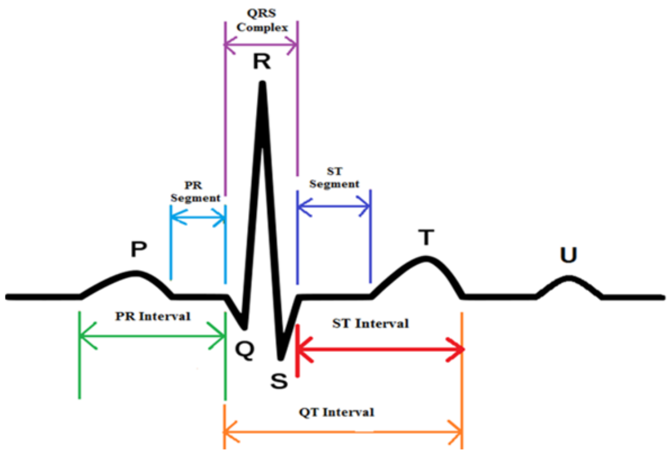

Fig. 1.4: Schematic representation of normal ECG waveform.

leads V1 and V2, QRS = -ve because, the chest electrode in these leads is nearer to the base of the heart, which is the direction of electronegativity during most of the ventricular depolarization process. In leads V4, V5, V6, QRS = +ve because the chest electrode in these leads is nearer the heart apex, which is the direction of electropositivity during most of depolarization [5].

1.4 ECG Waves and Interval

1.4.1 P Wave

P wave represents the sequential activation of the right and left atria, and it is common to see notched or biphasic P waves of right and left atrial activation. It is very difficult to analyze P waves with a high signal-to-noise ratio in ECG signal.

A clear P wave before the QRS complex represents sinus rhythm. Absence of P waves may suggest atrial fibrillation, sinus node arrest, junctional rhythm or ventricular rhythm.

1.4.2 PR Segment

The PR segment connects the P wave and the QRS complex. The impulse vector is from the AV node to the bundle of His to the bundle branches and then to the Purkinje Fibers. This electrical activity does not produce a contraction directly and is merely traveling down towards the ventricles and this shows up flat on the ECG. The PR interval is more clinically relevant than PR segment to any abnormality.

1.4.3 PR Interval

The PR interval is measured from the beginning of the P wave to the first part of the QRS complex. It includes time for atrial depolarization, conduction through the AV node, and conduction through the His-Purkinje system. Disruption at any point can prolong the PR interval. The length of the PR interval changes with heart rate.

Long PR interval suggests 1st degree atrioventricular block whereas varying PR interval implies Mobitz type I atrioventricular block or multifocal atrial tachycardia.

1.4.4 QRS complex

The QRS complex is the largest voltage deflection of approximately 10-20 mV but may vary in size depending on age, and gender. The QRS represents the simultaneous activation of the right and left ventricles, although most of the QRS waveform is derived from the larger left ventricular musculature.

Duration of the QRS complex indicates the time for the ventricles to depolarize and may give information about conduction problems. Wide QRS complex indicates right or left bundle branch block, ventricular flutter or fibrillation etc.

1.4.5 T wave

T wave represents ventricular repolarization. The interval from the beginning of the QRS complex to the apex of the T wave is referred to as the absolute refractory period.

Tall T wave may suggest left bundle branch block, ventricular hyper trophy, hyperkalemia, stroke whereas small, flattened or inverted T wave implies myocardial ischemia, myocarditis, anxiety, certain drugs, right bundle branch block, hypokalemia etc.

1.4.6 ST Segment

The ST segment occurs after ventricular depolarization has ended and before repolarization has begun. The ST segment is usually isoelectric and has a slight upward concavity. It is always measured from the J point, where the QRS and ST segments meet.

Elevation of ST segment implies myocardial ischemia, acute MI, LBBB, left ventricular hypertrophy, hyperkalemia, hypothermia whereas depression of ST segment may suggest myocardial ischemia, acute posterior MI, LBBB, RBBB etc.

1.4.7 ST Interval

The ST interval is measured from the J point to the end of the T wave.

1.4.8 QT Interval

The QT interval consists of the QRS complex (representing only a brief part of the interval), along with the ST segment and T wave, which constitutes the majority of the duration. The QT interval is used primary as a measure of membrane repolarization. Since the QT interval varies with heart rate, the QT interval is "corrected" (QTc) to make comparisons between ECG beats.

A prolonged QT interval is a risk factor for ventricular tachyarrhythmias and sudden death. Short QT interval may suggest hypercalcemia, hypomagnesemia, Graves' disease etc.

1.4.9 U wave

The U wave is hypothesized to be caused by the repolarization of the interventricular septum. Their amplitude is normally one-third of the following T wave and even more often completely absent. It may be seen following the T wave and can make interpretation of the QT interval especially difficult.

This is associated with metabolic disturbances, typically hypokalemia, hypomagnesemia and ischemia.

1.5 Arrhythmias in ECG Signal

The normal rhythm of the heart where there is no disease or disorder in the morphology of ECG signal is called Normal sinus rhythm (NSR) (Fig. 1.5(a)). The heart rate of NSR is generally characterized by 60 to 100 beats per minute. The regularity of the R-R interval varies slightly with the breathing cycle. The source of the rhythm is the Sino-atrial node, which is the normal pacemaker of the heart.

Table 1.2: Amplitude and duration of waves, intervals and segments of ECG signal

Features	Amplitudes (mV)	Duration (ms)
P Wave	0.1 -0.2	60-80
PR Segment	-	50-120
PR interval	-	120-200
QRS complex	1	80-120
T wave	0.1-0.3	120-160
ST segment	-	80-120
ST interval	-	320
QT interval	-	300-420
RR interval	-	(0.4-1.2) s

Hence another characteristic feature of NSR is a normal P-wave followed by a normal QRS-complex.

When the heart rate increases above 100 beats per minute, the rhythm is known as sinus tachycardia (Fig. 1.5(b)). This is not an arrhythmia but a normal response of the heart which demand for higher blood circulation [1]. If the heart rate is too slow then this is known as bradycardia and this can adversely affect vital organs. When the heart rate is too fast, the ventricles are not completely filled before contraction for which pumping efficiency drops, adversely affecting perfusion. Rhythms that deviate from NSR are called arrhythmias (or dysrhythmias) since they are abnormal and dysfunctional. Arrhythmias may be easily understood by categorizing them in the following manner:

1. Sinus Node Arrhythmias

2. Atrial Arrhythmias

3. Junctional Arrhythmias

4. Ventricular Arrhythmias

5. Atrioventricular Blocks

6. Bundle Branch and Fascicular Blocks

1.5.1 Sinus Node Arrhythmias

This type of arrhythmia arises from the S-A node of heart. As the electrical impulse is generated from the normal pacemaker, the characteristic feature of these arrhythmias is that P- wave morphology of the ECG is normal. These arrhythmias are the following types: Sinus arrhythmia, Sinus bradycardia, and Sinus arrest etc.

Sinus Arrhythmia

This is not a disorder or a true arrhythmia, but a normal, physiologic variation in the sinus rate with the phases of respiration. The slowest instantaneous heart beat may be less than 60 beats per minute, while the highest may exceed 100 beats per minute.

Sinus Bradycardia

In sinus bradycardia, the rhythm originates from the S-A node but at a rate of less than 60 beats per minute (Fig. 1.5(c)). The ECG appears normal except for the slow heart rate. Mild sinus bradycardia (50-59 beats per minute) is usually asymptomatic, while marked sinus bradycardia (30-45 beats per minute) may lead to hypotension and result in insufficient perfusion of the brain and other vital organs. Treatment is indicated if the bradycardia is symptomatic (e.g. giddiness, fainting, shortness of breath or chest pain).

Sinus Arrest

In sinus arrest, the S-A node intermittently fails to fire. There is no P-wave and therefore no accompanying QRS-complex and no T-wave (Fig. 1.5(d)). Bradycardia (slow average heart rate) may result if the occurrence of sinus arrests is frequent. Sinus arrest results from a marked depression of the automaticity of the S-A node. Since the automaticity of the S-A node is abnormal, the longest P-P interval (i.e. the "pause" on the ECG) will not be a multiple of the shortest P-P interval; unlike Sino-atrial exit block.

1.5.2 Atrial Arrhythmias

Atrial arrhythmias originate outside the S-A node but within the atria in the form of electrical impulses. These arrhythmias types are given bellow

(a) The normal sinus rhythm has regular, repeating waveforms of P, QRS, T waves and stable time segments between the waves

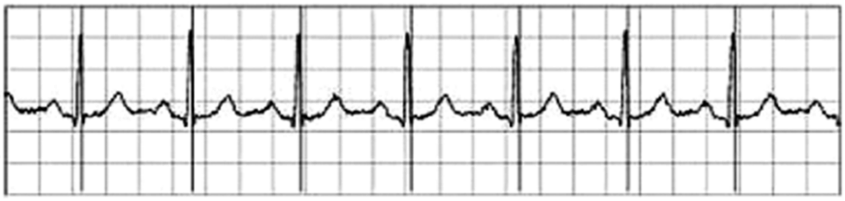

(b) In sinus tachycardia, the heart beats quickly, resulting in very short R-R Intervals

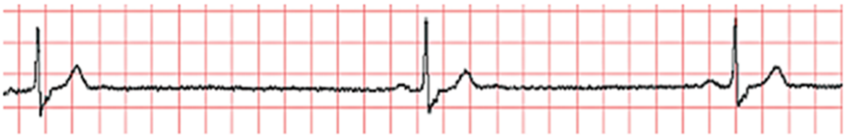

(c) In bradycardia, the heart beats at a slow rate, resulting in long R-R intervals

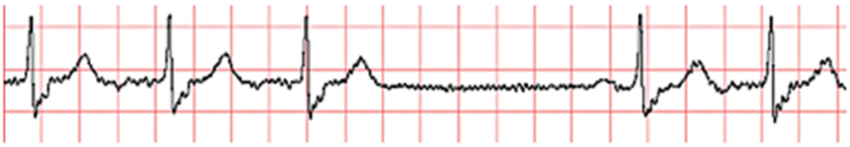

(d) Sinus arrest is characterised by a missing beat (P-QRS-T) that occurs repeatedly

Fig. 1.5: Sinus arrhythmias [1].

Premature Atrial Contractions (PAC)

This arrhythmia results an abnormal P-wave morphology followed by a normal QRS-complex and a T-wave. This happens because of an ectopic pacemaker firing before the S-A node. PACs may occur as a couplet where two PACs are generated consecutively. When three or more consecutive PACs occur, the rhythm is considered to be atrial tachycardia.

Atrial Tachycardia

The heart rate atrial tachycardia is fast and ranges from 160 to 240 beats per minute in atrial tachycardia. Frequently atrial tachycardia is accompanied by feelings of palpitations, nervousness, or anxiety.

Atrial Flutter

In atrial flutter, the atrial rate is very fast, ranging from 240 to 360 per minute. The abnormal P-waves occur regularly and so quickly that they take morphology of saw-tooth waveform which is called flutter (F) waves.

Atrial Fibrillation

The atrial rate exceeds 350 beats per minute in this type of arrhythmias. This arrhythmia occurs because of uncoordinated activation and contraction of different parts of the atria. The higher atria rate and uncoordinated contraction leads to ineffective pumping of blood into the ventricles. Atrial fibrillation may be intermittent, occurring in paroxysms (short bursts) or chronic [1].

1.5.3 Junctional Arrhythmias

Junctional arrhythmias are originated within the A-V junction in the form of the impulse comprising the A-V node and it's Bundle. The abnormal in P wave morphology occurs because of these arrhythmias [1]. The polarity of the abnormal P-wave would be opposite to that of the normal sinus P-wave since depolarization is propagated in the opposite direction - from the A-V node towards the atria.

Premature Junctional Contractions (PJC)

It is a ventricular contraction initiated by an ectopic pacemaker in the atrioventricular (A-V) node. In premature junctional escape contraction, a normal-looking QRS complex prematurely appears, but without a preceding P-wave, but the morphology of T-wave is normal [1].

Paroxysmal Supraventricular Tachycardia

In paroxysmal supraventricular tachycardia, the heart rate ranges from 160 to 240 beats per minute (Fig. 1.7(b)). PSVT may occur as a result of a reentry circuit in the A-V junction (Atrioventricular nodal re-entry tachycardia or AVNRT). It may also occur as a result of a re-entry circuit involving an accessory pathway between the atria and ventricles (Atrioventricular re-entry tachycardia or AVRT). The onset and

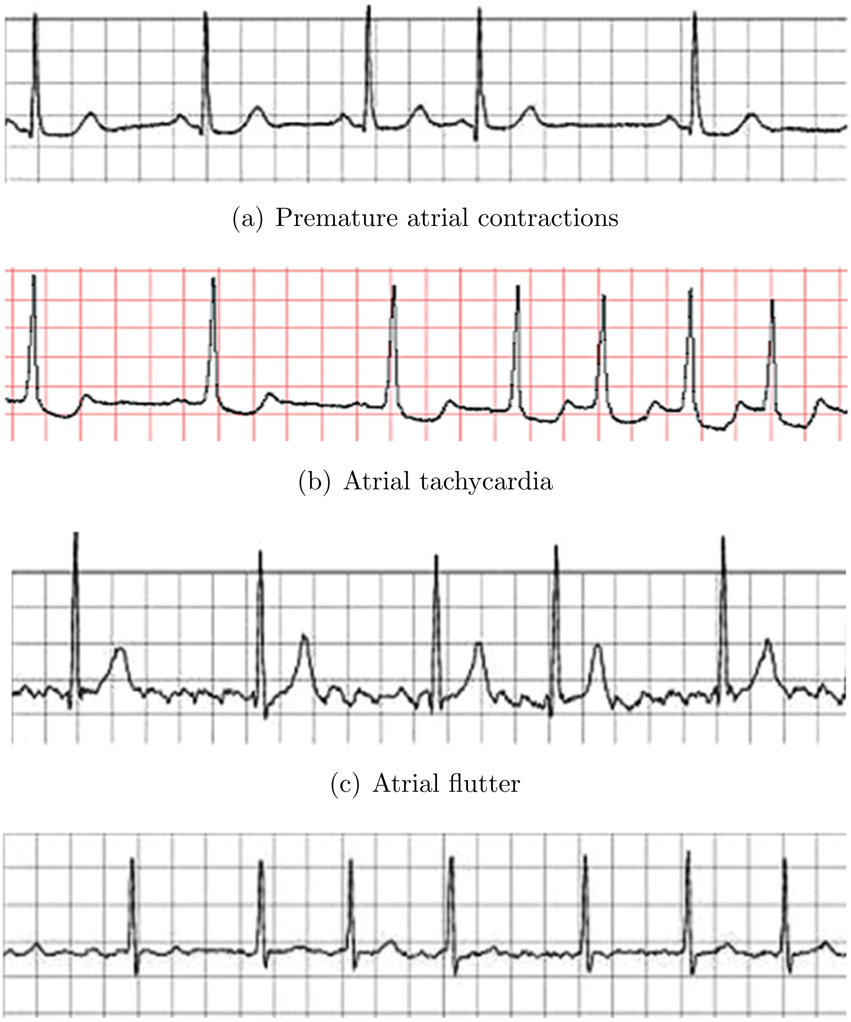

(a) Premature atrial contractions

(b) Atrial tachycardia

(c) Atrial flutter

(d) Atrial fibrillation

Fig. 1.6: Atrial arrhythmias [1].

termination of PSVT is abrupt, and may occur in repeated episodes (paroxysms) that last for seconds, hours or days. In AVNRT, P-waves are usually buried in the QRS complex and hence not visible; whereas for AVRT the P waves may be visible.

1.5.4 Ventricular arrhythmias

In this type of arrhythmia, the impulses originate from the ventricles and move outwards to the rest of the heart. In Ventricular arrhythmias, the QRS-complex is wide and bizarre in shape.

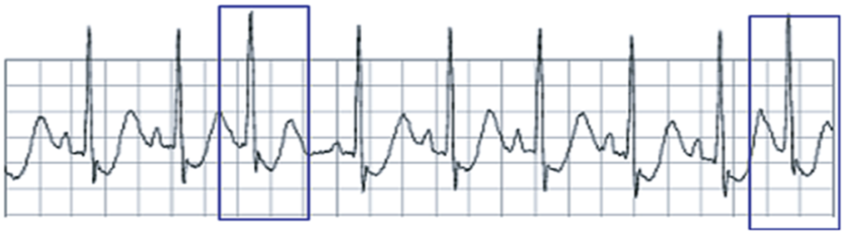

(a) Premature junctional arrhythmia

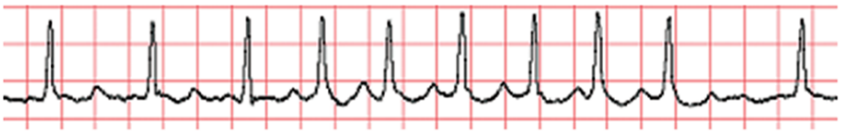

(b) Paroxysmal supraventricular tachycardia

Fig. 1.7: Junctional arrhythmias [1].

Premature Ventricular Contractions (PVC)

In PVC the abnormality is originated from ventricles. PVCs usually do not depolarize the atria or the S-A node and hence the morphology of P-waves maintains their underlying rhythm and occurs at the expected time. PVCs may occur anywhere in the heart beat cycle. PVCs are described as isolated if they occur singly, and as couplets if two consecutive PVCs occur.

Ventricular Tachycardia (VT)

The heart rate of ventricular tachycardia is 110 to 250 beats per minute. In VT the QRS complex is abnormally wide, out of the ordinary in shape, and of a different direction from the normal QRS complex. VT is considered life-threatening as the rapid rate may prevent effective ventricular filling and result in a drop in cardiac output.

Ventricular Fibrillation

Ventricular fibrillation occurs when numerous ectopic pacemakers in the ventricles cause different parts of the myocardium to contract at different times in a non-synchronized fashion. Ventricular flutter exhibits a very rapid ventricular rate with a saw-tooth like ECG waveform.

(a) Premature ventricular contractions

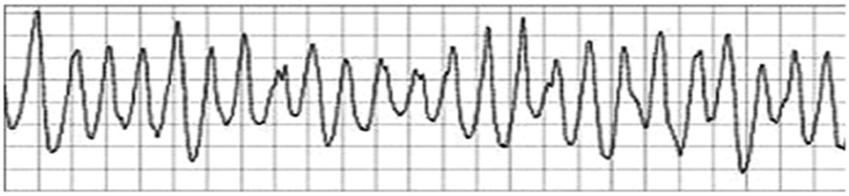

(b) Ventricular tachycardia

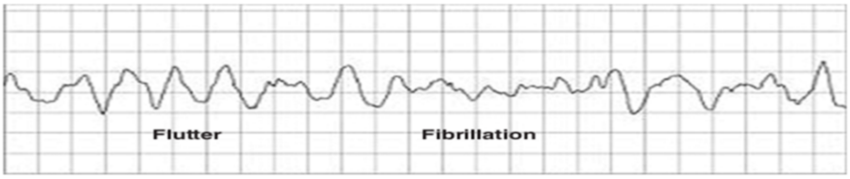

(c) Ventricular fibrillation

Fig. 1.8: Ventricular arrhythmias [1].

1.5.5 Atrioventricular Blocks

It is the normal propagation of the electrical impulse along the conduction pathways to the ventricles, but the block may delay or completely prevent propagation of the impulse to the rest of the conduction system.

First-Degree AV Block

A first-degree AV block is occurred when all the P-waves are conducted to the ventricles, but the PR-interval is prolonged.

Second-Degree AV Block

Second-degree AV blocks are occurred when some of the P- waves fail to conduct to the ventricles. Here, conduction intermittently fails to go down the bundle of His and bundle branches. There is usually a pre-existing complete block in one bundle branch, such that when an intermittent block occurs in the remaining bundle branch, conduction down to the ventricles fails. As a result of the pre-existing bundle branch block, the QRS-complex is commonly wide. Commonly the conduction ratio is 4:3

or 3:2 P-waves to QRS-complexes. This type of AV block is dangerous as complete heart block can occur unpredictably, and is an indication for implantation of an artificial pacemaker.

Third-Degree AV Block

In third-degree AV block, the rhythm of the P-waves is completely dissociated from the rhythm of the QRS-complexes. The atria and the ventricles beat independently, each beat at their own rate [1].

Paced Beat (Implant)

Hearts implanted with an artificial pacemaker will generally beat around 60 to 70 beats per minute depending on the setting of the artificial pacemaker. The pacing electrode is commonly attached to the apex of the right ventricular cavity (ventricular pacemaker) or the right atrium (atrial pacemaker), or both (dual chamber pacemaker). The artificial pacemaker produces a narrow, often biphasic spike. A pacemaker lead positioned in an atrium produces a pacemaker spike followed by a P -wave. A pacemaker lead positioned in a ventricle produces a pacemaker spike followed by a wide, bizarre QRS-complex (Fig. 1.10). Sometimes it is also called pacemaker rhythm.

1.5.6 Bundle Branch Blocks

Bundle branch block, cease in the conduction of the impulse from the AV-node to the whole conduction system. Due to this block there may occur myocardial infarction or cardiac surgery [1].

Right Bundle Branch Block (RBBB)

When the right bundle branch is blocked, the electrical impulse from the AV node is not able propagate to the Purkinje network to depolarize the right ventricular myocardium. Instead, the impulse propagates in a convoluted manner through the left ventricular myocardium to reach the right ventricular myocardium. Since propagation through the myocardium is much slower than through the specialized conducting tissue, the QRS-complex becomes widened. The morphology of the QRS-complex also changes and takes on a bizarre appearance because of the different

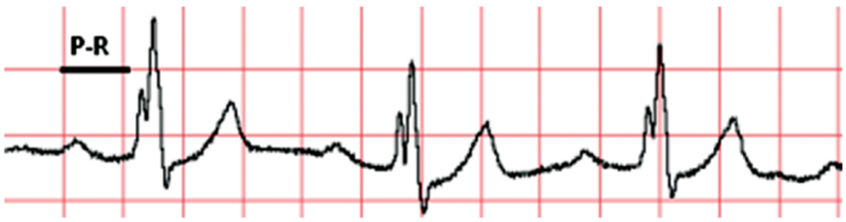

(a) First degree AV block

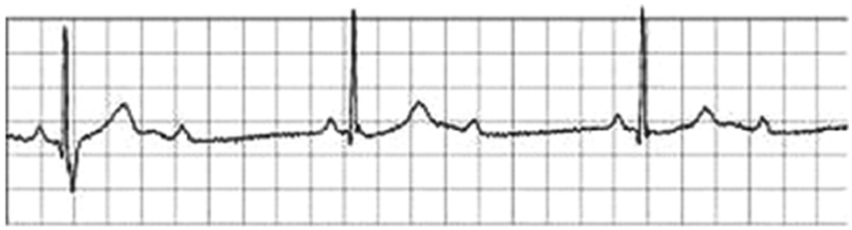

(b) Second degree AV block

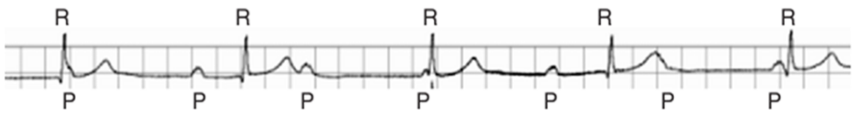

(c) Third degree AV block

Fig. 1.9: Atrioventricular blocks [1].

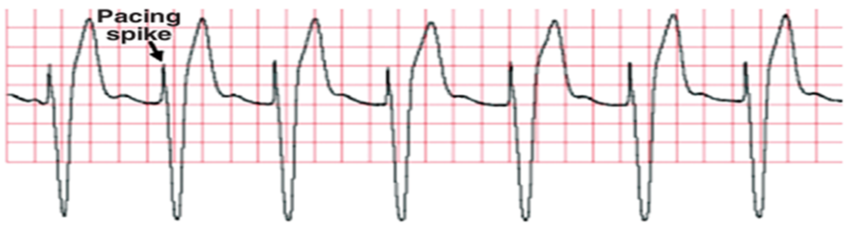

Fig. 1.10: A ventricular pacemaker generates a normal heart rate but with a bizarre-shaped QRS-complex. The pacemaker spike precedes each QRS-complex [1].

direction of depolarization.

Left Bundle Branch Block (LBBB)

Similar to right bundle branch block, a block in the left bundle branch will prevent the electrical impulses from the A-V node from depolarizing the left ventricular myocardium in the normal way. For LBBB, the right ventricle is depolarized primarily, generating an electrical wavefront that eventually spreads to the left ventricular myocardium causing the myocardium to depolarize.

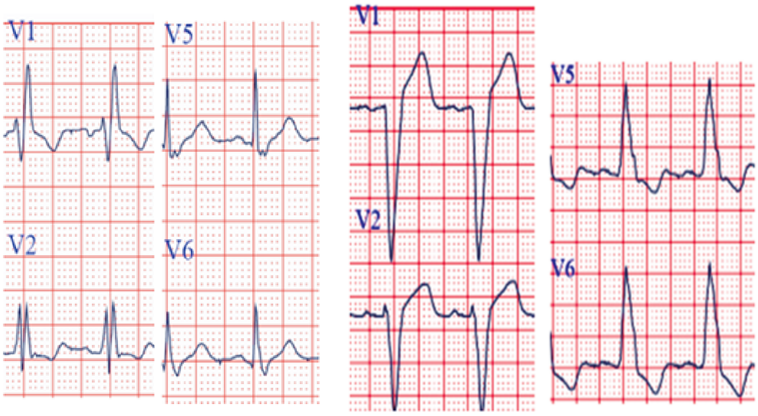

(a) Right bundle branch block (b) Left bundle branch block

Fig. 1.11: Bundle branch blocks [1].

1.6 Problem Definition

The state of cardiac heart is generally reflected in the shape of ECG waveform and heart rate. Any disturbance in the activity of heart can cause irregular heart rhythm known as cardiac arrhythmia. Electrocardiogram (ECG) is one of the most promising tools for classification of different types of arrhythmia, which is necessary until it goes fatal and causes loss of life. For ECG arrhythmia classification, a wide range of signal processing techniques extracting features have been reported in the literature. Most of them use time, frequency and time-frequency domain representation of the ECG waveforms, on the basis of which many specific features are defined in order to classify different types of ECG arrhythmia. The most difficult problem faced by today's automatic ECG analysis is the large variation in the morphologies of ECG waveforms. It is to be noted that methods capable of classifying multi-class arrhythmia in stringent conditions, such as lack of enough training dataset and random selection of training and testing dataset have been limitedly reported. Thus, in order to handle the practical situations of real life applications as mentioned above, development of a multi-class arrhythmia classification method, apart from providing simplicity in computation, is needed to be capable of providing performance with greater sensitivity, specificity and accuracy.

1.7 Objective of the Thesis

The objectives of this thesis are:

1. To develop a set of fractal dimension features based on empirical mode decomposition (EMD) of ECG signals.

2. To derive another set of fractal dimension features based on wavelet packet decomposition (WPD) of ECG signals.

3. To form a simple feature set based on energy and entropy of only the 4th level WPD detail coefficients of ECG signals in order to avoid complexity and computational burden.

4. To investigate the performance of the proposed feature sets for the classification of five types of arrhythmia using ECG signals available from the MIT-BIH arrhythmia database.

The outcome of this thesis is the development of an ECG based method exploiting features extracted from EMD and WPD, which is able to classify different types of ECG arrhythmia with greater sensitivity and specificity even in case of reduction of training dataset as well as random selection of training and testing dataset.

1.8 Organization of the Thesis

This thesis is organized as follows; The heart anatomy, different types of ECG arrhythmia and the importance of ECG arrhythmia classification are introduced in chapter 1. Chapter 2 provides a comprehensive review for the state-of-the-art ECG arrhythmia classification methods. Chapter 3 describes an empirical mode decomposition based fractal dimension feature for ECG arrhythmia classification. A wavelet packet based fractal dimension feature for ECG arrhythmia classification is discussed in chapter 4. Finally an approach for ECG arrhythmia classification based on energy and entropy of only the 4th level detail wavelet packet coefficients are proposed in chapter 5. Simulation results and quantitative performance comparison of all the proposed methods are shown in detail in chapter 6. Finally, concluding remarks, contribution and suggestions for future works of the thesis are highlighted in chapter 7.

Chapter 2

Literature Review

2.1 Introduction

ECG arrhythmia classification is very essential to the serious patients suffering from dangerous heart condition. If life threatening arrhythmia like PVC or VT is detected timely, the patients can be treated with necessary measures and saved from sudden death. It is a very time consuming job for doctors to analyze long ECG records of a patient. Therefore, many signal processing techniques have been utilized in order to extract features capable of classifying different ECG arrhythmia when fed to a classifier. The main principles of such methods are based on pattern recognition techniques. Several methods based on various signal processing techniques have been reported in the literature for cardiac arrhythmias classification based on time or frequency or time-frequency domain. In order to extract features from ECG, researchers have used fractal dimension [6–15], wavelet transform [16–21], behavioural modeling [22], cross spectral density [23], empirical mode decomposition (EMD) [24], artificial neural networks (ANN) [25–27], support vector machines (SVM) [28, 29], cluster analysis (CA) method [30], principal component analysis (PCA) [31] and independent component analysis (ICA) [32, 33]. Simple template matching methods have also been incorporated in the classification process [34]. The performance of these methods in classifying different types of ECG arrhythmia are evaluated in terms of different performance evaluation criteria e.g. sensitivity, specificity and accuracy.

It is to be noted that methods capable of classifying multi-class arrhythmia in practical conditions like performance after reducing training dataset and random selected training and testing dataset have been limitedly reported. This chapter presents review on the literature survey of the different cardiac arrhythmia classification methods used to date.

2.2 Time Domain Approaches

Features extracted from ECG morphology and RR intervals are the most popular time domain feature for cardiac arrhythmia classification. Overview of some recently reported methods exploiting features directly from time domain ECG signals are described here.

Chazal et al. developed a method for classifying five different ECG groups: normal beats, VEBs, SVEBs, fusion of normal and VEBs and unknown beat types using MIT-BIH arrhythmia database. In this study heart beat fudicial points were calculated manually. This paper derived 4 features on RR intervals, 3 features on heart beat intervals and 8 representations on ECG morphology. Twelve classifier configurations were set to test the effect on classification performance for different feature selections and finally choose the best configuration for an independent assessment. This showed that multiple lead configurations outperform single lead configurations processing the same feature sets. Single and double linear discriminants (LD) classifiers were implemented for classifying different ECG beats for single lead and multiple leads configurations respectively. Beat by beat performance of this study provides that 1904 normal beats and 3509 normal beats were misclassified as SVEB and fusion beats respectively. Since fusion beats are the combination of ventricular and normal beats, differentiating normal beats from fusion beats is really a challenging task [35].

Ince et al. proposed an automated patient-specific ECG heart beat classification system feature extraction process utilizing morphological wavelet transform features and temporal features from the ECG data. The morphological features are further reduced to a lower-dimensional feature space using principal component analysis (PCA). For the classification purpose, multi-dimensional particle swarm optimization (MD PSO) technique has been proposed in order to form artificial neural networks (ANNs) optimally by designing MLPs automatically. By using relatively small common and patient-specific training data, the proposed classification method can withstand significant inter-patient variations in ECG morphology by deriving the optimal network structure and thus makes it applicable to any ECG database without any modifications [36].

Yeh et al. proposed a method of analyzing ECG signal to classify 4 different types of arrhythmia plus normal heartbeats exploiting the cluster analysis (CA) method. In analyzing ECG signal for classification, it performs three consecutive steps: (i) QRS waveform detection; (ii) qualitative features selection; and (iii) classifying arrhythmia types. This method can easily be performed and carries no complex computational burden [30].

Time domain features only capture detail information from different aspects of time resolution representation of ECG signals. It cannot represent any frequency resolution characteristics of an ECG. Since ECG is a non-stationary signal, it has certain time and frequency resolution characteristics which can accurately represent the ECG signal as a whole. Only time domain features are not sufficient in order to represent detail characteristics regarding different types of ECG arrhythmia. Thus it is not capable of classifying ECG arrhythmia with greater accuracy for different conditions.

2.3 Frequency Domain Approaches

According to the concept that upon appearance of changes in the morphology of ECG signal caused by arrhythmia, corresponding changes are seen in the frequency domain, therefore, some arrhythmia classifiers have been designed based on the appropriate features obtained from signal fast Fourier transform (FFT), short-time Fourier transform (STFT), auto regressive (AR) models and power spectral density (PSD).

Dutta et al. proposed a heartbeat detection method exploiting a feature extractor coupled with an Artificial Neural Network (ANN) classifier. All the preprocessed ECG beats are cross-correlated with the normal heartbeat to form cross correlation sequences for every beat. These cross-correlation sequences are then transformed to frequency domain using Fourier transform in order to extract final feature vectors from its magnitude and phase cross-spectral density curves. The Learning Vector Quantization (LVQ) methods based classifiers are employed in this study in classifying three different types of beats: normal, Premature Ventricular Contraction

(PVC) and other beats, because this method adjusts the boundary between the clusters in order to minimize classification error. To demonstrate the efficiency of the proposed method, a large testing dataset is validated by classifying them against a small training dataset [23].

Since frequency analysis methods offer only frequency domain characteristics of an ECG ignoring time domain features, it alone is not sufficient for complete feature extraction in order to classify cardiac arrhythmia.

2.4 Time-Frequency Domain Approaches

Time-frequency signal analysis methods offer simultaneous interpretation of the signal in both time and frequency which allows local, transient or intermittent components to be elucidated. Such components are often obscured due to the averaging inherent within spectral only methods, i.e. the FFT.

The wavelet transform is a technique for analyzing signals. It was developed as an alternative to the Short Time Fourier Transform (STFT) to overcome problems related to its frequency and time resolution properties. More specifically, unlike the STFT that provides uniform time resolution for all frequencies the DWT provides high time resolution and low frequency resolution for high frequencies and high frequency resolution and low time resolution for low frequencies. In that respect it is similar to the human ear which exhibits similar time frequency resolution characteristics.

However, wavelet transformation (WT) is still the most popular one used for extracting features from ECG signals. This is because ECG signal is a highly non-stationary signal, and the inherent properties of WT include good time-frequency location and cross sub-band similarity. Due to its time frequency localization properties, the wavelet transform is an efficient tool for analyzing non-stationary signals like ECG. The wavelet transform can be used to decompose an ECG signal according to scale, allowing separation of the relevant ECG waveform morphology descriptors from the noise, interference, baseline wandering, and amplitude variation of the original signal. In the consequence, DWT has attracted interests in ECG pattern recognition and R-peak detection of ECG signals [18, 19, 37].

Chen et al. has presented higher order statistics of subband components to be effective in characterizing ECG signal for heartbeat classification. In order to select the most effective and less redundant features, two nonlinear correlation based filters (NCBFs), which apply feature-feature correlation, are employed in this study. The application of NCBFs with prior redundancy reduction further improves the efficiency of the methods with a little reduction in classification rates. Finally the performance of the best NCBF is compared with that of the linear correlation based filter (LCBF) and other filters reported in literature [38].

Khorrami et al. have proposed and compared use of CWT (Continues Wavelet Transform) with two popular and powerful data transformation techniques DWT (Discrete Wavelet Transform), and DCT (Discrete Cosine Transform) which have already been in use, in order to improve the capability of two pattern classifiers in ECG arrhythmias classification. The classifiers under examination are MLP (Multi-Layered Perceptron) and SVM (Support Vector Machine). The training or learning algorithms used in MLP and SVM are Back Propagation (BP) and Kernel-Adatron (K-A), respectively. The classification performance among four different arrhythmias together with normal ECG of MLP and SVM classifiers in terms of training performance, testing performance or generalization ability and training time are compared. For both classifiers, training and testing stages have been carried out twice. The final performance reveal that selection of the best feature extraction technique depends on the substantial value considered for training time, training and testing performance. Here, MLP outperforms SVM in case of testing performance with only the single lead [19].

Homaeinezhad et al. proposed a new ECG arrhythmia classification method utilizing hybrid learning machine with a new QRS complex geometrical feature extraction technique. After detecting and delineating the events of ECG using wavelet-based algorithm, each QRS region and also its corresponding discrete wavelet transform (DWT) are considered as virtual images and each of them is divided into eight polar sectors. Next, the curve length of each excerpted segment is calculated in order to form the final feature vector. To increase the classification performance as well as robustness of the proposed algorithm, a fusion structure consisting of six different classifiers namely as SVM, KNN and four MLP-BP neural networks with different topologies were designed and applied. Proposed learning machine was employed to classify 7 arrhythmias belonging to 15 different records [28].

Shen et al. presented an adaptive feature selection method for ECG arrhythmia classification exploiting modified support vector machines (SVMs). At first large number of trial features are extracted via considering Wavelet Transform based coefficients and signal amplitude or interval parameters, but finally as few as possible number of features are adaptively selected for the classification purpose. In order to increase the classification accuracy, a new classifier integrated with k-means clustering, one-against-one SVMs, and a modified majority voting mechanism, is proposed as well as employed [29].

Sahab et al. proposed an ECG arrhythmia classification technique utilizing discreet wavelet transform (DWT) and multi layer perceptron (MLP) neural network. In the preprocessing stage noises and artifacts are removed by a new method exploiting DWT. Then, using DWT, Daubechies (DB6) mother wavelet is incorporated in order to obtain eight-level decomposition and the minimum, maximum, variance and standard deviation of the signal are obtained. Finally combining time features with DWT features an array of final features are constructed to train and test 3 layer MLP neural networks [20].

Yu et al. proposed an electrocardiogram (ECG) beat classification system based on wavelet transformation and probabilistic neural network (PNN) to discriminate six ECG beat types. The ECG beat signals are first decomposed into components in different subbands using discrete wavelet transformation. Three sets of statistical features of the decomposed signals as well as the AC power and the instantaneous RR interval of the original signal are exploited to characterize the ECG signals. A PNN follows to classify the feature vectors. Only 11 features are required to attain this high accuracy, which is substantially smaller in quantity than that in other methods. These observations prove the effectiveness and efficiency of the proposed method for computer-aided diagnosis of heart diseases based on ECG signals [21].

Mahesh et al. presents a diagnostic system for classification of cardiac arrhythmia from ECG data, using Logistic Model Tree (LMT) classifier. Clinically useful information in the ECG is found in the intervals and amplitudes of the characteristic waves. The amplitude and duration of the characteristic waves of the ECG can be more accurately obtained using Discrete Wavelet Transform (DWT) analysis. Further, the non-linear behavior of the cardiac system is well characterized by Heart Rate Variability (HRV). Hence, DWT and HRV techniques have been employed to extract a set of linear (time and frequency domain) and nonlinear characteristic features from the ECG signals. These features are used as input to the LMT classifier to classify 11 different arrhythmias. The system can be deployed for practical use after validation by experts [39].

Wavelet packet decomposition method is an extension of wavelet transform. WPD is capable of dividing the whole time-frequency plane while classical WT can provide analysis only for low-band frequencies. The multi-resolution capability of WPD allows the decomposition of a signal into a number of scales, each scale representing a particular feature of the signal under study. The top level of the WPD is the time representation of the signal whereas bottom level has better frequency resolution. Thus using WPD, a better frequency resolution can be achieved over WT for the decomposed ECG signal. The advantage of wavelet packet analysis is that it is possible to combine the different levels of decomposition in order to construct the original signal.

Kutla et al. proposed an automatic heart beat recognition system exploiting features extracted from higher order statistics (HOS) of wavelet packet decomposition (WPD) coefficients. First of three stages involves the calculation of wavelet packet coefficients (WPC) for each different ECG beat. Then, feature vectors are extracted by calculating higher order statistics, namely second, third and fourth cumulants of each level of WPC. After applying normalization to all extracted features, final feature set is formed, which is applied as input to the k-NN algorithm based classifier. The proposed method has its ability to handle Gaussian noise which is ineffective since the system is based on cumulants [40].

2.5 Other Approaches

Yu et al. proposed a novel independent components (ICs) arrangement approach to collaborate with the independent component analysis (ICA) method used for classifying different ECG beat. The ICs extracted by fast ICA algorithm are rearranged according to the L2 norms of the rows of the de-mixing matrix. The efficacy and efficiency of the proposed method and three other general ICs arrangement strategies are studied. Two kinds of classifiers, including probabilistic neural network and support vector machines, are employed to calculate the performance of the proposed method in classifying eight different ECG beat types. The classification results reveal that the proposed ICs arrangement strategy outperforms the other strategies in eliminating the number of features required for the classifiers [41].

Moavenian et al. proposed a novel use of Kernel-Adatron (K-A) training algorithm collaborating with SVM (Support Vector Machine) for classifying six types of ECG arrhythmia plus normal ECG. The proposed pattern classifier is compared with MLP (multi-layered perceptron) using back propagation (BP) learning algorithm. The MLP and SVM training and testing stages were carried out twice. They were first trained only with one ECG lead signal and then a second ECG lead signal was added to the training and testing datasets in order to investigate its influence on training and testing performance and training time for both classifiers. The results designate that SVM in comparison to MLP is much faster in training stage and nearly seven times higher in performance, but MLP generalization ability in terms of mean square error is more than three times less [26].

Castillo et al. described a hybrid intelligent system for classification of cardiac arrhythmias exploiting three methods of classification: Fuzzy KNN, Multi-Layer Perceptron (MLP) Gradient Descent with momentum Backpropagation, and MLP Scaled Conjugate Gradient Backpropagation. Since the mentioned classifiers capture different knowledge about classification, all of them produced good classification results individually. Finally, a Mamdani type fuzzy inference system was used to aggregate the outputs of the individual classifiers, and a very high classification rate was achieved [27].

Ozbay et al. proposed a novel technique in classifying ECG arrhythmia exploiting neural network models with three types of adaptive activation function, namely NNAAF-1, NNAAF-2 and NNAAf-3. Different activation functions with adjustable free parameters were employed in hidden neurons of these models to improve classical MLP network. In addition, these three NNAAF models were compared with the MLP model implemented in similar conditions. Ten different types of ECG arrhythmias were selected to train NNAAFs and MLP models [42].

Lin et al. proposed a method for cardiac arrhythmias recognition using the nonlinear interpolation fractal classifier. A typical electrocardiogram (ECG) consists of P-wave, QRS-complexes, and T-wave. Iterated function system (IFS) uses the nonlinear interpolation in the map and uses similarity maps to construct various data sequences including the fractal patterns of supraventricular ectopic beat, bundle branch ectopic beat, and ventricular ectopic beat. Grey relational analysis (GRA) is proposed to recognize normal heart beat and cardiac arrhythmias. The nonlinear interpolation terms produce family functions with fractal dimension (FD), the so-called nonlinear interpolation function (NIF), and make fractal patterns more distinguishing between normal and ill subjects. Compared with other methods, the proposed hybrid methods demonstrate greater efficiency and higher accuracy in recognizing ECG signals [8].

Wang et al. introduced a new classification method of arrhythmia by combining empirical mode decomposition (EMD) with singular value decomposition (SVD), using support vector machines (SVM) for classifying. First, ECG signal is decomposed into a set of intrinsic mode function (IMF) using empirical mode decomposition method. The initial feature vector matrix is formed by these IMFs. Then, the initial feature vector matrix is decomposed using singular value decomposition, and values of the matrix can be calculated. Singular values are regarded as the feature vector of ECG signal, support vector machines used as classifiers are established to identify the condition of arrhythmia. Experimental results show that, this method can classify the types of arrhythmia accurately and effectively, and can be used for the field of ECG pathological auxiliary diagnosis [43].

Mishra et al. proposed a local fractal dimension based nearest neighbor classifier for ECG based classification of arrhythmia. Local fractal dimension (LFD) at each sample point of the ECG waveform is taken as the feature. A nearest neighbor method in the feature space is used to find the class of the test ECG beat. The nearest neighbor is found based on the RR-interval-information-biased Euclidean distance, proposed in the current work. Based on the two methods used for estimating the LFD, two classification methods are validated in the current work, e.g. variance based fractal dimension estimation based nearest neighbor classifier and power spectral density based fractal dimension estimation based nearest neighbor classifier [6].

2.6 Conclusion

In this chapter, a brief literature survey of the recent state-of-the-art ECG arrhythmia classification methods is presented. All the methods have their pros and cons. In order to handle the practical situations of real life applications such as reduced training dataset and random selection of training and testing feature set, design of a multi-class arrhythmia classification method, apart from providing simplicity in computation, is needed to be capable of providing performance with greater sensitivity, specificity and accuracy. Thus, development of a multi-class arrhythmia classification method, which is simple yet effective in handling practical conditions as mentioned above, is still a challenging task.

Chapter 3

An Empirical Mode Decomposition Based Fractal Dimension Feature for ECG Arrhythmia Classification

3.1 Introduction

In literature, there exist a numerous methods to extract fractal dimension, such as box counting methods, fractional Brownian motion methods, area measurement methods, power spectrum density based methods and variance based methods etc. Again, fractal dimension of a signal can be estimated by calculating Hurst exponent of the signal. There are various methods available e.g. rescaled ranged method, standard method, wavelet method with different mother wavelets, wavelet packet based method and empirical mode decomposition method (EMD) for estimating the Hurst exponent. In order to extract effective as well as distinguishable features based on localized information for different types of ECG arrhythmia, estimation of local fractal dimension (LFD) of neighboring sample points of segments within an ECG beat instead of taking a global fractal dimension of the whole beat is preferred in the proposed work.

In this chapter, our objective is to develop a set of LFD features based on empirical mode decomposition (EMD) of ECG signals [44]. In the EMD domain, the basic functions are directly derived from the original ECG signal. Therefore, a set of LFD features is calculated using the Hurst exponent (HE) derived from the intrinsic mode functions (IMFs) obtained via EMD operation of ECG signals [45]. We have used state-of-the-art methods PSDFE and VFE for comparison of ECG arrhythmia classification performance with the proposed method based on LFD estimation in EMD domain in terms of different performance evaluation criteria.

3.2 Preliminaries

3.2.1 Fractals and Fractal Dimension

Fractals are of rough or fragmented geometric shape that can be sub divided in parts. Unlike conventional geometry, which deals with lines, triangles, circles, spheres and cones, fractal geometry is concerned with broken or fractured shapes as so commonly found in nature. Images and shapes within images which cannot be represented by Euclidean geometry have been analyzed by fractal geometry. Natural objects are not union of exact reduced copies of whole. A magnified view of one part will not precisely reproduce the whole object, but it will have the same qualitative appearance. This property is called statistical self-similarity or semi-self similarity. In general, we can extract fractal information from self-similarity of an object. Self-similarity is defined as a property, where a subset, when magnified to the size of the whole, is indistinguishable from the whole [46]. Thus, fractal is a mathematical model to represent self-similar structures as well as to describe scale invariant random processes. Fractals are often characterized by their fractional dimensions [47]. It measures the degree of fractal boundary fragmentation or irregularity over multiple scales. It determines how fractal differs from Euclidean objects. According to Mandelbrot, analytically, the relationship between the object or data measuring scale δ and the length L can be expressed as [46]

$$L(\delta) = k \cdot \delta^{1-D}, \tag{3.1}$$

where, k is a constant and D is known as the fractal dimension, a number very often a non integer (fractional) [10]. The fractal dimension of a straight line is 1 and it approaches 2 for highly convoluted signals [48].

ECG signal of a human heart is a self-similar object. Thus it can be well modeled as self-affined fractal set with a fractal dimension. Broadly speaking, a fractal structure has the same statistics under any scale of magnification [10,49,50]. Thus, fractal dimension has the unique advantage of being not strongly related to the mean and variance of signals. A normal ECG signal, upward and downward baseline shifted ECG signals and a scaled ECG signal are presented in Fig. 3.1(a) through Fig. 3.1(d). It is seen from Fig. 3.1 that ECG signal yields the same fractal dimension regardless of change in mean and variance due to baseline shifting or scaling of the normal ECG signal.

Morphology of ECG signal changes under different arrhythmia conditions causing corresponding fractal dimension to change. Since the fractal dimension varies under different arrhythmia conditions, classification of different ECG arrhythmia is possible by using fractal dimension. Fractal dimensions of normal ECG (N), left bundle branch block (L) and right bundle branch block (R) ECGs, atrial premature (A) and premature ventricular contraction (V) ECGs, and paced beat (PB) ECG are computed and plotted in Fig. 3.2(a) through Fig. 3.2(f). For each class of arrhythmia N through PB, ten beats are considered for computing fractal dimensions. It is clear from Fig. 3.2 that fractal dimension of all beats in the same class vary a little.

In Fig. 3.3, a bar graph plotting mean value of fractal dimensions with their standard deviation (SD) in error-bar considering ten beats of each class of arrhythmia is shown. It is vivid from this figure that the mean value of fractal dimension is different from class to class. Since the standard deviation against the mean value of fractal dimension does not overlap among the classes, it is obvious that fractal dimension is capable of providing separability among all classes of ECG arrhythmia. Therefore, in this work we are motivated to employ fractal dimension as a feature for classifying different ECG arrhythmia.

3.2.2 Recent Methods for Computing Fractal Dimension

Power spectrum density based fractal dimension estimator (PSDFE) and variance based fractal dimension estimator (VFE) are recently proposed for classification of ECG arrhythmia [6].

Power Spectrum Density Based Fractal Dimension Estimator

PSDFE is a well-known method to estimate the fractal dimension of biological signals [7]. The power spectrum of a discrete ECG signal $x[n]$, can be calculated by

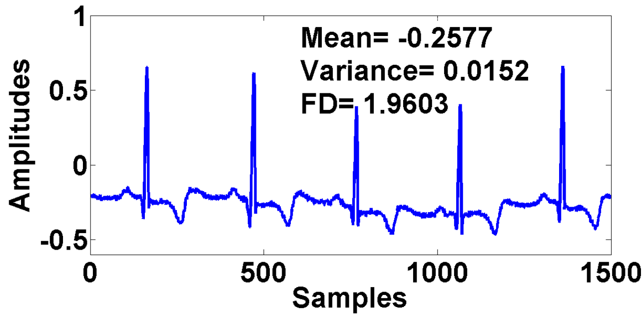

(a) Normal ECG

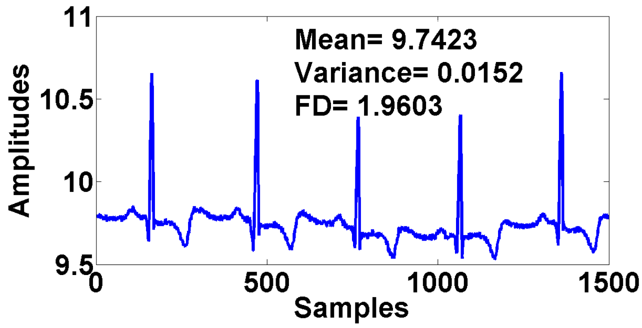

(b) Upward baseline shifted ECG

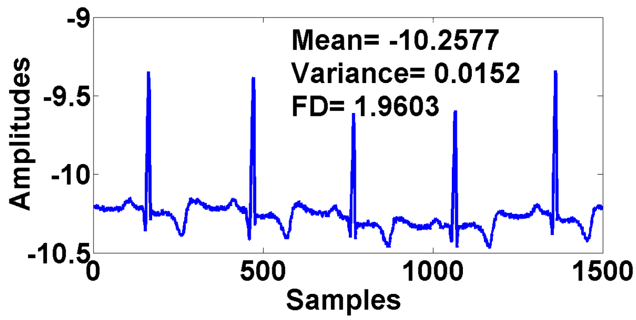

(c) Downward baseline shifted ECG

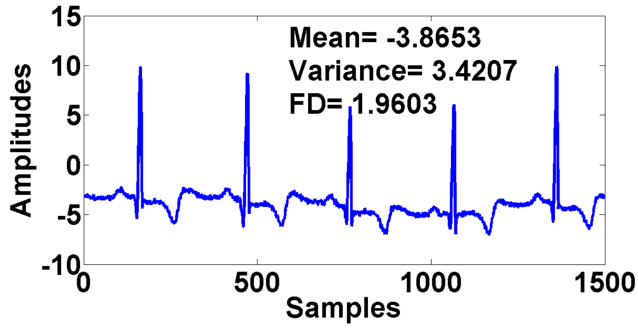

(d) Scaled ECG

Fig. 3.1: Fractal dimensions of (a) normal ECG (b) upward baseline shifted ECG (c) downward baseline shifted ECG and (d) scaled ECG

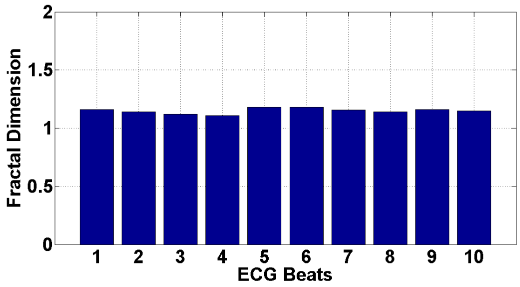

(a) Class N

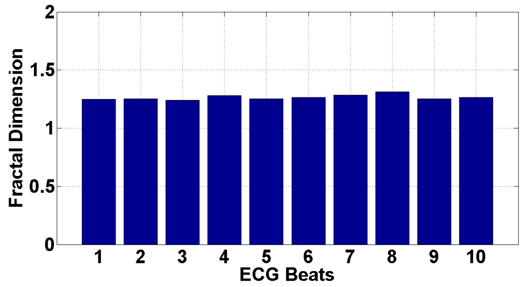

(b) Class L

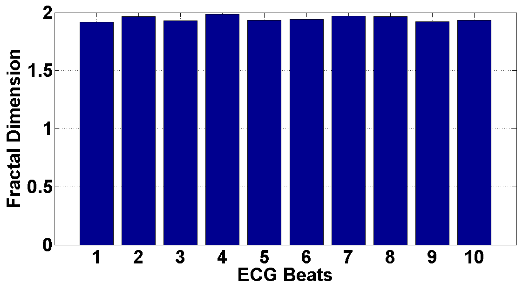

(c) Class R

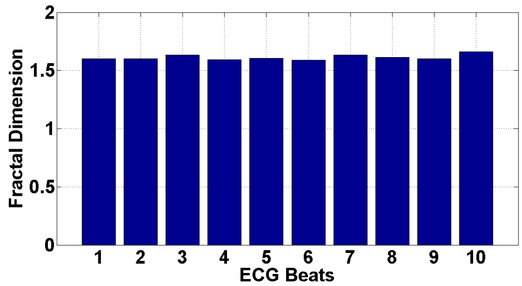

(d) Class PB

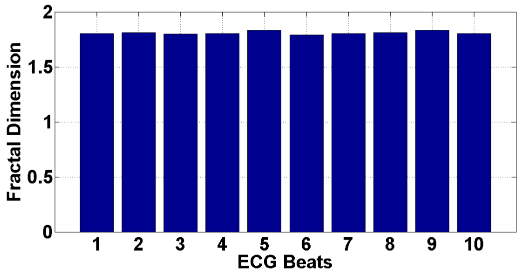

(e) Class V

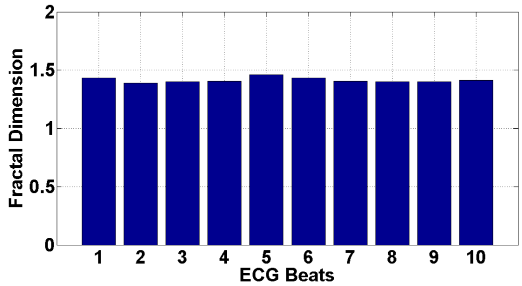

(f) Class A

Fig. 3.2: Fractal dimension of normal ECG and five classes of ECG arrhythmia.

the square of its discrete Fourier Transform (DFT) $X[k]$, which is given by

$$X[k] = \sum_{n=0}^{N-1} x[n]e^{-j2\pi nk/N}, 0 \leq k \leq 1. \tag{3.2}$$

For a fractal process, in the frequency domain, the power spectrum $|X[k]|^2$ follows a power law relationship with the discrete frequency k as

$$|X[k]|^2 \sim pk^{-\gamma}. \tag{3.3}$$

Taking logarithm of the both sides of Eq. (3.3), we get

$$\log(|X[k]|^2) \sim (\log p - \gamma \log k). \tag{3.4}$$

The PSD curve, mainly the log-log plot of the power spectrum $|X[k]|^2$ versus discrete frequency k is plotted. The slope of the line fitting the log-log plot by a least square

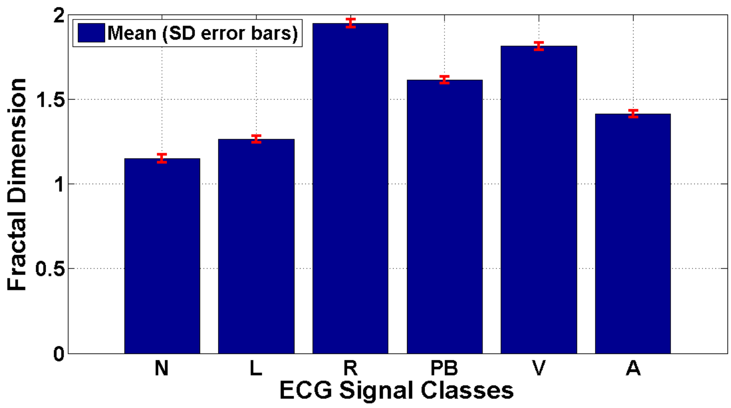

Fig. 3.3: Mean Fractal dimension with standard deviation (SD) error bars for different ECG arrhythmias.

method in the linear frequency range is employed to estimate the spectral exponent γ. The spectral exponent γ thus obtained from the PSD curve is utilized to find the fractal dimension D as follows

$$D = \frac{5-\gamma}{2}. \tag{3.5}$$

Variance Based Fractal Dimension Estimator

VFE is another method of estimating fractal dimension of any time series signal, where the spread of the increments in the signal amplitude is utilized [6]. For a discrete time series ECG signal $x[n]$, the variance of the amplitude increment is related to the time increment over a given time increment according to the following power law

$$\begin{aligned} var\{(x[n_2]-x[n_1])\} &\sim |n_2-n_1|^{2H}, \\ var(\Delta x)_{\Delta n_m} &\sim \Delta n_m^{2H}, \end{aligned} \tag{3.6}$$

where, $\Delta n = |n_2 - n_1|$,$(\Delta x)_{\Delta n} = x[n_2] - x[n_1]$, $(\Delta n)_m$ is the discrete time increment at the m-th order scale, $var(\Delta x)_{\Delta n_m}$ is the variance of the amplitude increment over that time increment at the m-th order scale, and H is defined as the Hurst exponent. From Eq. (3.6), it is clear that H can be estimated from a log-log plot of $(\Delta n)_m$ versus $var(\Delta x)_{\Delta n_m}$. For this purpose, the slope s of the line fitting the log-log plot is first estimated by the least square method. Then, the Hurst exponent H is found from half of the slope s. Fractal dimension of an ECG signal can be calculated by subtracting H from 2 [6].

3.3 Proposed Method

3.3.1 Empirical Mode Decomposition

EMD is intuitive and adaptive signal processing technique used for nonlinear, non-stationary time series data, such as ECG. Unlike Fourier Transform (FT) or Wavelet Transform (WT), the basic functions in EMD are derived fully from the data signal under consideration. Moreover, the computation of EMD does not require any previously known value of the signal [24]. The key task here is to identify the intrinsic oscillatory modes by their characteristic time scales in the signal empirically, and accordingly, decompose the signal into intrinsic mode functions (IMFs) [44, 51]. A function is considered to be an IMF if it satisfies two conditions; first, in the whole data set, the number of local extrema and that of zero crossings must be equal to each other or different by at most one and second, at any point, the mean value of the envelope defined by the local maxima and that defined by the local minima should be zero. The systematic way to decompose the data into IMFs, known as the “sifting” process, is described as follows

1. All the local maxima of the data are determined and joined by cubic spline line thus constructing an upper envelope.

2. All the local minima of the data are found and connected by cubic spline line to obtain the lower envelope.

3. The mean m_1 of both the envelopes are calculated and the difference between the signal $x[n]$ and m_1 is computed as $h_1[n]$.

$$h_1[n] = x[n] - m_1. \tag{3.7}$$

4. If $h_1[n]$ satisfies the conditions of IMF, then it is the first frequency and amplitude modulated oscillatory mode (IMF) of $x[n]$.

5. If $h_1[n]$ dissatisfies the conditions to be an IMF, it is treated as the data in the second sifting process, where steps 1, 2 and 3 are repeated on $h_1[n]$ to derive the second component $h_2[n]$ as

$$h_2[n] = h_1[n] - m_2, \tag{3.8}$$

in which m_2 is the mean of upper and lower envelopes of $h_1[n]$.

6. Let after w cycles of operation, if $h_w[n]$, given by

$$h_w[n] = h_{w-1}[n] - m_w, \tag{3.9}$$

becomes an IMF, it is designated as $c_1[n] = h_w[n]$, the first IMF component of the original signal.

7. Subtracting $c_1[n]$ from $x[n]$, $r_1[n]$ is calculated as

$$r_1[n] = x[n] - c_1[n], \tag{3.10}$$

which is treated as the original data for the next cycle for calculating the next IMF.

8. Repeating the above process for L times, L no. of IMFs is obtained along with the final residue $r_L[n]$. A popular stopping criteria for the sifting process is to have the value of standard difference (SD) within a predefined threshold [52] as

$$SD = \sum_{n=1}^{N} \frac{|h_w[n] - h_{w-1}[n]^2}{h_w[n]^2}, \tag{3.11}$$

here, w and $(w-1)$ are index terms indicating two consecutive sifting processes.

Thus the decomposition process is stopped since $r_L[n]$ becomes a monotonic function from which no more IMF can be extracted. To this end, for L level of decomposition, the original signal can be reconstructed by the following formula,

$$x[n] = \sum_{k=1}^{L} c_k[n] + r_L[n]. \tag{3.12}$$

A typical ECG signal and the resulting IMFs are shown in Fig. 3.4.

3.3.2 Computation of Fractal Dimension Feature

The IMFs $c_1, c_2, ..., c_L$ in Eq. (3.12) represent the finally obtained amplitude and frequency modulated output set. Their frequency gradually decreases as the order of the IMFs increases. It is seen from the Fig. 3.4 that the lower order IMFs represent the high frequency oscillations and upper order IMFs correspond to low frequency oscillations. For the purpose of fractal dimension computation, we need to obtain the variance of each IMF by the following formula

$$V[k] = \frac{1}{N-1} \sum_{n=1}^{N} (c_k[n] - \overline{c_k})^2, k = 1, 2, 3, ..., L, \tag{3.13}$$

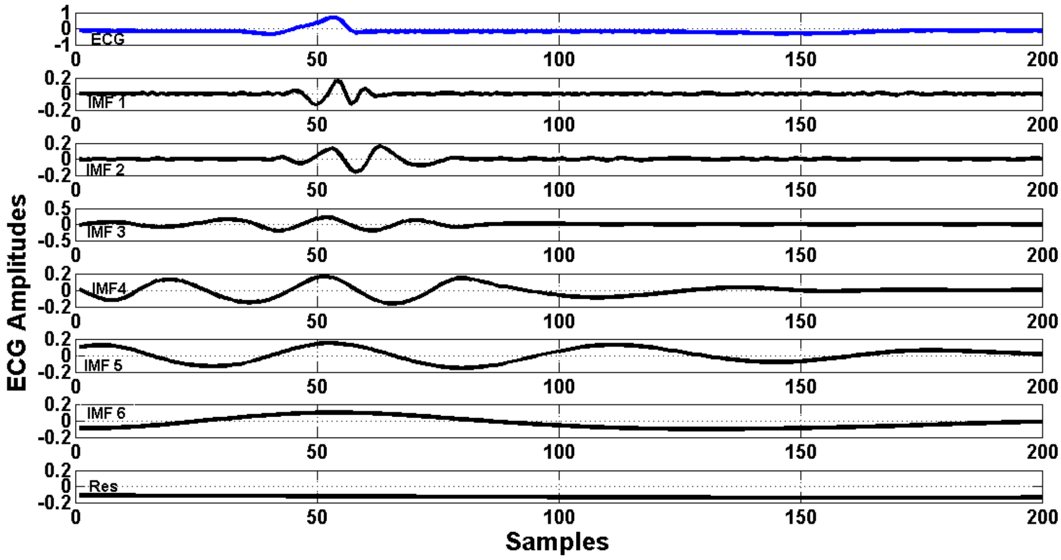

Fig. 3.4: Empirical mode decomposition to ECG signal.

where, N is the length of the ECG time series data, $k = 1, 2, ..., L$ is the level of IMF decomposition and $\overline{c_k}$ is the mean value of the IMF corresponding to the k-th level. The variance of each IMF $V[k]$ is related to the corresponding level of IMF decomposition by the Hurst exponent H. The relationship follows a power law expressed as [44]

$$V[k] \sim 2^{2kH}. \tag{3.14}$$

Taking logarithm on both sides of Eq. (3.14), we get

$$\log_2(V[k]) \sim 2kH. \tag{3.15}$$

By plotting the curve with $\log_2(V[k])$ as y-axis and level of IMF decomposition, k as x-axis results in a line. By fitting the line utilizing the least square method, the slope s corresponding to the line is obtained. From Eq. (3.15), it is clear that the slope s of the line is related to the Hurst Exponent H as

$$s = 2H. \tag{3.16}$$

From Eq. (3.16), H can be calculated as

$$H = \frac{s}{2}. \tag{3.17}$$

Denoting E as the Euclidean dimension [10], the fractal dimension D can be calculated from the Hurst exponent

$$D = E + 1 - H. \tag{3.18}$$

Since for ECG signal $E = 1$, a simplified form of fractal dimension D in Eq. (3.18) can be written as

$$D = 2 - H. \tag{3.19}$$

In a particular arrhythmia condition, morphological changes occur in different sections of a normal ECG beat and such changes vary from beat to beat under the same arrhythmia. Thus instead of taking a global fractal dimension of the whole beat, local fractal dimension (LFD) of neighboring sample points of segments within an ECG beat can capture detail information of the arrhythmia. Since LFD facilitates more accurate characterization of the ECG arrhythmia, LFD is preferred in the proposed work.

3.3.3 Selection of Window Length

Conventionally, LFD is estimated from an ECG beat using a fixed length window sliding over the whole beat [6]. So, the sliding window of size W converts the N-point ECG beat into $(N - W + 1)$ segments. For each segment, an LFD is estimated thus resulting in a time series of LFD of size $(N - W + 1)$.

In the proposed method, two or more IMFs are needed to be extracted from a sliding window of ECG in order to calculate the slope required for the estimation of the Hurst exponent as well as that of the LFD. However, it is found that at least three level of IMF decomposition can better approximate the slope. But the process of IMF decomposition strongly depends on the length of the sliding window. The effect of increase in window length on average number of IMF per window is shown in Fig. 3.5 for class N, class L and class PB ECG beat types. It is clearly seen from the figure that average number of IMF per window increases with the increase in window length for all the classes. It is also observed from the figure that window length 30 and 50 can ensure the average number of IMF greater than three for a beat of class N or class L, whereas window length 150 is enough for providing three IMFs per window on average in case of a beat of PB class. So a fixed window length cannot ensure the required number of IMF per window for each type of ECG arrhythmia. Therefore, the selection of a proper length for the window is an important task. In order to extract feature vector containing LFDs estimated from an ECG beat, the length of the sliding window needs to be optimized for each

ECG beat.

Although, we need to ensure three IMFs at each window for all the ECG classes, analyzing the average no. of IMF per window with varying window length may provide us a clue that there may be several windows yielding less than or equal to two IMFs. So, the effect of increase in window length with respect to the percentage of window containing single or double or multiple no. of IMF is further studied for the same three types of ECG beats and shown in Fig. 3.6. It is clear from this figure that, for class N, window length 30 can ensure the absence of any window with single IMF and window length 50 can ensure at least three IMFs for all the windows. Again, for class L, window length 60 can ensure that there is no window with single IMF and the window length 70 guarantees that all the windows contain more than two IMFs. But for ECG class PB, window length 80 can ensure that there is no window with single IMF, but it becomes difficult to find any proper window length that could guarantee at least three IMFs at each window of the ECG beat.

In our method, for a particular beat of size N, among $(N - W + 1)$ segments, at each segment while sliding the window over the whole beat, window length $W = 30$ is primarily selected on which EMD decomposition is applied for calculating the IMFs. Then, we keep on increasing the window length until at least three IMFs are found and the corresponding window length is taken as the optimum for that particular segment. Thus, for the next segment of the sliding window, starting from the initial window length of $W = 30$, the similar window length increasing process is continued until the condition of obtaining three IMFs is satisfied for the segment. In each segment of the whole beat, such a window length selection process, which is adaptive to the condition of extracting three IMFs is effective for obtaining the slope required for determining the Hurst exponent as well as the LFD feature vector. Even after choosing adaptive window, if in any segment, less than three IMFs are found, LFD is set to zero for that segment.

3.3.4 Classification

In the proposed method, for the purpose of ECG arrhythmia classification using the extracted LFD feature vector, a distance based similarity measure is used. The

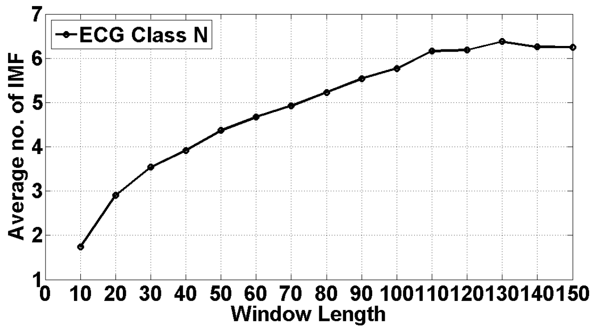

(a) Class N

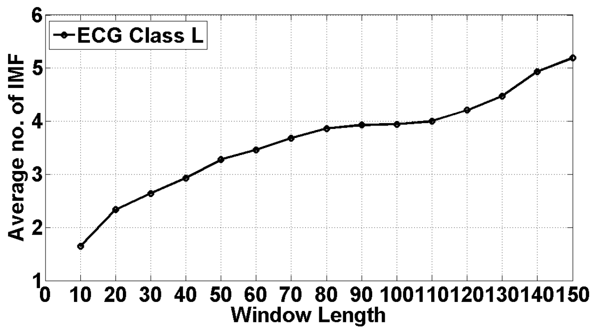

(b) Class L

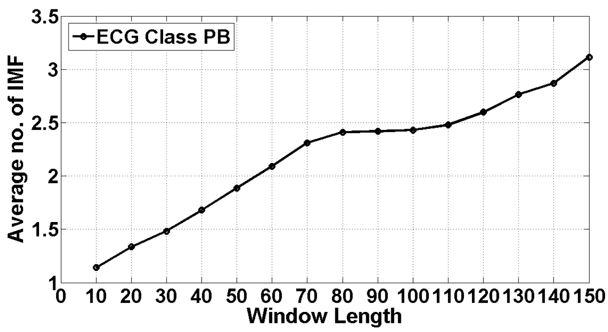

(c) Class PB

Fig. 3.5: Average no. of IMF per window with the increase in window length for a) class N, b) class L and c) class PB ECG arrhythmia.

classification task is carried out based on the Euclidean distances between the feature vectors of the training ECG and the feature vectors of the testing ECG. Given the N-dimensional feature vector for the f-th training ECG belonging to class z arrhythmia be $\{\alpha_{zf}(1), \alpha_{zf}(2), ..., \alpha_{zf}(N)\}$ and a v-th test ECG with a feature vector $\{\beta_v(1), \beta_v(2), ..., \beta_v(N)\}$, Euclidean distance is measured between the test ECG v and the training ECG f belonging to class z as

$$ED_{zf}^{v} = \sqrt{\sum_{l=1}^{N} |\alpha_{zf}(i) - \beta_v(i)|^2}. \tag{3.20}$$

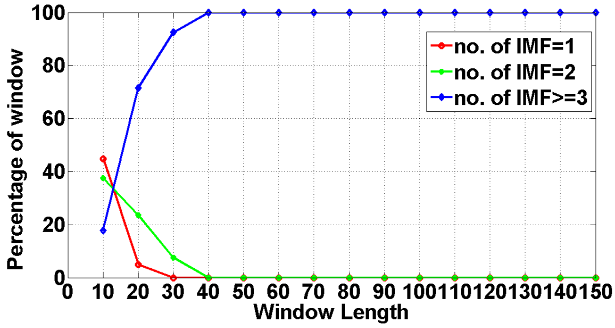

(a) Class N

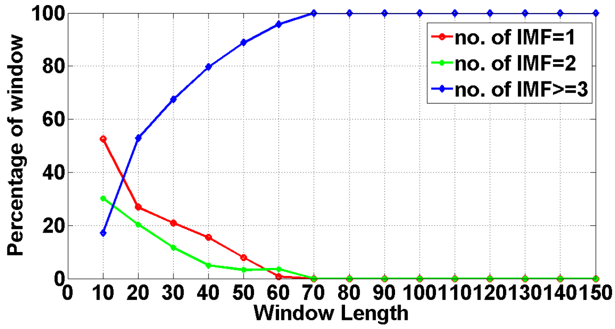

(b) Class L

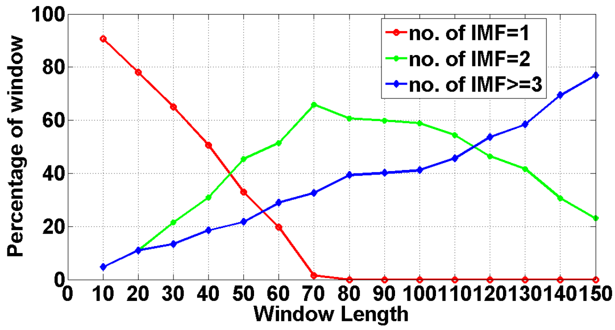

(c) Class PB

Fig. 3.6: Percentage of window involving single or double or multiple IMFs with respect to varying window length for a) class N b) class L and c) class PB ECG arrhythmia.

Considering total u training ECG beats belonging to class z arrhythmia, minimum Euclidean distance is obtained from

$$ED_z^v = \min_{f=1}^{u} ED_{zf}^v. \tag{3.21}$$

Therefore, test ECG beat will be classified as z class arrhythmia among P number of classes if it satisfies the condition

$$ED_z^v < ED_g, \forall z \neq g, and, \forall g \in 1, 2, .., P. \tag{3.22}$$

In this thesis, we are interested to handle a six-class problem ($P = 6$), i.e. to discriminate among six classes from the mixture of normal ECG and five classes of arrhythmia as mentioned before.

3.4 Conclusion

The Electrocardiogram (ECG) is the most important bio-signal which is analyzed for the diagnosis of any heart-related diseases. The term arrhythmia suggests abnormalities in the heart rate, although it is commonly used to refer to changes in the shape of the heart wave which is reflected in ECG. Since conventional time or frequency domain analysis is found inadequate to describe the characteristics of a non-stationary signal, such as ECG, in this chapter, we propose to transform the ECG data by empirical mode decomposition in order to facilitate the transfer domain analysis by sliding a window of optimal length. The transformed data thus obtained is exploited to formulate a feature vector consisting of local fractal dimension (LFD) that can better model detail characteristics of the ECG data. The feature vector is fed to Euclidean distance classifier in order to classify ECG arrhythmia of five different types along with normal ECG. A number of simulations are carried out using selected number of ECG beats from records of the MIT-BIH (Massachusetts Institute of Technology - Boston's Beth Israel Hospital) arrhythmia database. It is shown that the proposed method based on LFD estimation in EMD domain is capable of producing greater accuracy in comparison to that obtained by using a state-of-the-art method of ECG arrhythmia classification using the same classifier and ECG beats.

Chapter 4

A Wavelet Packet Based Fractal Dimension Feature for ECG Arrhythmia Classification

4.1 Introduction

In the EMD based LFD estimation method, for better approximation of LFD at each sample point, at least three IMFs are to be determined, which is dependent on the length of the segment of an ECG signal used for EMD operation. For some types of ECG arrhythmia, it is difficult to optimize the segment length in order to ensure the extraction of at least three IMFs. This problem can be overcome by analyzing the ECG signal in time-frequency domain via Wavelet Packet Decomposition (WPD). In this chapter, time-frequency analysis of ECG signal in WPD domain is performed for calculating the HE as well as deriving a set of more effective LFD features. Features extracted from these WPD coefficients can efficiently represent the characteristics of the original ECG signal in different details, because in WPD the wavelet space is also decomposed along with the scale space decomposition thus making the higher frequency band decomposition possible [53]. We have used state-of-the-art methods PSDFE and VFE for comparison of ECG arrhythmia classification performance with the proposed method based on LFD estimation in WPD domain in terms of different performance evaluation criteria.

4.2 Proposed Method

Wavelet transform is popular because it satisfies energy conservation law and original signal can be reconstructed [54]. In this section discrete wavelet transform, wavelet packet transform, selection of mother wavelet and rationale behind selection of detail coefficients are described separately.

4.2.1 Wavelet Transform

Discrete wavelet Transform (DWT) is a multi-resolution transform with a very fast implementation. DWT is a lost less linear transformation of a signal or data into coefficients on a basis of mother wavelet functions [16, 17]. A family of mother wavelet is available having the energy spectrum concentrated around the low frequencies like the ECG signal as well as better resembling the QRS complex of the ECG signal [55]. Therefore, for the analysis of an ECG signal $x[n]$ at different scales, wavelet transform (DWT) is used in practice. A general equation for the DWT transformed signal is written as [56]

$$Z(a,b) = \sum_{n=-\infty}^{\infty} x[n]\phi_{a,b}[n], \tag{4.1}$$

where, $x[n]$ is the given ECG signal to be transformed and

$$\phi_{a,b}[n] = \frac{1}{\sqrt{2}}) \times \phi[\frac{n-b}{a}]. \tag{4.2}$$

In DWT, the function represents a window of finite length, where b is a real number known as window translation parameter and a is a positive real number named as dilation or contraction parameter.

In discrete wavelet transform (DWT), for analyzing both the low and high frequency components in $x[n]$, it is passed through a series of low-pass and high-pass filters with different cut-off frequencies. This process results in a set of approximate and detail DWT coefficients, respectively. The filtering operations in DWT result in a change in the signal resolution [57]. Thus, DWT decomposes the signal into approximate and detail information thereby helping in analyzing it at different frequency bands with different resolutions. In wavelet analysis, only scale space is decomposed, but wavelet space is not decomposed. This results in a logarithmic frequency resolution, which does not work well for all the signals. By the restriction of Heisenberg's uncertainty principle, the spatial resolution and spectral resolution of high frequency band become poor thus limiting the application of wavelet transform.

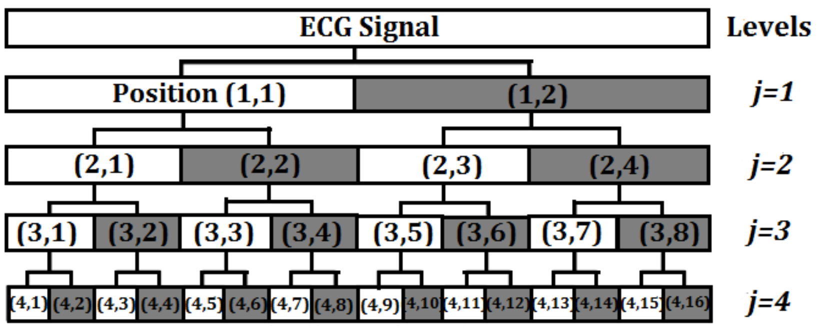

Fig. 4.1: Wavelet packet decomposition.

4.2.2 Wavelet Packet Transform

In order to overcome the drawback as mentioned above, it is desirable to iterate the high pass wavelet branch as well as the low pass scaling function branch. Such a wavelet decomposition produced by these arbitrary subband trees is known as wavelet packet (WP) decomposition. A method based on the Wavelet Packet Transform is a generalization of the Wavelet Transform based decomposition process that offers a richer range of probabilities for the analysis of signals, namely ECG.

In wavelet packet analysis, the wavelet space is also decomposed thus making the higher frequency band decomposition possible. Since, both the approximation and the detail coefficients are decomposed into two parts at each level of decomposition, a complete binary tree with superior frequency localization can be achieved as shown in Fig. 4.1, where detail coefficients are shadowed. Thus the wavelet packet transform provides a closer approximation of the dataset, compared to the wavelet transform. Features extracted from these wavelet packet decomposition (WPD) coefficients can efficiently represent the characteristics of the original ECG signal in different details. Therefore, recently WPD has drawn attention of the researchers in ECG pattern recognition [40].

4.2.3 Selection of Mother Wavelet

The selection of the mother wavelet is an important task in the WPD procedure. But, there is no universal rule that is suggested to select a particular mother wavelet. The choice of the mother wavelet depends upon the characteristics of the signal to be analyzed. The mother wavelet having similarity or resemblance to the signal being analyzed is usually chosen [58]. There are several wavelet families, namely

Harr, Daubechies, Biorthogonal, Coiflets, Symlets, Morlet, Mexican Hat, Meyer etc. and several other real and complex wavelets. In Fig. 4.2, plots representing the shapes of some mother wavelets are shown. An ECG beat is superimposed on each plot in Fig. 4.2 in order to compare it with the mother wavelet. It is seen from this figure that Daubechies (db6) and Symlets (sym11) provide better resemblance to the ECG beat. Detail analysis demonstrates that since, for the sym11 wavelet, energy spectrum is mainly concentrated around low frequencies as that in ECG, it is chosen for extracting features in the proposed method of ECG arrhythmia classification [58].

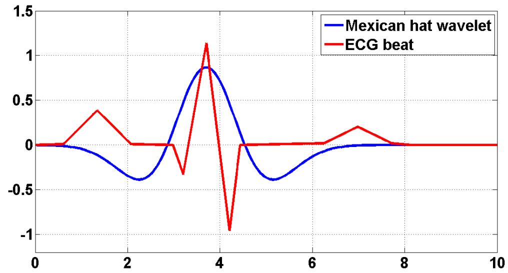

(a) Mexican hat wavelet

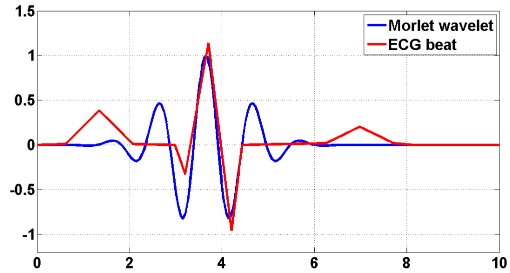

(b) Morlet wavelet

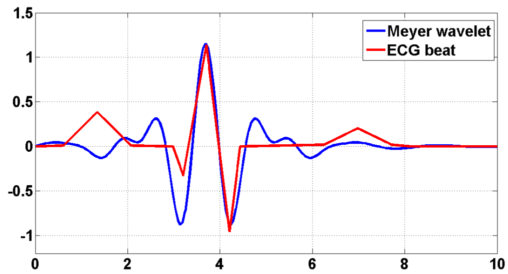

(c) Meyer wavelet

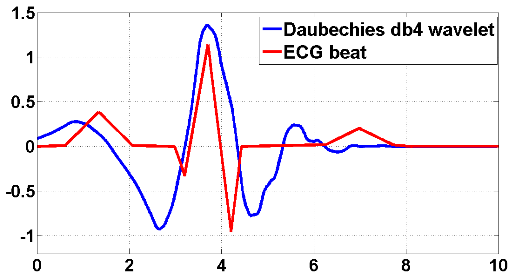

(d) Daubechies (db4) wavelet

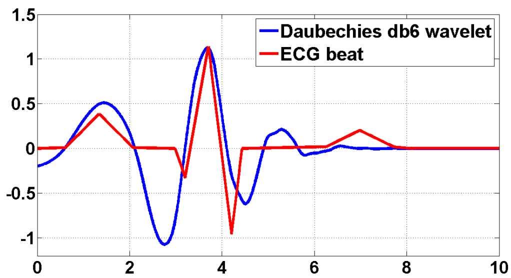

(e) Daubechies (db6) wavelet

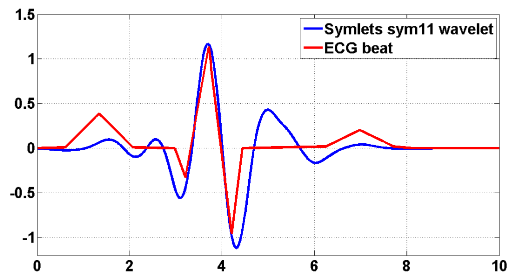

(f) Symlets (sym11) wavelet

Fig. 4.2: Different mother wavelets along with ECG beat: a) Mexican hat wavelet b) Morlet wavelet c) Meyer wavelet d) Daubechies (db4) wavelet e) Daubechies (db6) wavelet and f) Symlets (sym11) wavelet.

4.2.4 Rationale behind Selection of Detail Coefficients

In DWT of fractal Brownian motion, it is shown that details coefficients are stationary compared to the approximation coefficients [59]. The same conclusion can be drawn directly for WPD, since the WPD technique is the natural extension of the DWT. Consequently detail coefficients are chosen for extracting feature in this study. For each class of arrhythmia, detail and approximate coefficients of five different ECG beats are obtained and shown in plots of Fig. 4.3. From these plots, it is clear that detail coefficients remain almost same for a particular class of arrhythmia, whereas approximate coefficients vary within a class. It is also noticeable from this figure that baseline is always same for detail coefficients but is shifted for approximate coefficients. Even if the original test ECG with a particular arrhythmia may contain baseline wandering or shifting as an artifact, the corresponding detail coefficients is independent of the baseline wandering. Thus the removal of baseline wandering prior to feature extraction is no longer needed.

In Fig. 4.4, a bar graph plotting mean value of detail coefficients with their SD in error-bar considering five beats of each class of arrhythmia is shown. It is vivid from this figure that the mean value of detail coefficients is different from class to class. Since the SD against the mean value of detail coefficients does not overlap among the classes, it is obvious that detail coefficients are capable of providing separability among all classes of ECG arrhythmia. On the other hand, In Fig. 4.5, a bar graph plotting mean value of approximate coefficients with their SD in error-bar considering five beats of each class of arrhythmia is shown. It is found from this figure that the SD against the mean value of approximate coefficients shows overlapping regions among the classes. Thus, the approximate coefficients cannot provide separability among different classes of ECG arrhythmias. That is why, detail WPD coefficients are considered to form the feature vector for ECG arrhythmia classification.

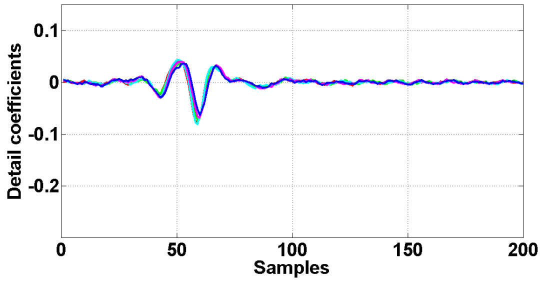

(a) Class N (detail)

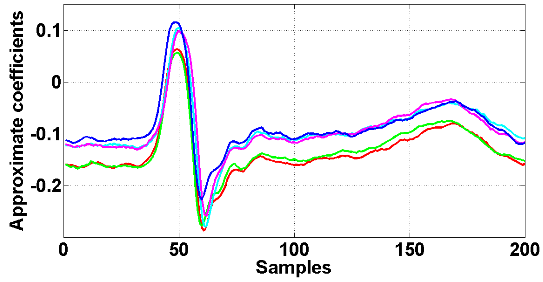

(b) Class N (approximate)

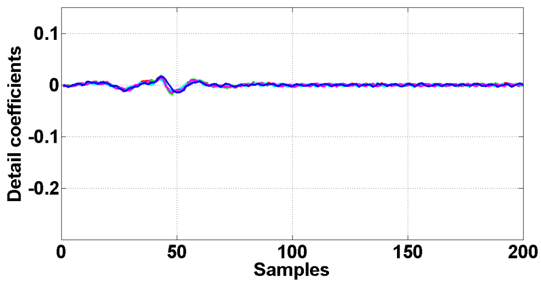

(c) Class L (detail)

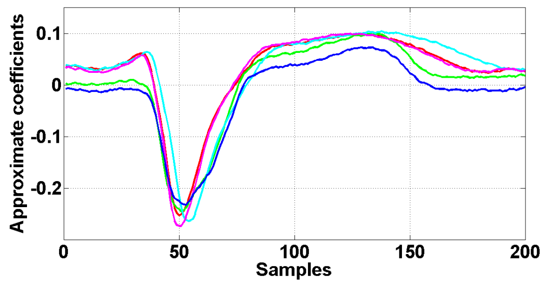

(d) Class L (approximate)

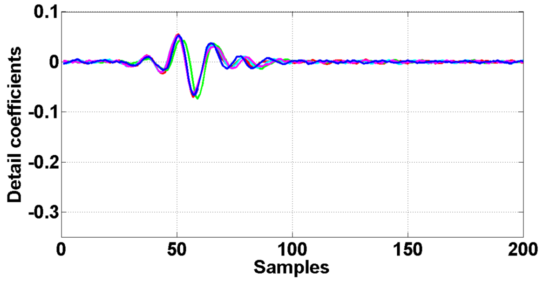

(e) Class R (detail)

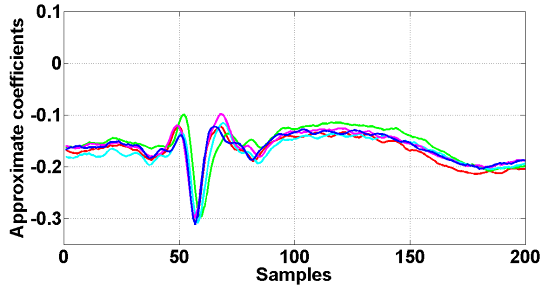

(f) Class R (approximate)

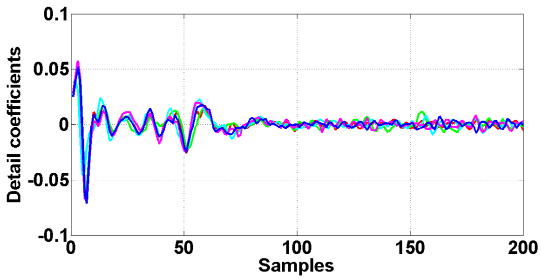

(g) Class PB (detail)

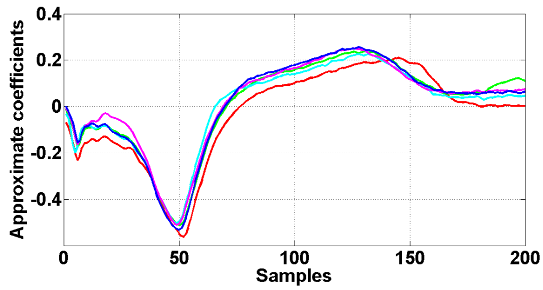

(h) Class PB (approximate)

4.2.5 Computation of Fractal Dimension Feature and Classification

For a j level WPD, the ECG signal $x[n]$ with frame length L is decomposed into 2^j subbands. The l-th WPD coefficients of the r-th subband is expressed as

$$c_{j,r}[l] = WPD[x[n], j], n = 1, 2, 3, ..., L, \tag{4.3}$$

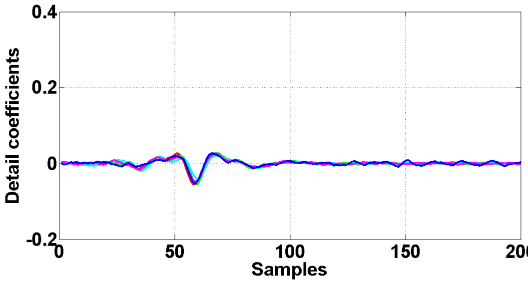

(i) Class V (detail)

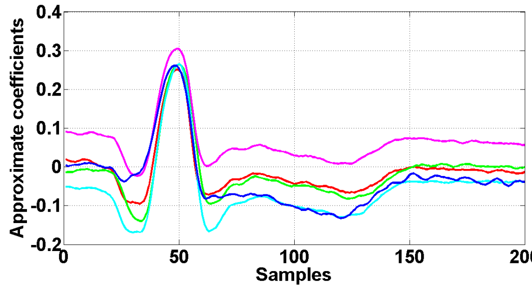

(j) Class V (approximate)

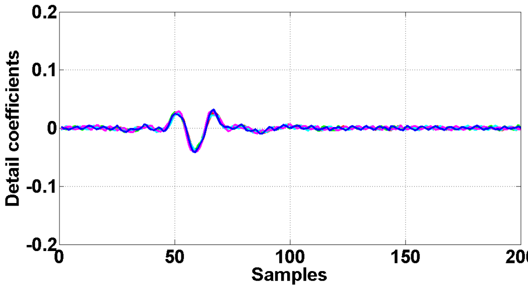

(k) Class A (detail)

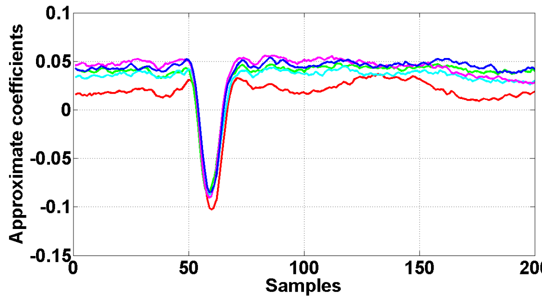

(l) Class A (approximate)

Fig. 4.3: Detail and approximate coefficients of different classes of arrhythmias a) class N (detail), b)class N (approximate) c) class L (detail) d) class L (approximate) e) class R (detail) f) class R (approximate) g) class PB (detail) h) class PB (approximate) i) class V (detail) j) class V (approximate) k) class A (detail) l) class A (approximate).

where, $l = 1, 2, ..., L/2^j$ and $r = 1, 2, ..., 2^j$.

From Fig. 4.1, it is seen that at each level j, there are 2^{j-1} shadowed regions containing detail coefficients $c_{j,q}$ where $q = 2, 4, ..., 2^j$ is the position of subband containing detail coefficients at level j. We determine the normalized energy from all the detail coefficients at each level j by the following formula

$$E_{j,q} = \frac{1}{L/2^j} \sum_{l=1}^{L/2^j} c_{j,q}[l]^2. \tag{4.4}$$

Then, for each level j, the average normalized energy over all subbands containing detail coefficients is calculated as

$$E_j = \frac{1}{2^{j-1}} \sum_{q=1}^{2^{j-1}} E_{j,q}. \tag{4.5}$$

The average normalized energy E_j is related to the corresponding level j by the Hurst exponent H. The relationship follows a power law expressed as [9]

$$E_j \sim 2^{2jH}. \tag{4.6}$$

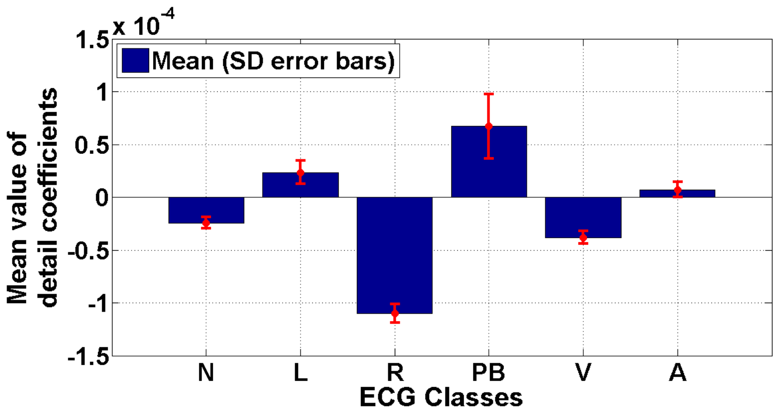

Fig. 4.4: Mean value of detail coefficients with SD in errorbars for different ECG arrhythmias.

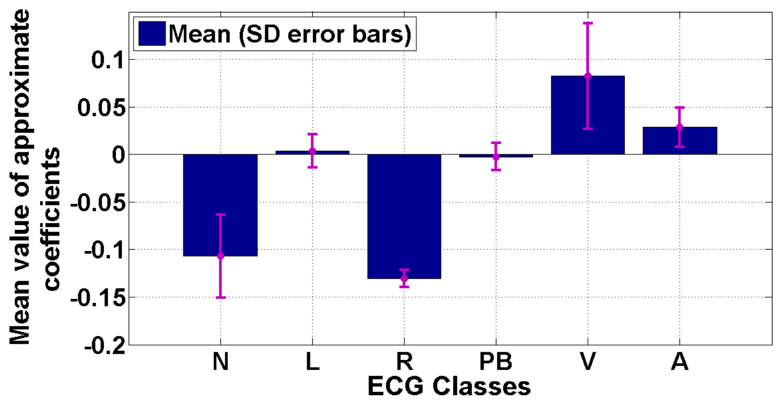

Fig. 4.5: Mean value of approximate coefficients with SD in errorbars for different ECG arrhythmias.

Taking logarithm on both sides of Eq. (4.6), we get

$$\log_2(E_j) \sim 2jH. \tag{4.7}$$

By plotting the curve with $\log_2(E_j)$ as y-axis and level j as x-axis results in a line. By fitting the line utilizing the least square method, the slope s corresponding to the line is obtained. From Eq. (4.7), it is clear that the slope s of the line is related to the Hurst Exponent H as

$$s = 2H. \tag{4.8}$$

From Eq. (4.8), H can be calculated as

$$H = \frac{s}{2}. \tag{4.9}$$

Denoting E as the Euclidean dimension [10], the fractal dimension D can be calculated from the Hurst exponent

$$D = E + 1 - H. \tag{4.10}$$

Since for ECG signal $E = 1$, a simplified form of fractal dimension D in Eq. (4.10) can be written as

$$D = 2 - H. \tag{4.11}$$

In a particular arrhythmia condition, morphological changes occur in different sections of a normal ECG beat and such changes vary from beat to beat under the same arrhythmia. Thus instead of taking a global fractal dimension of the whole beat, local fractal dimension (LFD) of neighboring sample points of segments within an ECG beat can capture detail information of the arrhythmia. Since LFD facilitates more accurate characterization of the ECG arrhythmia, LFD is preferred in the proposed work.

For this proposed method, in order to classify ECG arrhythmia using the extracted LFD feature vector, the same Euclidean distance classifier as described in chapter 3 is used.

4.3 Conclusion

The Electrocardiogram (ECG) is the most important bio-signal which is analyzed for the diagnosis of any heart-related diseases. The term arrhythmia suggests abnormalities in the heart rate, although it is commonly used to refer to changes in the shape of the heart wave which is reflected in ECG. Since conventional time or frequency domain analysis is found inadequate to describe the characteristics of a non-stationary signal, such as ECG, in this chapter, we propose to transform the ECG data by wavelet packet decomposition in order to facilitate the time-frequency analysis by sliding a window of optimal length. The transformed data thus obtained is exploited to formulate a feature vector consisting of local fractal dimension (LFD) that can better model detail characteristics of the ECG data. The feature vector is fed to Euclidean distance classifier in order to classify ECG arrhythmia of five different types along with normal ECG. A number of simulations are carried out using selected number of ECG beats from records of the MIT-BIH (Massachusetts Institute of Technology - Boston's Beth Israel Hospital) arrhythmia database. It is shown that the proposed method based on LFD estimation in WPD domain is capable of producing greater accuracy in comparison to that obtained by using a state-of-the-art method of ECG arrhythmia classification using the same classifier and ECG beats.

Chapter 5

An Approach for ECG Arrhythmia Classification Based on Energy and Entropy of the 4th Level Detail Wavelet Packet Coefficients

5.1 Introduction

Modern era of medical science is supported by computer aided feature extraction and disease diagnostics in which various signal processing techniques have been utilized in extracting features from the biomedical signals and analyzes these features. The objective of computer aided digital signal processing of ECG signal is to reduce the time taken by the cardiologists in interpreting the results. Considering the complexity and ease of implementation as an important criterion, a feature set based on energy and entropy of only the 4th level detail WPD coefficients is found to be simple yet the highest capable of solving a multi-class ECG arrhythmia problem. Based on the detail analysis in terms of energy, frequency and cross-correlation, it is found that instead of considering all the detail WPD coefficients, only the 4th level detail WPD coefficients are enough for extracting features containing detail information of different arrhythmia which are capable of classifying ECG arrhythmia [60]. We have used state-of-the-art methods PSDFE and VFE for comparison of ECG arrhythmia classification performance with the proposed method based on energy and entropy of detail WPD coefficients in terms of different performance evaluation criteria.

5.2 Proposed Method

5.2.1 Rationale behind Taking 4th Level Detail WPD Coefficients

Wavelet packet transform is chosen rather than wavelet transform for extracting features from ECG beat in this chapter. The reason behind the choice of WPD is discussed in chapter 4. Again between detail and approximate coefficients present at different levels, only detail coefficients are taken for the proposed method. The rationale for taking only detail coefficients is described in chapter 4. For a four level WP decomposition, among the detail coefficients at different levels, sum of all the detail coefficients at the 4th level has been chosen for extracting the feature in ECG arrhythmia classification. The choice of the 4th level detail coefficients is based on the following analysis of energy, frequency and cross-correlation.

Energy Analysis

The normalized energy of an ECG signal $x[n]$ of length N is determined as

$$E = \frac{1}{N}\sum_{n=1}^{N} x^2[n]. \tag{5.1}$$

In comparison to the normalized energy of ECG signal, normalized energy of sum of detail WPD coefficients at a particular level j expressed as $E_{C_{jd}}$ can be found more suitable for extracting distinguishable feature of different classes of ECG arrhythmia, where C_{jd} represents the sum of detail WPD coefficients at any level j.
The normalized energy $E_{C_{jd}}$ for classes N, R and A is shown in Figs. 5.1(a) - 5.1(c), respectively. For each class, six ECG beats are considered while plotting Figs. 5.1(a) - 5.1(c) for six levels of WPD. It is seen from Fig. 5.1 that for each beat of all classes of arrhythmia, the normalized energy of the sum of detail WPD coefficients at the 4th level $E_{C_{4d}}$ is the highest among that of the detail WPD coefficients at the other levels. Since, the 4th level detail WPD coefficients carry the dominant information of ECG signal in terms of normalized energy, it is reasonable to consider the 4th level detail WPD coefficients for feature extraction.

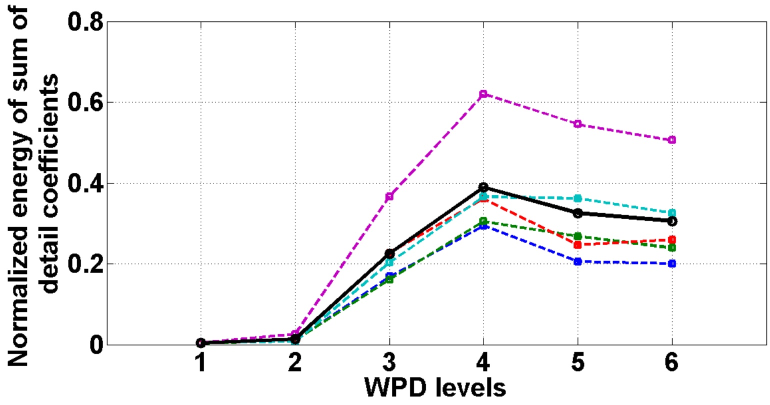

(a) Class N

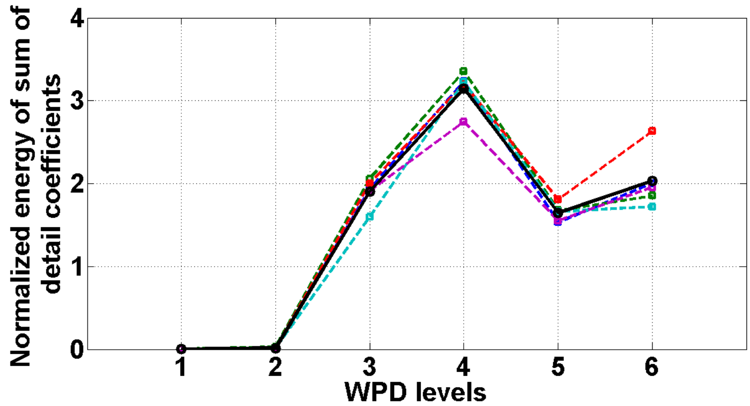

(b) Class R

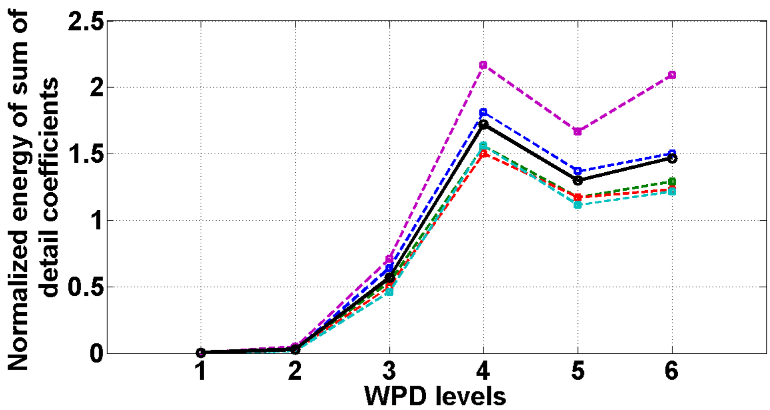

(c) Class A

Fig. 5.1: Normalized energy of sum of detail coefficients at different levels of WPD for a) Class N b) Class R and c) Class A.

Frequency Analysis

The DFT of an ECG signal $x[n]$ can be expressed as

$$X[k] = \sum_{n=0}^{N-1} x[n]e^{-j2\pi nk/N}, 0 \leq k \leq (N-1), \tag{5.2}$$

where, $X[k]$ represents the DFT coefficients. An efficient computation of $X[k]$ is performed via Fast Fourier Transform (FFT). It is known that the bandwidth of an ECG beat ranges from 0.67-40 Hz [61]. The FFT plot of an ECG signal along with the FFT plots of sum of detail WPD coefficients at each level C_{jd} are shown in Fig. 5.2 for N type ECG signal. Among the six levels considered for plotting Fig. 5.2, it is clear that the bandwidth of FFT of the 4th level detail WPD coefficients and that of the ECG signal lie approximately in the same range, such as 7-38 Hz and 1-35 Hz, respectively. Since, the available dominant frequency components in ECG and that in the sum of the 4th level detail WPD coefficients C_{4d} are comparable, the 4th level detail WPD coefficients are found appropriate in extracting distinctive features for classifying different types of ECG arrhythmia.

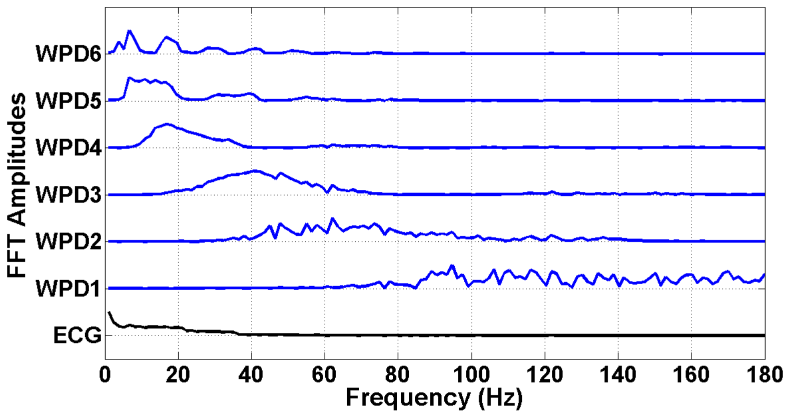

Fig. 5.2: Frequency contents of ECG signal and that of sum of detail WPD coefficients at different levels for N type ECG signal.

Cross-correlation Analysis

Cross-correlation coefficient between ECG signal $x[n]$ and the sum of detail WPD coefficients at any level j (C_{jd}) can be expressed as

$$\rho = \frac{\sum_{n=1}^{N}(x[n]-\overline{x})(C_{jd}[n]-\overline{C_{jd}})}{\sqrt{\sum_{n=1}^{N}(x[n]-\overline{x})^2}\sqrt{\sum_{n=1}^{N}(C_{jd}[n]-\overline{C_{jd}})^2}}. \tag{5.3}$$

where, $\overline{x}$ and $\overline{C_{jd}}$ represent the mean of ECG beat and that of C_{jd}. Cross-correlation analysis in terms cross-correlation coefficient between the ECG signal $x[n]$ and C_{jd} for classes N, R and A are summarized in Table 5.1 for six levels of WPD. For each class, six beats are considered for calculating ρ and the average value is shown in Table 5.1. It is observable from Table 5.1 that the average ρ is the highest for the

WPD coefficients at the 4th level for each class of arrhythmia. Since, the WPD coefficients at the 4th level are highly correlated with the ECG signal, it is justified to use the 4th level WPD coefficients for feature extraction in the task of classifying different ECG arrhythmia.

Table 5.1: Average value of cross-correlation coefficients

WPD	Cross-correlation coefficient		
levels	Class N	Class R	Class A
1	0.0710	0.0244	0.0331
2	0.1313	0.0544	0.0964
3	0.5514	0.6250	0.4453
4	**0.7283**	**0.8046**	**0.7761**
5	0.6692	0.5904	0.6828
6	0.6678	0.6892	0.7489

5.2.2 Feature Extraction and Classification

Conventionally, energy defined in Eq. (5.1) can be estimated from an ECG beat using a fixed length window sliding over the whole beat. So, the sliding window of size W converts the N-point ECG beat into $(N - W + 1)$ segments. For each segment, we propose to estimate the energy of sum of the 4th level detail WPD coefficients (C_{4d}) as

$$E_{C_{4d}} = \sum_{l=1}^{W} C_{4d}^2[l], \tag{5.4}$$

thus resulting in a time series of energy of size $(N - W + 1)$. Entropy is first introduced in physics to describe the system disorganization, which is later adopted in signal processing for the same purpose. The definition of entropy in signal processing is based on the hypothesis that noise is totally disorganized thus carrying the highest entropy. For each segment, entropy of sum of the 4th level detail WPD coefficients (C_{4d}) can be computed as

$$Entropy_{C_{4d}} = -\sum_{l=1}^{W} [p(C_{4d}[l]) \log_2 p(C_{4d}[l])], \tag{5.5}$$

thus obtaining a time series of entropy of size $(N - W + 1)$. In Eq. (5.5), p represents the probability distribution function. The proposed feature vector is formed by incorporating both the energy and entropy of the 4th level detail WPD coefficients.

In this proposed method, for the purpose of classification task among different ECG arrhythmia using the energy and entropy based feature vectors, the same Euclidean distance classifier as described in chapter 3 is utilized herein.

5.3 Conclusion

The Electrocardiogram (ECG) is the most important bio-signal which is analyzed for the diagnosis of any heart-related diseases. The term arrhythmia suggests abnormalities in the heart rate, although it is commonly used to refer to changes in the shape of the heart wave which is reflected in ECG. Since conventional time or frequency domain analysis is found inadequate to describe the characteristics of a non-stationary signal, such as ECG, in this chapter, we propose to transform the ECG data by wavelet packet decomposition (WPD) in order to facilitate the time-frequency analysis by sliding a window of optimal length. The transformed data thus obtained is exploited to formulate a feature vector consisting of energy and entropy of only the 4th level WPD detail coefficients that can better model detail characteristics of the ECG data. The feature vector is fed to Euclidean distance classifier in order to classify ECG arrhythmia of five different types along with normal ECG. A number of simulations are carried out using selected number of ECG beats from records of the MIT-BIH (Massachusetts Institute of Technology - Boston's Beth Israel Hospital) arrhythmia database. It is shown that the proposed method based on energy and entropy of detail WPD coefficients is capable of producing greater accuracy in comparison to that obtained by using a state-of-the-art method of ECG arrhythmia classification using the same classifier and ECG beats.

Chapter 6

Simulation Results and Performance Evaluation

6.1 Introduction

Performance evaluation of the proposed methods for classifying five types of ECG arrhythmia plus normal ECG is an important task. For this purpose the evaluation criteria taken into account in this chapter are clustering analysis, confusion matrix, receiver operating characteristics (ROC) curves, reduction of training dataset and representation of error-bar graph. The popular MIT-BIH arrhythmia database is used for extracting ECG beats of different arrhythmia for simulation. State-of-the-art methods PSDFE and VFE are used for performance comparison with the proposed methods.

6.2 Simulation Results

6.2.1 Database

In the proposed method, we have employed MIT-BIH (Massachusetts Institute of Technology-Boston's Beth Israel Hospital) arrhythmia database [62]. The ECG recordings are sampled at 360 samples per second per channel with 11-bit resolution over a 10 mV range. But normal beats are frequently difficult to discern in the lower signal of each ECG record, on the other hand, normal QRS complexes are usually prominent in the upper signal. Thus the ECG records of upper signal namely modified limb lead II (MLII) are used in this work, from which the heartbeat waveform is extracted by taking 50 samples before the R peak and 150 samples after the R peak thus forming 201 samples of ECG beat. From the database, we have considered normal ECG beats (N) and that belonging to five types of arrhythmia, namely left bundle branch block beat (L), right bundle branch block beat (R), atrial premature beat (A), premature ventricular contraction (V), and paced beat (PB). In Table 6.1, the number of the ECG file that is used from the MIT-BIH database and the number of QRS complexes taken from each type of class including normal and arrhythmia are shown. It is seen from this table that we have employed ECG signals from 22 patients. For each class, 32 beats are considered resulting in a total 192 ECG beats. Out of these ECG beats, approximately 38% are selected for training and the remaining is left for testing or validating the classifiers.

Table 6.1: The MIT-BIH database file number and the number of QRS complexes used in this study

Type	MIT-BIH file number	No. of QRS complexes taken	No. of QRS complexes left for validation
N	100,112,122,123	32	20
L	109,111,207,214	32	20
R	118,124,212,231	32	20
PB	102,104,107,217	32	20
V	119,221,200,233	32	20
A	207,209	32	20

6.2.2 Simulation Conditions

It is not required to normalize the ECG beats in the proposed methods based on LFD estimation since, linear change on ECG signal due to base line shift or amplification or attenuation do not change the LFD of the ECG signal. For the proposed method based on LFD estimation in EMD domain as described in chapter 3, LFD is calculated at each sample of an ECG beat considering the fractal information of neighboring samples. A window of size W is taken around each sample of an ECG beat. Sliding such a window of size W converts the 201 samples of ECG beat into $(201 - W + 1)$ segments and LFD is computed for each segment using Eq. (3.13) to Eq. (3.19) thus yielding a time series of LFD of size $(201 - W + 1)$.

For the proposed method based on LFD estimation in WPD domain as discussed in chapter 4, LFD is computed for each segment using Eq. (4.4) to Eq. (4.11) thus yielding a time series of LFD of size $(201 - W + 1)$.

For the finally proposed method based on energy and entropy of detail WPD coefficients as derived in chapter 5, features are extracted at each sample of an ECG beat considering the neighboring samples utilizing a sliding window of optimal length. A window of size W is taken around each sample of an ECG beat. Sliding such a window of size W converts the 201 samples of ECG beat into $(201 - W + 1)$ segments and energy and entropy is computed from sum of WPD detail coefficients at 4-th level using Eq. (5.4) and Eq. (5.5) thus yielding a feature vector of size $2(201 - W + 1)$.

For feature extraction methods via WPD domain, the selection of mother wavelet is an important task as performance of the proposed method varies with the change of mother wavelets. However, we have selected Symlets (sym11) for WPD procedure since apart from showing close resemblance to the QRS complex, sym11 provides better performance in ECG arrhythmia classification compared to that of other mother wavelets when applied to the proposed method.

On extracting the the proposed feature set and using the set in classifying different ECG arrhythmia based on Euclidean distance based classifier, performance is evaluated through 50 iterations by random selection of training and testing data sets of signals at each step of iteration. At each iteration, from 192 beats, we have randomly selected 72 ECG beats as the training dataset consisting of equal number of beats for each class of arrhythmia and the rest 120 beats are employed for validation purpose at the testing phase. Finally, average classification performance over all iterations is considered for detail analysis and comparison.

6.2.3 Performance Evaluation Criteria

For the performance evaluation of the proposed methods, criteria considered in our simulation study are: 1) Clustering analysis 2) Confusion matrix 3) Receiver operating characteristics (ROC) curves 4) Reduced training dataset 5) Error-bar calculation. For the purpose of comparison, we use state-of-the-art methods PSDFE and VFE [6]. We have implemented the PSDFE and VFE methods independently using the parameters specified therein on the basis of the criteria described as follows

Clustering Analysis

The effectiveness of the proposed feature sets in classifying different types of ECG arrhythmia in terms of clusters is justified by the inter-class separability and intra-class compactness of the feature. Among different statistical measures, we employ Geometrical Separability Index (GSI) and Bhattacharya distance (BD) to quantitatively show the cluster-to-cluster distance and cluster dispersion in case of different classes of ECG arrhythmia.

Geometrical Separability Index (GSI) Assuming a nearest neighbor type classifier, GSI is a measure that gives an idea about the degree to which two classes are separable in the nearest neighbor sense [63]. For two data clusters formed from two classes of feature vectors each consisting of Q number of data, GSI is given by

$$GSI = \frac{\sum_{i=1}^{Q}[(G(y_i) + G(y_{iNeighbor}) + 1)mod2]}{Q}, \tag{6.1}$$

here, y_i is one of the feature data and $y_{iNeighbor}$ is its nearest neighbor. Function G represents the binary decision classification giving the class number of the data in a feature vector. Q is the total number of data in a feature vector. If the GSI value approximates to zero, it indicates that two classes are inseparable, whereas as GSI approximates to 1, the two classes are declared as separable.

Bhattacharya distance (BD) For two Gaussian distributed data-clusters formed from two feature vectors, BD is a measure of separability, which is given by [64,65]

$$BD = \frac{1}{8}(E_1 - E_2)^T[\frac{V_1 + V_2}{2}]^{-1}(E_1 - E_2) + \frac{1}{2}\ln\frac{|\frac{V_1+V_2}{2}|}{\sqrt{|V_1||V_2|}}, \tag{6.2}$$

here, E_1 and E_2 are the mean vectors of clusters 1 and 2, respectively, whereas V_1 and V_2 are the covariance matrices of clusters 1 and 2, respectively.

For the two feature vectors, the first term in the expression of BD gives the class separability due to the mean difference between the vectors, while the second term gives the class separability due to the covariance-difference between them. Using a feature, the less the value of BD for a particular class, the more compact or inseparable the feature is for the same class.

		Classified by the classifier					
		N	L	R	PB	V	A
Actual Class	N	TP_N	FN_N				
	L						
	R						
	PB	FP_N	TN_N				
	V						
	A						

Fig. 6.1: Confusion matrix.

Confusion Matrix

For the performance evaluation of the proposed method, parameters considered in our simulation study are: 1) Sensitivity 2) Specificity 3) Accuracy.

All the parameters as mentioned above can be derived from the confusion matrix, which is a form of representing the result from a classification exercise. The rows in the matrix stand for the actual classes to be tested and columns provide the class classified by a method. In particular, any $[row, column]$ entry in the confusion matrix indicates the number of cases from the test database that belongs to the class corresponding to the *row* but classified as the class corresponding to the *column*. In Fig. 6.1, a general confusion matrix for a six class problem (N, L, R, PB, V, A) is shown, where TP, FP, FN and TN are represented for N class. In general,

TP_i, true positive for any class i, measures the number of testing cases, which are correctly classified as class i.

FP_i, false positive for any class i, denotes the number of testing cases, which are incorrectly classified as class i.

FN_i, false negative for any class i, indicates the number of testing cases, which are incorrectly classified as other than class i.

TN_i, true negative for any class i, means the number of testing cases, which are correctly classified as other than class i.

Sensitivity of a class relates the number of positive testing cases which are correctly classified to the number of testing cases of that particular class. Thus, sensitivity, for a particular class i, can be defined as

$$Sen_i = \frac{TP_i}{TP_i + FN_i}. \tag{6.3}$$

A classifier, which always indicates positive, regardless of the class of the testing case, provides 100% sensitivity for that class. Therefore the sensitivity alone cannot be used to determine the usefulness of the classifier in practice.

Specificity of a class relates the number of negative testing cases which are correctly classified to the total number of testing cases belonging to other classes rather than class i. Therefore, specificity for a particular class i, can be expressed as

$$Sp_i = \frac{TN_i}{TN_i + FP_i}. \tag{6.4}$$

Accuracy of a class relates the number of testing cases which are correctly classified to the number of total testing cases. Therefore, accuracy, for a particular class i, can be written as

$$Acc_i = \frac{TP_i + TN_i}{TP_i + TN_i + FP_i + FN_i}. \tag{6.5}$$

For the purpose of comparison, we use state-of-the-art methods in [6].

Receiver Operating Characteristics (ROC) Curves

The ROC curve, a plot of $(1-specificity)$ in x-axis and *sensitivity* in y-axis, is a way to measure the efficiency of a classification method in classifying a particular class. While testing any unknown class but comparing the test feature vector only with the feature vectors of a particular arrhythmia class z, a threshold Γ_z of Euclidean distance between training and testing feature vectors is considered. Considering total u training ECG beats belonging to class z arrhythmia, minimum Euclidean distance is obtained as

$$ED_z^v = \min_{f=1}^{u} \left\{ \sqrt{\sum_{l=1}^{N} |\alpha_{zf}(i) - \beta_v(i)|^2} \right\}, \tag{6.6}$$

where, $\{\alpha_{zf}(1), \alpha_{zf}(2), ..., \alpha_{zf}(N)\}$ represents N-dimensional feature vector for the f-th training ECG belonging to class z and $\{\beta_v(1), \beta_v(2), ..., \beta_v(N)\}$ symbolizes a feature vector for a v-th test ECG. Therefore, the test ECG beat will be classified as z class arrhythmia if it satisfies the condition

$$ED_z^v < \Gamma_z. \tag{6.7}$$

Thus for a particular class z with a set threshold Γ_z, the confusion matrix as discussed before can be formed to calculate sensitivity and specificity. This process is repeated by changing the value of Γ_z and the values of sensitivity and specificity corresponding to each Γ_z are exploited to get the ROC curve for class z. Increasing the threshold Γ_z for class z, decreases the probability of a test beat to be classified as another class thus improving sensitivity but increases the possibility of another class to be misclassified as class z thus reducing specificity. For other classes, the similar procedure is adopted to obtain the corresponding ROC curves. Since any increase in sensitivity is accompanied by a decrease in specificity, the ROC curve thus shows the tradeoff between sensitivity and specificity of a particular class. While comparing different methods, in classifying a particular class using different threshold values, the method that reaches the 100% sensitivity with a faster rate and steeper slope is more accurate.

Reduced Training Dataset

The performance of a classification method in classifying different ECG arrhythmia can be evaluated in terms of change in average sensitivity over all classes with the reduction in training dataset. For this purpose the reduction factor r_f can be defined as

$$r_f = \frac{no.\ of\ test\ QRS\ complexes}{no.\ of\ training\ QRS\ complexes}. \tag{6.8}$$

Thus, a curve with indices on X-axis representing the reduction factor r_f and the indices on Y-axis plotting the average sensitivity over six classes (normal and five classes of arrhythmia) is useful for comparing the performance of different methods using reduced training dataset. Over the range of reduction factors, the method providing less deviation in average sensitivity is the better one.

Error-bar Calculation

The performance of a classification method in terms of average sensitivity of a particular class depends on the selection of training and testing datasets used. If there are K number of iterations while randomly selecting training and testing datasets, the average value of sensitivity Sen_{avg} of a particular class over all iterations can be given by

$$Sen_{avg} = \frac{1}{K}\sum_{j=1}^{K} Sen_j, \tag{6.9}$$

where, Sen_j represents the sensitivity of a particular class at j-th random selection of training and testing dataset. Again, standard deviation of the sensitivity Sen_{SD} of that particular class resulting over all iterations is expressed as

$$Sen_{SD} = \sqrt{\frac{1}{K}\sum_{j=1}^{K}(Sen_j - Sen_{avg})^2}. \tag{6.10}$$

For a particular class, average sensitivity and standard deviation as calculated using Eqs. (6.9) and (6.10) can be employed for plotting an error-bar graph. This graph helps to realize that a feature is termed effective if it yields a performance that changes as little as possible with any random variation in training and testing datasets. Thus for any class, a method with higher Sen_{avg} and lower Sen_{SD} is desirable.

6.3 Performance Comparison using LFD Estimation Method in EMD Domain

This section presents the results of the proposed method based on LFD estimation in EMD domain. All ECG beats mentioned in Table 6.1 are processed for extracting LFD feature vectors using the PSDFE, VFE and the proposed method. With an optimized length $W = 30$ for each segment of the window sliding over an $N = 201$-point ECG beat, 172 LFDs are estimated from each of the $(N - W + 1) = 172$ segments. The performance of the three methods is compared on the basis of the following performance evaluation criteria as described before.

6.3.1 Clustering Analysis

Two statistical measures are utilized in order to show the clustering analysis, where inter-class separability and intra-class compactness of the proposed LFD feature extracted from the EMD domain are highlighted.

Thornton's separability index or geometric separability index (GSI) is a term that signifies the ability of a particular classification method in separating the clusters of any two classes as well as in reflecting the compactness between the clusters of the same class [63]. The higher GSI value indicates the more separability between two classes under consideration, whereas lower GSI value stands for declaring the two classes as the same class. In Table 6.2 the GSI index obtained using the

Table 6.2: The GSI index obtained using the proposed method of LFD estimation in EMD domain for each pair of arrhythmia classes

ECG Classes	N	L	R	PB	V	A
N	0	0.9975	0.9962	0.9973	0.9984	0.9946
L	0.9969	0	0.9962	0.9967	0.9964	0.9978
R	0.9952	0.9946	0	0.9956	0.9949	0.9960
PB	0.9969	0.9957	0.9960	0	0.9960	0.9975
V	0.9979	0.9954	0.9960	0.9964	0	0.9983
A	0.9963	0.9977	0.9977	0.9985	0.9984	0

proposed method of LFD estimation in EMD domain for each pair of arrhythmia classes is shown. It is seen from Table 6.2 that each diagonal entry representing the same class has a value zero, whereas each entry other than the diagonal representing two different classes has a value close to one. Such GSI values indicate that the proposed LFD feature extracted from the EMD domain is capable of providing high separability between any two different classes of arrhythmia as well as yielding high compactness for the same class.

Bhattacharya distance (BD) is another term that signifies the ability of a particular classification method in reflecting the intra-class compactness of clusters of the same class [64]. Among different methods, the method yielding lower BD value indicates more compactness of its feature employed in the inter-patient analysis. The average inter-patient BD obtained using PSDFE, VFE and the proposed method of LFD estimation in EMD domain for each class of arrhythmia is shown in Fig. 6.2. It is vivid from this figure that in comparison to the methods as mentioned above, the proposed method results in less average BD for each class of arrhythmia thus offering the intra-class compactness of the proposed LFD feature extracted from the EMD domain.

From the clustering analysis done in terms of GSI index and BD value, it is clear that the proposed feature extracted from LFD estimation in EMD domain is effective and superior in classifying different ECG arrhythmia compared to that employed in the other two state-of-the-art methods.

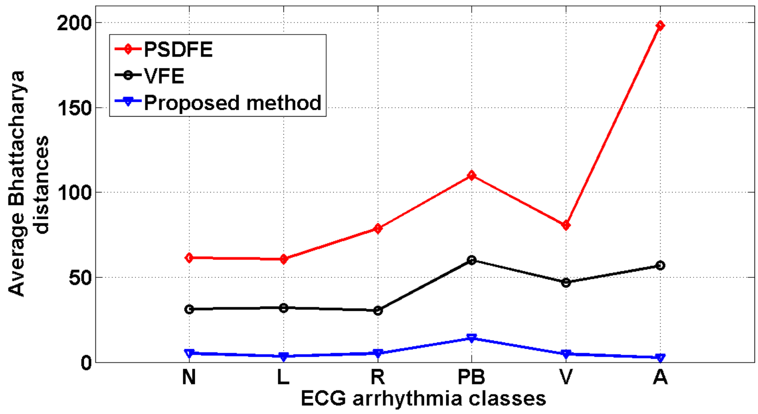

Fig. 6.2: Average inter-patient Bhattacharya distances obtained using PSDFE, VFE and the proposed method of LFD estimation in EMD domain for each class of arrhythmia.

6.3.2 Performance Comparison using Confusion Matrix

Among 50 iterations of random selection of training and testing datasets as mentioned in subsection 6.2.3, for each iteration, confusion matrix representing the test classes along with the classified classes is obtained and sensitivity, specificity and accuracy of each class are determined for the performance comparison.

Table 6.3, 6.4 and 6.5 represent the confusion matrices derived for PSDFE, VFE and the proposed method based on LFD estimation in EMD domain at a particular iteration. In each of these three tables, the diagonal entries stand for the number of cases when a particular class of ECG arrhythmia is correctly classified. From Table 6.3, it is found that while using PSDFE method, misclassification occurs for every classes of ECG arrhythmia except R class. On the other hand from the confusion matrix of VFE method in Table 6.4, it is seen that all the test beats for N, L and R classes are correctly classified, whereas, some of the PB, V and A beats are misclassified. Clearly it is obserbed from Table 6.5 that the proposed method based on LFD estimation in EMD domain is capable of reducing the misclassification cases in V and A classes while providing the similar correct classification rate for other classes of arrhythmia as found in the VFE method.

For the PSDFE, VFE and the proposed method, the average sensitivity, specificity and accuracy of all ECG arrhythmia classes are summarized in tables 6.6, 6.7 and 6.8 respectively. For all the methods, the sensitivity, specificity and accuracy found at each iteration are averaged over 50 iterations and shown in the tables as

Table 6.3: Confusion matrix for PSDFE method using Euclidean distance classifier

	N	L	R	PB	V	A
N	18	0	0	0	2	0
L	1	19	0	0	0	0
R	0	0	**20**	0	0	0
PB	0	2	0	18	0	0
V	0	3	0	1	16	0
A	1	0	0	0	2	17

Table 6.4: Confusion matrix for VFE method using Euclidean distance classifier

	N	L	R	PB	V	A
N	**20**	0	0	0	0	0
L	0	**20**	0	0	0	0
R	0	0	**20**	0	0	0
PB	0	0	0	19	0	1
V	0	0	3	0	17	0
A	2	0	0	0	0	18

Table 6.5: Confusion matrix for proposed method based on LFD estimation in EMD domain using Euclidean distance classifier

	N	L	R	PB	V	A
N	**20**	0	0	0	0	0
L	0	**20**	0	0	0	0
R	0	0	**20**	0	0	0
PB	0	1	0	19	0	0
V	0	0	1	0	18	1
A	1	0	0	0	0	19

mentioned above. It is evident from Table 6.6 that the PSDFE and VFE methods produce relatively lower values of sensitivity for all classes of arrhythmia, whereas the proposed method based on LFD estimation in EMD domain yields higher average sensitivity even in case of V types of arrhythmia for which the PSDFE method produces the least sensitivity. Such high values of average sensitivity attest the

Table 6.6: Comparison of average sensitivity obtained by using the PSDFE, VFE methods and the proposed method based on LFD estimation in EMD domain

Type of	Average Sensitivity		
ECG beat	PSDFE	VFE	Proposed
N	93.33	96.67	97.27
L	89.58	93.33	94.55
R	93.33	97.22	97.27
PB	87.50	95.00	95.45
V	82.50	87.78	88.64
A	85.42	91.67	95.91
Avg.	88.61	93.61	94.85

capability of the proposed method based on LFD estimation in EMD domain in successfully classifying different types of ECG arrhythmia.

It can be seen from Table 6.7 that for all classes of ECG arrhythmia, the PSDFE and VFE methods show lower values of average specificity but the average specificity is higher, as expected, for the proposed method based on LFD estimation in EMD domain. It is observable that the specificity is much lower in case of L types of arrhythmia while employing the PSDFE method. Since for a particular method , a higher specificity indicates a better classification, the proposed method based on LFD estimation in EMD domain is indeed better in performance even in classifying L types of arrhythmia.

As demonstrated from Table 6.8 that the average accuracy resulting from the other methods are comparatively lower for all types of arrhythmia, whereas the proposed method based on LFD estimation in EMD domain is able to result in better classification performance as it gives higher average accuracy for different classes considered.

6.3.3 Performance Comparison using ROC Curves

ROC curves for classes N, L, R, PB, V and A are shown in Fig. 6.3. From this figure it is clear that the PSDFE method shows the least specificity or the most false prediction to achieve 100% sensitivity for all classes of arrhythmia. It is seen that in VFE method, in order to attain the desired sensitivity the specificity improves

Table 6.7: Comparison of average specificity obtained by using the PSDFE, VFE methods and the proposed method based on LFD estimation in EMD domain

Type of	Average Specificity		
ECG beat	PSDFE	VFE	Proposed
N	97.92	98.33	98.45
L	95.08	97.33	98.36
R	99.25	99.33	99.45
PB	96.83	98.22	98.55
V	97.75	99.22	99.27
A	99.50	99.89	99.91
Avg.	97.72	98.72	99.00

Table 6.8: Comparison of average accuracy obtained by using the PSDFE, VFE methods and the proposed method based on LFD estimation in EMD domain

Type of	Average Accuracy		
ECG beat	PSDFE	VFE	Proposed
N	97.15	98.06	98.26
L	94.16	96.67	97.73
R	98.26	98.98	99.09
PB	95.28	97.69	98.03
V	95.21	97.31	97.50
A	97.15	98.52	99.24
Avg.	96.21	97.87	98.31

with respect to that obtained from the PSDFE method.

Although in case of R and V classes, the proposed method based on LFD estimation in EMD domain shows more false prediction at 100% sensitivity compared to that seen in the VFE method, it maintains steepest slope with least false prediction upto achieving approximately 95% sensitivity. However for all the other arrhythmia classes, the proposed method based on LFD estimation in EMD domain offers ROC curves with steeper slope and faster rate to reach 100% sensitivity thus proving its superiority in classifying ECG arrhythmia efficiently by increasing sensitivity without increasing false prediction.

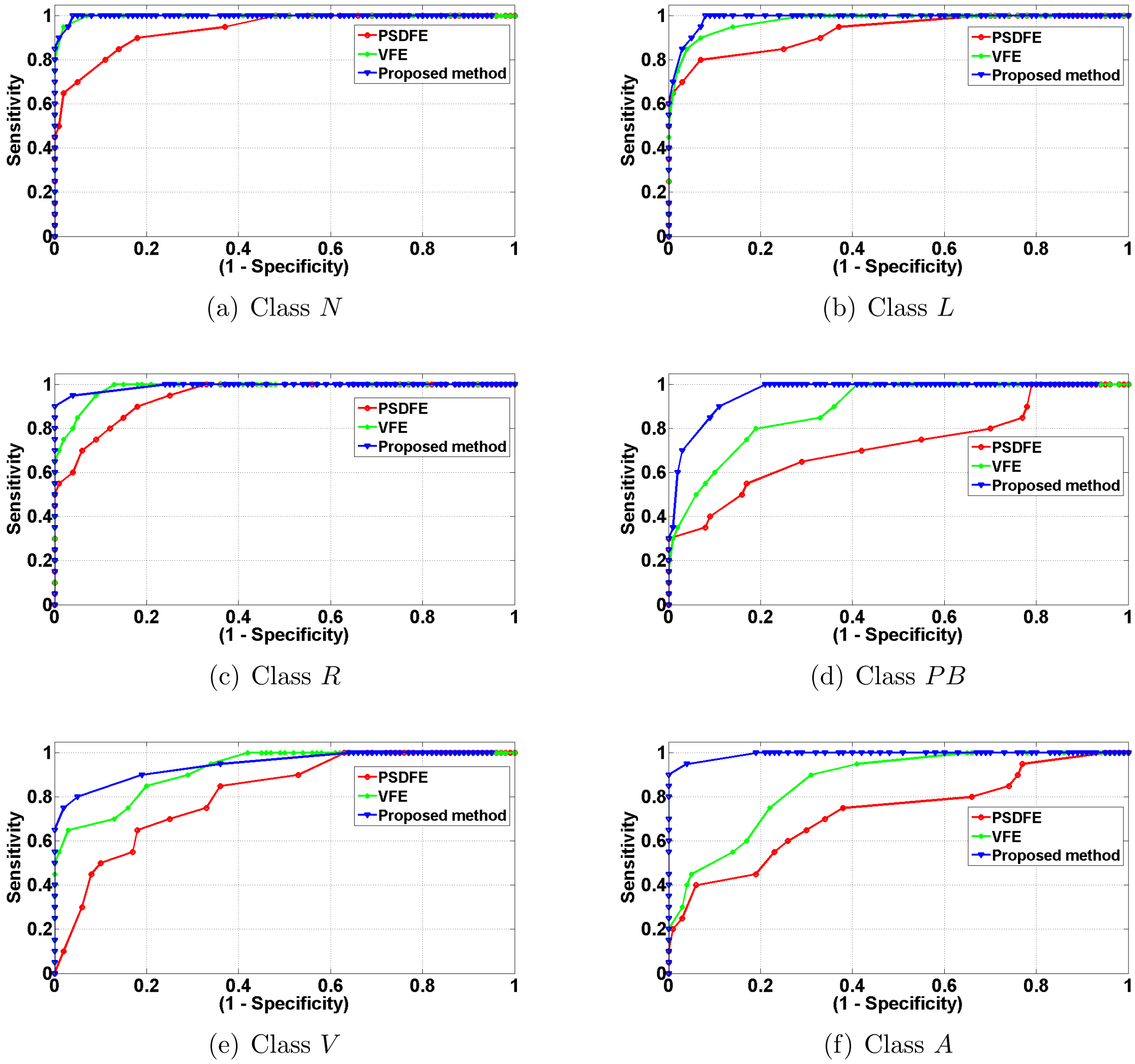

(a) Class N (b) Class L

(c) Class R (d) Class PB

(e) Class V (f) Class A

Fig. 6.3: Performance comparison in terms of ROC curves for the PSDFE, VFE methods and the proposed method based on LFD estimation in EMD domain.

6.3.4 Performance Comparison using Reduced Training Dataset

The change in average sensitivity with the change in reduction factor in training dataset with respect to testing dataset as defined before is shown in Fig. 6.4 for the PSDFE, VFE methods and the proposed method based on LFD estimation in EMD domain. This figure shows that with the increase of reduction factor, the deviation of average sensitivity in the PSDFE method is very high and that variation reduces in case of VFE method. On the other hand, even when the training dataset is one-eighth of the testing dataset, the proposed method yields an average sensitivity of 94% where it shows an average sensitivity of 95% with a reduction factor of two. Therefore, the proposed method offers less deviation in average sensitivity with the

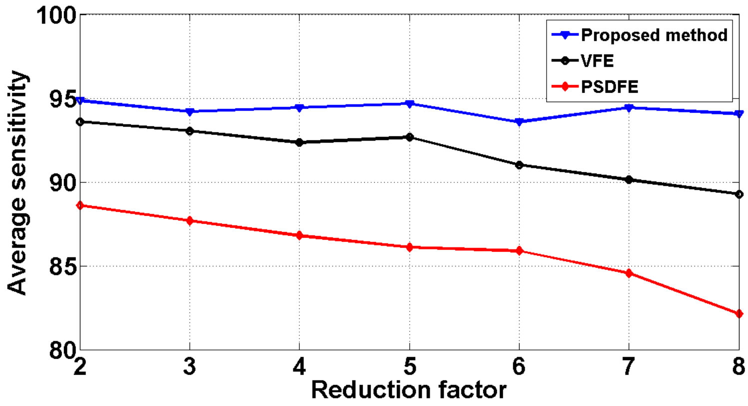

Fig. 6.4: Performance comparison in terms of average sensitivity vs reduction factor for the PSDFE, VFE methods and the proposed method based on LFD estimation in EMD domain.

reduction of training dataset thus showing less dependency on the size of the training dataset compared to that of the other methods.

6.3.5 Performance Comparison using Error-bar Calculation

This subsection provides the performance comparison of the proposed method based on LFD estimation in EMD domain with that of the PSDFE and VFE methods for random selection of training and testing datasets keeping the total number of training and testing datasets fixed at each iteration. For the confusion matrix derived at every selection, sensitivity is determined for all the classes of arrhythmia. Finally, for each class, average sensitivity over all selections and standard deviation of the sensitivity are calculated and shown in an error-bar plot in Fig. 6.5. It is illustrated from this plot that the other methods show lower average sensitivity with higher standard deviation of sensitivity for each class. On the other hand, average sensitivity over all selections obtained by using the proposed method is higher with comparatively lower standard deviation with respect to that of the other methods in case of all classes ECG arrhythmia.

6.4 Performance Comparison using LFD Estimation Method in WPD Domain

This section presents the results of the proposed method based on LFD estimation in WPD domain. All ECG beats mentioned in Table 6.1 are processed for extracting

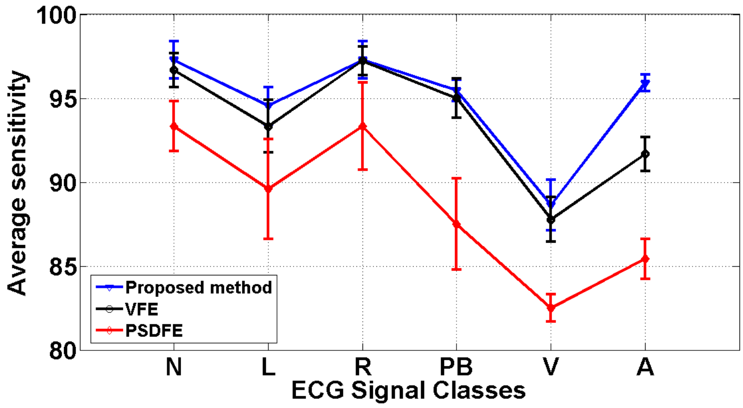

Fig. 6.5: Performance comparison in terms of Error-bar for the PSDFE, VFE methods and the proposed method based on LFD estimation in EMD domain.

LFD feature vectors using the PSDFE, VFE and proposed method. With an optimized length $W = 30$ for each segment of the window sliding over an $N = 201$-point ECG beat, 172 LFDs are estimated from each of the $(N - W + 1) = 172$ segments. The performance of the three methods is compared on the basis of the following performance evaluation criteria as described before.

6.4.1 Clustering Analysis

Two statistical measures are utilized in order to show the clustering analysis, where inter-class separability and intra-class compactness of the proposed LFD feature extracted from the WPD domain are highlighted.

Thornton's separability index or geometric separability index (GSI) is a term that signifies the ability of a particular classification method in separating the clusters of any two classes as well as in reflecting the compactness between the clusters of the same class [63]. The higher GSI value indicates the more separability between two classes under consideration, whereas lower GSI value stands for declaring the two classes as the same class. In Table 6.9 the GSI index obtained using the proposed method of LFD estimation in WPD domain for each pair of arrhythmia classes is shown. It is seen from Table 6.9 that each diagonal entry representing the same class has a value zero, whereas each entry other than the diagonal representing two different classes has a value close to one. Such GSI values indicate that the proposed LFD feature extracted from the WPD domain is capable of providing high separability between any two different classes of arrhythmia as well as yielding high

Table 6.9: The GSI index obtained using the proposed method of LFD estimation in WPD domain for each pair of arrhythmia classes

ECG Classes	N	L	R	PB	V	A
N	0	0.9974	0.9972	0.9982	0.9980	0.9970
L	0.9962	0	0.9961	0.9973	0.9967	0.9963
R	0.9958	0.9957	0	0.9967	0.9952	0.9969
PB	0.9966	0.9967	0.9959	0	0.9964	0.9971
V	0.9966	0.9952	0.9950	0.9964	0	0.9971
A	0.9960	0.9957	0.9966	0.9976	0.9973	0

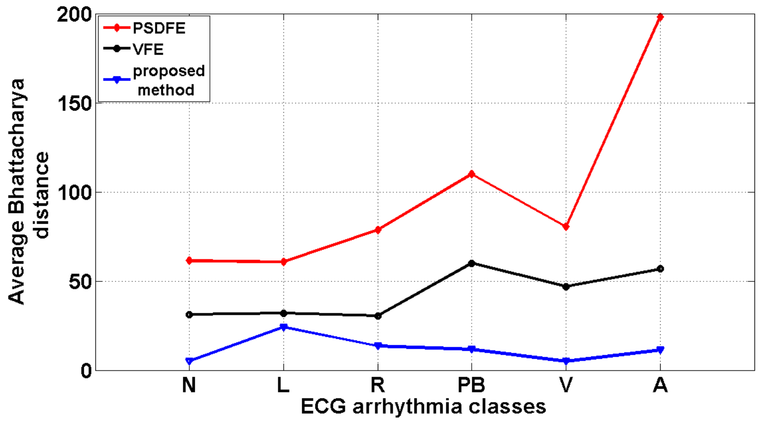

Fig. 6.6: Average inter-patient Bhattacharya distances obtained using the PSDFE, VFE methods and the proposed menthod of LFD estimation in WPD domain.

compactness for the same class.

Bhattacharya distance (BD) is another term that signifies the ability of a particular classification method in reflecting the intra-class compactness of clusters of the same class [64]. Among different methods, the method yielding lower BD value indicates more compactness of its feature employed in the inter-patient analysis. The average inter-patient BD obtained using PSDFE, VFE and the proposed method of LFD estimation in WPD domain for each class of arrhythmia is shown in Fig. 6.6. It is vivid from this figure that in comparison to the methods as mentioned above, the proposed method results in less average BD for each class of arrhythmia thus offering the intra-class compactness of the proposed LFD feature extracted from the WPD domain.

From the clustering analysis done in terms of GSI index and BD value, it is clear that the proposed feature is effective and superior in classifying different ECG arrhythmia compared to that employed in the other two state-of-the-art methods.

Table 6.10: Confusion matrix for proposed method based on LFD estimation in WPD domain using Euclidean distance classifier

	N	L	R	PB	V	A
N	**20**	0	0	0	0	0
L	0	**20**	0	0	0	0
R	0	0	**20**	0	0	0
PB	0	0	0	**20**	0	0
V	0	1	0	0	19	0
A	0	0	0	0	0	**20**

6.4.2 Performance Comparison using Confusion Matrix

Among 50 iterations of random selection of training and testing datasets as mentioned in subsection 6.2.3, for each iteration, confusion matrix representing the test classes along with the classified classes is obtained and sensitivity, specificity and accuracy of each class are determined for the performance comparison.

Table 6.3, 6.4 and 6.10 represent the confusion matrices derived for PSDFE, VFE and the proposed method based on LFD estimation in WPD domain at a particular iteration. In each of these three tables, the diagonal entries stand for the number of cases when a particular class of ECG arrhythmia is correctly classified. From Table 6.3, it is found that while using PSDFE method, misclassification occurs for every classes of ECG arrhythmia except R class. On the other hand from the confusion matrix of VFE method in Table 6.4, it is seen that all the test beats for N, L and R classes are correctly classified, whereas, some of the PB, V and A beats are misclassified. Clearly it is observed from Table 6.10 that the proposed method based on LFD estimation in WPD domain is capable of reducing the misclassification cases in V class while providing 100% correct classification for other classes of arrhythmia.

For the PSDFE, VFE and the proposed method, the average sensitivity, specificity and accuracy of all ECG arrhythmia classes are summarized in tables 6.11, 6.12 and 6.13 respectively. For all the methods, the sensitivity, specificity and accuracy found at each iteration are averaged over 50 iterations and shown in the tables as mentioned above. It is evident from Table 6.11 that the PSDFE and VFE methods

Table 6.11: Comparison of average sensitivity obtained by using the PSDFE, VFE methods and the proposed method based on LFD estimation in WPD domain

Type of	Average Sensitivity		
ECG beat	PSDFE	VFE	Proposed
N	93.33	96.67	100
L	89.58	93.33	95.00
R	93.33	97.22	99.33
PB	87.50	95.00	98.67
V	82.50	87.78	93.67
A	85.42	91.67	96.67
Avg.	88.61	93.61	97.22

produce relatively lower values of sensitivity for all classes of arrhythmia, whereas the proposed method based on LFD estimation in WPD domain yields higher average sensitivity even in case of V types of arrhythmia for which the PSDFE method produces the least sensitivity. Such high values of average sensitivity attest the capability of the proposed method based on LFD estimation in WPD domain in successfully classifying different types of ECG arrhythmia.

It can be seen from Table 6.12 that for all classes of ECG arrhythmia, the PSDFE and VFE methods show lower values of average specificity but the average specificity is higher, as expected, for the proposed method based on LFD estimation in WPD domain. It is observable that the specificity is much lower in case of L types of arrhythmia while employing the PSDFE method. Since for a particular method , a higher specificity indicates a better classification, the proposed method based on energy and entropy of detail WPD conefficients is indeed better in performance even in classifying L types of arrhythmia.

As demonstrated from Table 6.13 that the average accuracy resulting from the other methods are comparatively lower for all types of arrhythmia, whereas the proposed method based on LFD estimation in WPD domain is able to result in better classification performance as it gives higher average accuracy for different classes considered.

Table 6.12: Comparison of average specificity obtained by using the PSDFE, VFE methods and the proposed method based on LFD estimation in WPD domain

Type of	Average Specificity		
ECG beat	PSDFE	VFE	Proposed
N	97.92	98.33	99.33
L	95.08	97.33	99.47
R	99.25	99.33	99.60
PB	96.83	98.22	98.87
V	97.75	99.22	99.40
A	99.50	99.89	100
Avg.	97.72	98.72	99.44

Table 6.13: Comparison of average accuracy obtained by using the PSDFE, VFE methods and the proposed method based on LFD estimation in WPD domain

Type of	Average Accuracy		
ECG beat	PSDFE	VFE	Proposed
N	97.15	98.06	99.44
L	94.16	96.67	98.72
R	98.26	98.98	99.56
PB	95.28	97.69	98.83
V	95.21	97.31	98.44
A	97.15	98.52	99.44
Avg.	96.21	97.87	99.07

6.4.3 Performance Comparison using ROC Curves

ROC curves for classes N, L, R, PB, V and A are shown in Fig. 6.7. From this figure it is clear that the PSDFE method shows the least specificity or the most false prediction to achieve 100% sensitivity for all classes of arrhythmia. It is seen that in VFE method, in order to attain the desired sensitivity the specificity improves with respect to that obtained from the PSDFE method.

On the other hand, for all the types of ECG arrhythmia, the proposed method based on LFD estimation in WPD domain offers ROC curves with steeper slope and faster rate to reach 100% sensitivity thus proving its superiority in classifying ECG arrhythmia efficiently by increasing sensitivity without increasing false prediction.

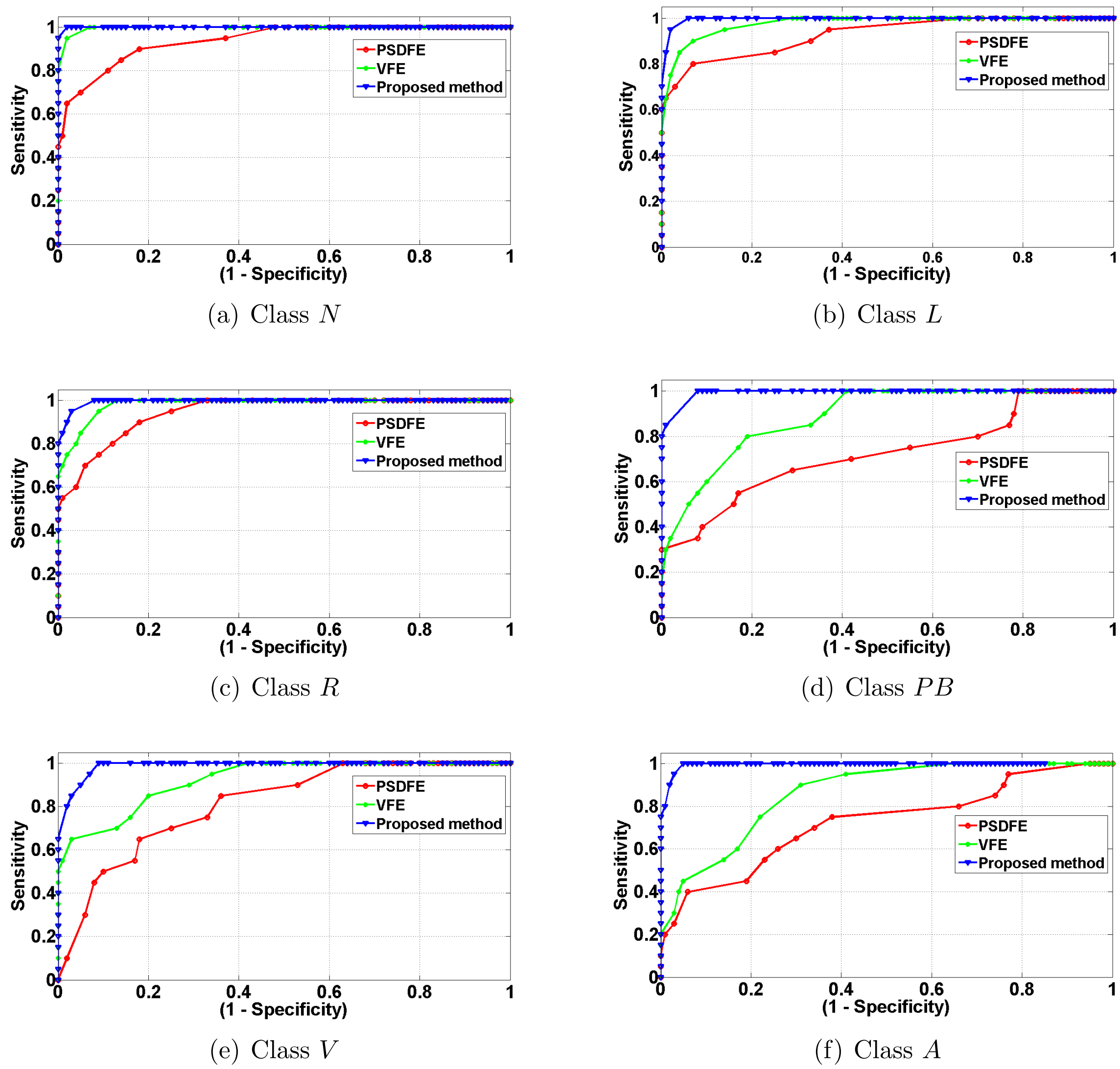

(a) Class N (b) Class L

(c) Class R (d) Class PB

(e) Class V (f) Class A

Fig. 6.7: Performance comparison in terms of ROC curves for the PSDFE, VFE methods and the proposed method based on LFD estimation in WPD domain.

6.4.4 Performance Comparison using Reduced Training Dataset

The change in average sensitivity with the change in reduction factor in training dataset with respect to testing dataset as defined before is shown in Fig. 6.8 for the PSDFE, VFE methods and the proposed method based on LFD estimation in WPD domain. This figure shows that with the increase of reduction factor, the deviation of average sensitivity in the PSDFE method is very high and that variation reduces in case of VFE method. On the other hand, even when the training dataset is one-eighth of the testing dataset, the proposed method yields an average sensitivity of

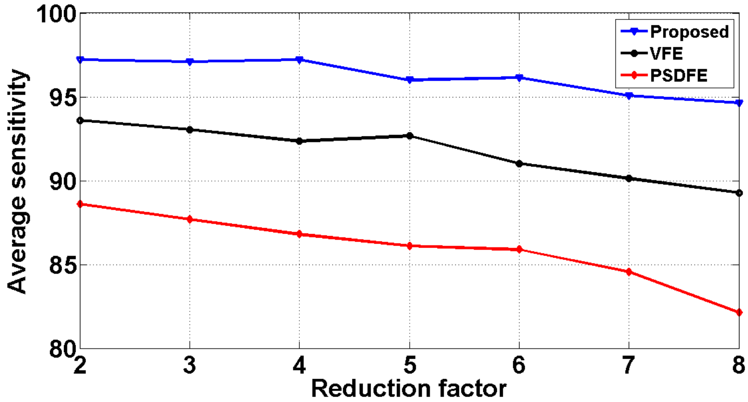

Fig. 6.8: Performance comparison in terms of average sensitivity vs reduction factor for the PSDFE, VFE methods and the proposed method based on LFD estimation in WPD domain.

95% where it shows an average sensitivity of 97% with a reduction factor of two. Therefore, the proposed method offers less deviation in average sensitivity with the reduction of training dataset thus showing less dependency on the size of the training dataset compared to that of the other methods.

6.4.5 Performance Comparison using Error-bar Calculation

This subsection provides the performance comparison of the proposed method based on LFD estimation in WPD domain with that of the PSDFE and VFE methods for random selection of training and testing datasets keeping the total number of training and testing datasets fixed at each iteration. For the confusion matrix derived at every selection, sensitivity is determined for all the classes of arrhythmia. Finally, for each class, average sensitivity over all selections and standard deviation of the sensitivity are calculated and shown in an error-bar plot in Fig. 6.9. It is illustrated from this plot that the other methods show lower average sensitivity with higher standard deviation of sensitivity for each class. On the other hand, average sensitivity over all selections obtained by using the proposed method is higher with comparatively lower standard deviation with respect to that of the other methods in case of all classes ECG arrhythmia.

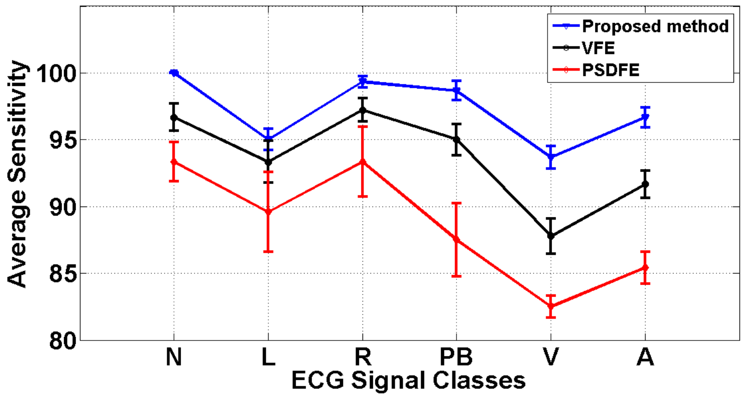

Fig. 6.9: Performance comparison in terms of Error-bar for the PSDFE, VFE methods and the proposed method based on LFD estimation in WPD domain.

6.5 Performance Comparison using Energy and Entropy of Detail WPD Coefficients

This section presents the results of the proposed method based on energy and entropy of detail WPD coefficients. All ECG beats mentioned in Table 6.1 are processed for extracting feature vectors using the PSDFE, VFE methods and the proposed method. With an optimized length $W = 30$ for each segment of the window sliding over an $N = 201$-point ECG beat, 172 energy and 172 entropy resulting in total 344 features are calculated from each of the $(N - W + 1) = 172$ segments. The performance of the three methods is compared on the basis of the following performance evaluation criteria as described before.

6.5.1 Clustering Analysis

Two statistical measures are utilized in order to show the clustering analysis, where inter-class separability and intra-class compactness of the proposed energy and entropy based feature extracted from the detail WPD coefficients are highlighted.

Thornton's separability index or geometric separability index (GSI) is a term that signifies the ability of a particular classification method in separating the clusters of any two classes as well as in reflecting the compactness between the clusters of the same class [63]. The higher GSI value indicates the more separability between two classes under consideration, whereas lower GSI value stands for declaring the two classes as the same class. In Table 6.14 the GSI index obtained using the proposed method based on energy and entropy of detail WPD coefficients for each

Table 6.14: The GSI index between each arrhythmia for the proposed method based on energy and entropy of detail WPD coefficients

ECG Classes	N	L	R	PB	V	A
N	0	0.9942	0.9936	0.9948	0.9950	0.9941
L	0.9947	0	0.9954	0.9958	0.9959	0.9945
R	0.9929	0.9945	0	0.9945	0.9934	0.9937
PB	0.9936	0.9941	0.9932	0	0.9939	0.9949
V	0.9931	0.9942	0.9923	0.9946	0	0.9939
A	0.9954	0.9954	0.9959	0.9969	0.9962	0

pair of arrhythmia classes is shown. It is seen from Table 6.14 that each diagonal entry representing the same class has a value zero, whereas each entry other than the diagonal representing two different classes has a value close to one. Such GSI values indicate that the proposed energy and entropy based feature extracted from the detail WPD coefficients is capable of providing high separability between any two different classes of arrhythmia as well as yielding high compactness for the same class.

Bhattacharya distance (BD) is another term that signifies the ability of a particular classification method in reflecting the intra-class compactness of clusters of the same class [64]. Among different methods, the method yielding lower BD value indicates more compactness of its feature employed in the inter-patient analysis. The average inter-patient BD obtained using the PSDFE, VFE methods and the proposed method based energy and entropy of detail WPD coefficients for each class of arrhythmia is shown in Fig. 6.10. It is vivid from this figure that in comparison to the methods as mentioned above, the proposed method results in less average BD for each class of arrhythmia thus offering the intra-class compactness of the proposed energy and entropy based feature extracted from the WPD domain.

From the clustering analysis done in terms of GSI index and BD value, it is clear that the proposed feature is effective and superior in classifying different ECG arrhythmia compared to that employed in the other two state-of-the-art methods.

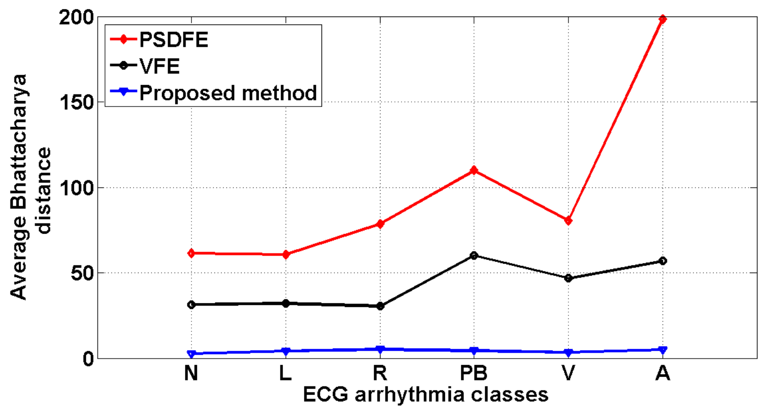

Fig. 6.10: Average inter-patient Bhattacharya distances obtained using the PSDFE, VFE methods and the proposed method based on energy and entropy of detail WPD coefficients.

6.5.2 Performance Comparison using Confusion Matrix

Among 50 iterations of random selection of training and testing datasets as mentioned in subsection 6.2.3, for each iteration, confusion matrix representing the test classes along with the classified classes is obtained and sensitivity, specificity and accuracy of each class are determined for the performance comparison.

Table 6.3, 6.4 and 6.15 represent the confusion matrices derived for PSDFE, VFE and the proposed method based on energy and entropy of detail WPD coefficients at a particular iteration. In each of these three tables, the diagonal entries stand for the number of cases when a particular class of ECG arrhythmia is correctly classified. From Table 6.3, it is found that while using PSDFE method, misclassification occurs for every classes of ECG arrhythmia except R class. On the other hand from the confusion matrix of VFE method in Table 6.4, it is seen that all the test beats for N, L and R classes are correctly classified, whereas, some of the PB, V and A beats are misclassified. Clearly it is observed from Table 6.15 that the proposed method based on energy and entropy of detail WPD coefficients is capable of providing 100% correct classification for all types of ECG classes of arrhythmia.

For the PSDFE, VFE and the proposed method, the average sensitivity, specificity and accuracy of all ECG arrhythmia classes are summarized in tables 6.16, 6.17 and 6.18 respectively. For all the methods, the sensitivity, specificity and accuracy found at each iteration are averaged over 50 iterations and shown in the tables as mentioned above. It is evident from Table 6.16 that the PSDFE and VFE methods

Table 6.15: Confusion matrix for proposed method based on energy and entropy of detail WPD coefficients using Euclidean distance classifier

	N	L	R	PB	V	A
N	**20**	0	0	0	0	0
L	0	**20**	0	0	0	0
R	0	0	**20**	0	0	0
PB	0	0	0	**20**	0	0
V	0	0	0	0	**20**	0
A	0	0	0	0	0	**20**

produce relatively lower values of sensitivity for all classes of arrhythmia, whereas the proposed method based on energy and entropy of detail WPD coefficients yields higher average sensitivity even in case of V types of arrhythmia for which the PSDFE method produces the least sensitivity. Such high values of average sensitivity attest the capability of the proposed method based on energy and entropy of detail WPD coefficients in successfully classifying different types of ECG arrhythmia.

It can be seen from Table 6.17 that for all classes of ECG arrhythmia, the PSDFE and VFE methods show lower values of average specificity but the average specificity is higher, as expected, for the proposed method based on energy and entropy of detail WPD coefficients. It is observable that the specificity is much lower in case of L types of arrhythmia while employing the PSDFE method. Since for a particular method, a higher specificity indicates a better classification, the proposed method based on energy and entropy of detail WPD coefficients is indeed better in performance even in classifying L types of arrhythmia.

As demonstrated from Table 6.18 that the average accuracy resulting from the other methods are comparatively lower for all types of arrhythmia, whereas the proposed method based on energy and entropy of detail WPD coefficients is able to result in better classification performance as it gives higher average accuracy for different classes considered.

6.5.3 Performance Comparison using ROC Curves

ROC curves for classes N, L, R, PB, V and A are shown in Fig. 6.11. From this figure it is clear that the PSDFE method shows the least specificity or the most false

Table 6.16: Comparison of average sensitivity obtained by using the PSDFE, VFE methods and the proposed method based on energy and entropy of detail WPD coefficients

Type of	Average Sensitivity		
ECG beat	PSDFE	VFE	Proposed
N	93.33	96.67	100
L	89.58	93.33	99.71
R	93.33	97.22	99.84
PB	87.50	95.00	99.48
V	82.50	87.78	98.47
A	85.42	91.67	98.99
Avg.	88.61	93.61	99.42

Table 6.17: Comparison of average specificity obtained by using the PSDFE, VFE methods and the proposed method based on energy and entropy of detail WPD coefficients

Type of	Average Specificity		
ECG beat	PSDFE	VFE	Proposed
N	97.92	98.33	99.84
L	95.08	97.33	99.79
R	99.25	99.33	99.84
PB	96.83	98.22	99.95
V	97.75	99.22	99.95
A	99.50	99.89	100
Avg.	97.72	98.72	99.90

prediction to achieve 100% sensitivity for all classes of arrhythmia. It is seen that in VFE method, in order to attain the desired sensitivity the specificity improves with respect to that obtained from the PSDFE method.

On the other hand, for all the types of ECG arrhythmia, the proposed method based on energy and entropy of detail WPD coefficients offers ROC curves with steeper slope and faster rate to reach 100% sensitivity thus proving its superiority in classifying ECG arrhythmia efficiently by increasing sensitivity without increasing false prediction.

Table 6.18: Comparison of average accuracy obtained by using the PSDFE, VFE methods and the proposed method based on energy and entropy of detail WPD coefficients

Type of	Average Accuracy		
ECG beat	PSDFE	VFE	Proposed
N	97.15	98.06	99.87
L	94.16	96.67	99.78
R	98.26	98.98	99.83
PB	95.28	97.69	99.87
V	95.21	97.31	99.69
A	97.15	98.52	99.84
Avg.	96.21	97.87	99.81

6.5.4 Performance Comparison using Reduced Training Dataset

The change in average sensitivity with the change in reduction factor in training dataset with respect to testing dataset as defined before is shown in Fig. 6.12 for the PSDFE, VFE methods and the proposed method based on energy and entropy of detail WPD coefficients. This figure shows that with the increase of reduction factor, the deviation of average sensitivity in the PSDFE method is very high and that variation reduces in case of VFE method. On the other hand, even when the training dataset is one-eighth of the testing dataset, the proposed method yields an average sensitivity of 98% where it shows an average sensitivity of 99% with a reduction factor of two. Therefore, the proposed method offers less deviation in average sensitivity with the reduction of training dataset thus showing less dependency on the size of the training dataset compared to that of the other methods.

6.5.5 Performance Comparison using Error-bar Calculation

This subsection provides the performance comparison of the proposed method based on energy and entropy of detail WPD coefficients with that of the PSDFE and VFE methods for random selection of training and testing datasets keeping the total number of training and testing datasets fixed at each iteration. For the confusion matrix derived at every selection, sensitivity is determined for all the classes of arrhythmia. Finally, for each class, average sensitivity over all selections and standard deviation

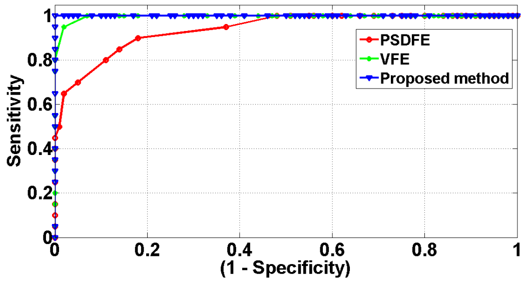

(a) Class N

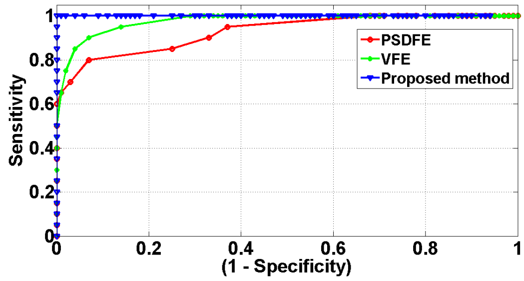

(b) Class L

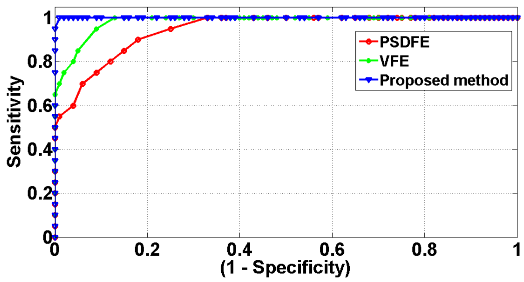

(c) Class R

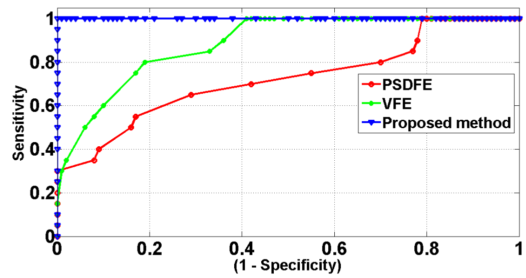

(d) Class PB

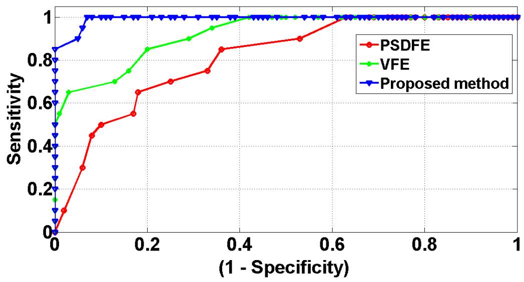

(e) Class V

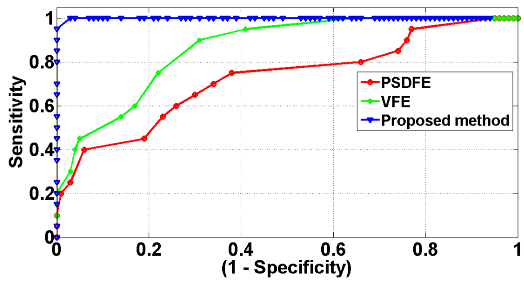

(f) Class A

Fig. 6.11: Performance comparison in terms of ROC curves for the PSDFE, VFE methods and the proposed method based on energy and entropy of detail WPD coefficients.

of the sensitivity are calculated and shown in an error-bar plot in Fig. 6.13. It is illustrated from this plot that the other methods show lower average sensitivity with higher standard deviation of sensitivity for each class. On the other hand, average sensitivity over all selections obtained by using the proposed method is higher with comparatively lower standard deviation with respect to that of the other methods in case of all classes ECG arrhythmia.

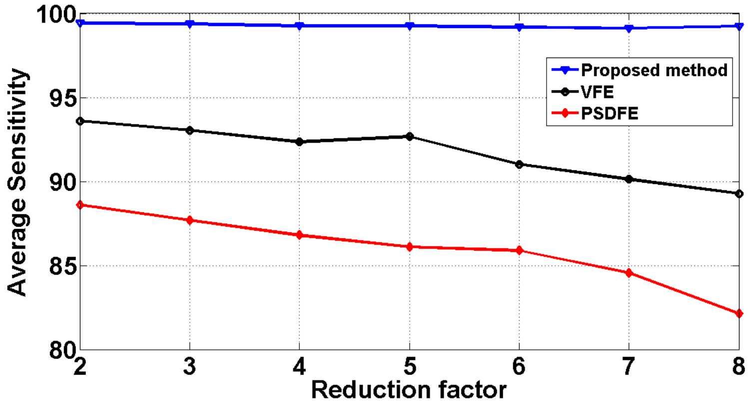

Fig. 6.12: Performance comparison in terms of average sensitivity vs reduction factor for the PSDFE, VFE methods and the proposed method based on energy and entropy of detail WPD coefficients.

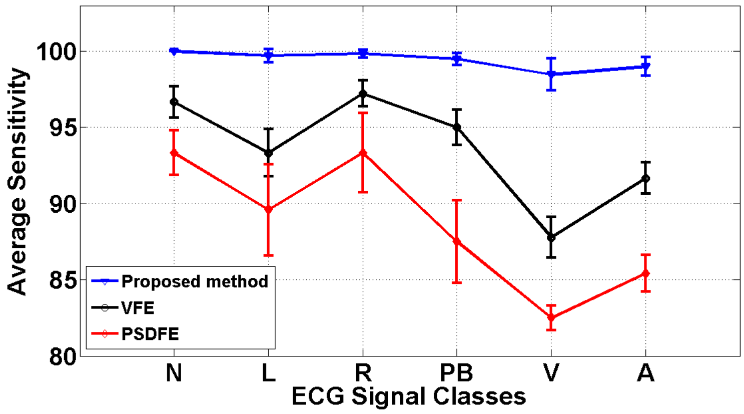

Fig. 6.13: Performance comparison in terms of Error-bar for the PSDFE, VFE methods and the proposed method based on energy and entropy of detail WPD coefficients.

6.6 Conclusion

Firstly an empirical mode decomposition based LFD estimation algorithm is employed along with Euclidean distance classifier in order to classify five types of ECG arrhythmia and normal ECG. Secondly a wavelet packet based LFD estimation method is employed along with Euclidean distance classifier in order to classify five types of ECG arrhythmia and normal ECG. Finally features extracted from energy and entropy of 4th level WPD detail coefficients are employed along with Euclidean distance classifier in order to classify five types of ECG arrhythmia and normal ECG. State-of-the-art ECG arrhythmia classification methods e.g. VFE and PSDFE [6] is also implemented for detail comparison with the proposed method. Two statistical measures e.g. GSI and BD are utilized in justifying inter-class separability and intra-class compactness of the proposed feature. Average sensitivity, specificity and accuracy are calculated from classification performance of 50 iterations, considering random selected training and testing datasets at each stage.

The performance of the proposed method based on LFD estimation in EMD domain for individual arrhythmia came quite high with average accuracy of 98.26% for normal beats, 97.73% for class L and 99.09%, 98.03%, 97.50% and 99.24% for classes R, PB, V and class A arrhythmia respectively resulting in total average accuracy of 98.31%.

The performance of another proposed method based on LFD estimation in WPD domain for individual arrhythmia came quite high with average accuracy of 99.44% for normal beats, 98.72% for class L and 99.56%, 98.83%, 98.44% and 99.44% for classes R, PB, V and class A arrhythmia respectively resulting in total average accuracy of 99.07%.

Finally the performance of the simplest yet effective proposed method based on energy and entropy of detail WPD coefficients for individual arrhythmia came quite high with average accuracy of 99.87% for normal beats, 99.78% for class L and 99.83%, 98.87%, 99.69% and 99.84% for classes R, PB, V and class A arrhythmia respectively resulting in total average accuracy of 99.81%.

Chapter 7

Conclusion

7.1 Concluding Remarks

Estimation of local fractal dimension (LFD) as a feature can be utilized in order to classify different types of ECG arrhythmia, because it is capable of capturing detail distinguished features regarding arrhythmia. Again, prior to feature extraction normalization of ECG signals is not necessary as LFD is independent of any scaling operation done on the signal. LFD can be calculated by estimating Hurst exponent (HE) which also can found via different methods. Firstly empirical mode decomposition (EMD) is employed to estimate HE as well as LFD feature sets for ECG arrhythmia classification. Though in EMD domain, the computation of IMFs does not require any previously known value of the signal, this method requires at least three IMFs for better LFD estimation, which depends on the length of the time series signal under consideration. To overcome this problem, time frequency analysis like wavelet packet domain is utilized for calculating LFD feature sets via estimation HE from detail WPD coefficients. Hence it is found that instead of considering all the detail WPD coefficients, taking only 4th level detail WPD coefficients is sufficient for extracting an effective feature set capable of classifying cardiac arrhythmia with higher accuracy. Hence by avoiding complexity and computational burden, feature set extracted from energy and entropy of sum of 4th level detail WPD coefficients is proposed. Euclidean distance classifier is employed for classification task for all the three proposed methods. All the three proposed methods can perform well even in case of reduced training dataset and random selection of training and testing ECG beats. Simulations are carried out to evaluate the performance of the proposed method in terms of sensitivity, specificity and accuracy. It is shown that the proposed method outperforms some of the state-of-the-art methods with superior efficacy.

7.2 Contribution of the Thesis

The major contributions of this thesis are:

1. A set of LFD features is developed exploiting Hurst exponent calculated from the IMFs obtained via empirical mode decomposition (EMD) of ECG signals.

2. Another set of LFD features is designed based on calculating the Hurst exponent using wavelet packet decomposition (WPD) of ECG signals.

3. Based on the analysis in terms of energy, frequency and cross-correlation, it is found that instead of taking all the detail WPD coefficients at each level, only the 4th level detail WPD coefficients are enough to extract features in order to classify different ECG arrhythmia. Thus, a simple feature set is formed based on energy and entropy of only the 4th level detail WPD coefficients of ECG signals.

4. Detail simulations have been carried out in order to investigate the performance of the proposed feature sets for the classification of five types of arrhythmia using ECG signals available from the MIT-BIH arrhythmia database.

5. The performance of our proposed method is compared with state-of-the-art methods PSDFE and VFE [6]. This is why PSDFE and VFE methods are implemented independently and classification performance has been carried out using the same dataset and the same Euclidian distance classifier.

6. Simulation results show that the proposed method is able to classify different types of ECG arrhythmia with greater sensitivity, specificity and accuracy even in case of reduction of training dataset as well as random selection of training and testing dataset.

7.3 Scopes for Future Work

In this thesis, LFD estimation methods exploiting Hurst exponent obtained individually from the EMD and WPD domain and an effective energy and entropy based method utilizing only the 4th level detail WPD coefficients are developed for ECG arrhythmia classification. However, there are still some scopes for future research, as mentioned below:

- In practical cases, where the unknown ECG comes from a different patient whose data is not present in the training dataset, the classification problem is termed as patient independent performance analysis. So, our proposed methods are needed to be fed into patient independent analysis for further justification in handling various practical situations.

- In practical cases, ECG signals are subject to various noises. So, noise analysis can be performed for all the proposed methods in order to verify their performance in noisy environment.

- Available databases other than MIT-BIH arrhythmia database need to be utilized for validating efficacy of our proposed methods.

Bibliography

[1] R. Acharya, J. Suri, and J. Spaan, *Advances in cardiac signal processing.* Springer Verlag, 2007.

[2] M. Khan, *Rapid ECG interpretation.* Humana Press, 2007.

[3] F. Morris, W. Brady, A. Camm, and I. ebrary, *ABC of clinical electrocardiography.* BMJ Books, 2003.

[4] C. Evans *et al.*, "Principles of human physiology." *Principles of human physiology, 9th Ed*, 1945.

[5] A. Moss, *Noninvasive electrocardiology: Clinical aspects of holter monitoring.* WB Saunders Co, 1996.

[6] A. Mishra and S. Raghav, "Local fractal dimension based ECG arrhythmia classification," *Biomedical Signal Processing and Control*, vol. 5, no. 2, pp. 114–123, 2010.

[7] S. Spasic, "Spectral and fractal analysis of biosignals and coloured noise," in *proc. 5th IEEE Int. Symposium Intelligent Systems and Informatics*, pp. 147–149, 2007.

[8] C. Lin, Y. Du, and T. Chen, "Nonlinear interpolation fractal classifier for multiple cardiac arrhythmias recognition," *Chaos, Solutions & Fractals*, vol. 42, no. 4, pp. 2570–2581, 2009.

[9] Z. Wang, D. Guo, X. Li, and Y. Fei, "Estimating hurst exponent with wavelet packet," in *proc. IEEE 7th Int. Conf. Computer-Aided Industrial Design and Conceptual Design*, pp. 1–4, 2006.

[10] B. Mandelbrot, *The fractal geometry of nature.* Wh Freeman, 1983.

[11] P. Muller, N. Contento, and H. Rix, "Fractal dimension on ECG," in *proc. IEEE 14th Annual Int. Conf. Engineering in Medicine and Biology Society*, vol. 3, pp. 977–978, 1992.

[12] K. Lai and K. Chan, "Real-time classification of electrocardiogram based on fractal and correlation analyses," in *Proc. IEEE 20th Annual Int. Conf. Engineering in Medicine and Biology Society*, pp. 119–122, 1998.

[13] A. Esgiar and P. Chakravorty, "Electrocardiogram signal classification based on fractal features," in *proc. IEEE Conf. Computers in Cardiology*, pp. 661–664, 2004.

[14] P. Ivanov, L. Amaral, A. Goldberger, S. Havlin, M. Rosenblum, Z. Struzik, and H. Stanley, "Multifractallity in human heartbeat dynamics," *Nature*, vol. 399, no. 6735, pp. 461–465, 1999.

[15] G. Wang, H. Huang, H. Xie, Z. Wang, and X. Hu, "Multifractal analysis of ventricular fibrillation and ventricular tachycardia," *Medical Engineering & Physics*, vol. 29, no. 3, pp. 375–379, 2007.

[16] L. Khadra, A. Al-Fahoum, and H. Al-Nashash, "Detection of life-threatening cardiac arrhythmias using the wavelet transformation," *Medical and Biological Engineering and Computing*, vol. 35, no. 6, pp. 626–632, 1997.

[17] S. Pal and M. Mitra, "Detection of ECG characteristic points using multiresolution wavelet analysis based selective coefficient method," *Measurement*, vol. 43, no. 2, pp. 255–261, 2010.

[18] S. Banerjee, R. Gupta, and M. Mitra, "Delineation of ECG characteristic features using multiresolution wavelet analysis method," *Measurement*, vol. 45, no. 3, pp. 474–487, 2012.

[19] H. Khorrami and M. Moavenian, "A comparative study of DWT, CWT and DCT transformations in ECG arrhythmias classification," *Expert systems with Applications*, vol. 37, no. 8, pp. 5751–5757, 2010.

[20] A. Sahab and Y. Gilmalek, "An automatic diagnostic machine for ECG arrhythmias classification based on wavelet transformation and neural networks,"

International journal of circuits, systems and signal processing, vol. 3, no. 5, pp. 255–262, 2011.

[21] S. Yu and Y. Chen, "Electrocardiogram beat classification based on wavelet transformation and probabilistic neural network," *Pattern Recognition Letters*, vol. 28, no. 10, pp. 1142–1150, 2007.

[22] M. Signes, H. Mora, and J. Garcia, "A computational framework based on behavioural modelling: Application to the matching of electrocardiogram (ECG) recordings," *Mathematical and computer modelling*, vol. 54, no. 7-8, pp. 1644–1649, 2011.

[23] S. Dutta, A. Chatterjee, and S. Munshi, "Identification of ECG beats from cross-spectrum information aided learning vector quantization," *Measurement*, vol. 44, no. 10, pp. 2020–2027, 2011.

[24] S. Pal and M. Mitra, "Empirical mode decomposition based ECG enhancement and QRS detection," *Computers in Biology and Medicine*, vol. 42, no. 1, pp. 83–92, 2012.

[25] İ. Güler *et al.*, "ECG beat classifier designed by combined neural network model," *Pattern recognition*, vol. 38, no. 2, pp. 199–208, 2005.

[26] M. Moavenian and H. Khorrami, "A qualitative comparison of artificial neural networks and support vector machines in ECG arrhythmias classification," *Expert Systems with Applications*, vol. 37, no. 4, pp. 3088–3093, 2010.

[27] O. Castillo, P. Melin, E. Ramírez, and J. Soria, "Hybrid intelligent system for cardiac arrhythmia classification with fuzzy k-nearest neighbors and neural networks combined with a fuzzy system," *Expert Systems with Applications*, vol. 39, no. 3, pp. 2947–2955, 2012.

[28] M. Homaeinezhad, S. Atyabi, E. Tavakkoli, H. Toosi, A. Ghaffari, and R. Ebrahimpour, "ECG arrhythmia recognition via a neuro-svm-knn hybrid classifier with virtual QRS image-based geometrical features," *Expert Systems with Applications*, vol. 39, no. 2, pp. 2047–2058, 2012.

[29] C. Shen, W. Kao, Y. Yang, M. Hsu, Y. Wu, and F. Lai, "Detection of cardiac arrhythmia in electrocardiograms using adaptive feature extraction and modified support vector machines," *Expert Systems with Applications*, vol. 39, no. 9, pp. 7845–7852, 2012.

[30] Y. Yeh, C. Chiou, and H. Lin, "Analyzing ECG for cardiac arrhythmia using cluster analysis," *Expert Systems with Applications*, vol. 39, no. 1, pp. 1000–1010, 2012.

[31] Y. Yeh, T. Chiang, and H. Lin, "Principal component analysis method for detection and classification of ECG beat," in *proc. IEEE 11th Int. Conf. Bioinformatics and Bioengineering (BIBE)*, pp. 318–322, 2011.

[32] S. Yu and K. Chou, "A switchable scheme for ECG beat classification based on independent component analysis," *Expert Systems with Applications*, vol. 33, no. 4, pp. 824–829, 2007.

[33] ——, "Selection of significant independent components for ECG beat classification," *Expert Systems with Applications*, vol. 36, no. 2, pp. 2088–2096, 2009.

[34] V. Krasteva and I. Jekova, "QRS template matching for recognition of ventricular ectopic beats," *Annals of Biomedical Engineering*, vol. 35, no. 12, pp. 2065–2076, 2007.

[35] P. De Chazal, M. O'Dwyer, and R. Reilly, "Automatic classification of heartbeats using ECG morphology and heartbeat interval features," *IEEE Transactions on Biomedical Engineering*, vol. 51, no. 7, pp. 1196–1206, 2004.

[36] T. Ince, S. Kiranyaz, and M. Gabbouj, "A generic and robust system for automated patient-specific classification of ECG signals," *IEEE Transactions on Biomedical Engineering*, vol. 56, no. 5, pp. 1415–1426, 2009.

[37] A. Pachauri and M. Bhuyan, "Robust detection of R-wave using wavelet technique," *World Academy of Science Engineering and Technology*, no. 56, pp. 901–905, 2009.

[38] Y. Chen and S. Yu, "Selection of effective features for ECG beat recognition based on nonlinear correlations," *Artificial Intelligence In Medicine*, vol. 54, no. 1, pp. 43–52, 2012.

[39] V. Mahesh, A. Kandaswamy, C. Vimal, and B. Sathish, "ECG arrhythmia classification based on logistic model tree," *Journal of Biomedical Science and Engineering*, vol. 2, no. 6, pp. 405–411, 2009.

[40] Y. Kutlu and D. Kuntalp, "Feature extraction for ecg heartbeats using higher order statistics of WPD coefficients," *Computer Methods and Programs in Biomedicine*, vol. 105, no. 3, pp. 257–267, 2012.

[41] S. Yu and K. Chou, "Selection of significant independent components for ECG beat classification," *Expert Systems with Applications*, vol. 36, no. 2, pp. 2088–2096, 2009.

[42] Y. Ozbay and G. Tezel, "A new method for classification of ecg arrhythmias using neural network with adaptive activation function," *Digital Signal Processing*, vol. 20, no. 4, pp. 1040–1049, 2010.

[43] Y. Wang, L. Song, and S. Kang, "Arrhythmia recognition based on EMD and support vector machines," in *proc. IEEE 4th Int. Conf. Bioinformatics and Biomedical Engineering*, pp. 1–4,2010.

[44] G. Rilling, P. Flandrin, and P. Gonçalves, "Empirical mode decomposition, fractional gaussian noise and hurst exponent estimation," in *Proc. IEEE Int. Conf. Acoustics, Speech, and Signal Processing (ICASSP'05)*, vol. 4, pp. 489–492, 2005.

[45] R. Sinha and C. Shahnaz, "An empirical mode decomposition based fractal dimension feature for ECG arrhythmia classification," *Submitted to Signal, Image and Video Processing, Springer.*

[46] B. Mandelbrot, "How long is the coast of britain? statistical self-similarity and fractional dimension," *Science*, vol. 156, no. 3775, pp. 636–638, 1967.

[47] J. Theiler, "Estimating fractal dimension," *JOSA A*, vol. 7, no. 6, pp. 1055–1073, 1990.

[48] M. Katz, "Fractals and the analysis of waveforms," *Computers in Biology and Medicine*, vol. 18, no. 3, pp. 145–156, 1988.

[49] A. Pentland, "Fractal-based description of natural scenes," *IEEE Transactions on Pattern Analysis and Machine Intelligence*, no. 6, pp. 661–674, 1984.

[50] E. Bayraktar, H. Poor, and K. Sircar, "Estimating the fractal dimension of the S&P 500 index using wavelet analysis," *International Journal of Theoretical and Applied Finance*, vol. 7, no. 5, pp. 615–644, 2004.

[51] J. Salisbury and Y. Sun, "Assessment of chaotic parameters in nonstationary electrocardiograms by use of empirical mode decomposition," *Annals of Biomedical Engineering*, vol. 32, no. 10, pp. 1348–1354, 2004.

[52] N. Huang and N. Attoh-Okine, *The Hilbert-Huang transform in engineering.* CRC Press, 2005.

[53] R. Sinha and C. Shahnaz, "A wavelet packet based fractal dimension feature for ECG arrhythmia classification," *Submitted to Computers in Biology and Medicine, Elsevier.*

[54] J. Sahambi, S. Tandon, and R. Bhatt, "Using wavelet transforms for ECG characterization. an on-line digital signal processing system," *Engineering in Medicine and Biology Magazine*, vol. 16, no. 1, pp. 77–83, 1997.

[55] S. Mahmoodabadi, A. Ahmadian, M. Abolhasani, M. Eslami, and J. Bidgoli, "Ecg feature extraction based on multiresolution wavelet transform," in *proc. IEEE 27th Annual Int. Conf. Engineering in Medicine and Biology Society*, pp. 3902–3905, 2006.

[56] S. Saxena, V. Kumar, and S. Hamde, "QRS detection using new wavelets," *Journal of Medical Engineering & Technology*, vol. 26, no. 1, pp. 7–15, 2002.

[57] R. Polikar, "The wavelet tutorial," 1996.

[58] S. Mahmoodabadi, A. Ahmadian, M. Abolhasani, M. Eslami, and J. Bidgoli, "ECG feature extraction based on multiresolution wavelet transform," in *proc.*

IEEE 27th Annual Int. Conf. Engineering in Medicine and Biology Society, pp. 3902–3905, 2006.

[59] P. Flandrin, "Wavelet analysis and synthesis of fractional brownian motion," *IEEE Transactions on Information Theory*, vol. 38, no. 2, pp. 910–917, 1992.

[60] R. Sinha and C. Shahnaz, "An approach for ECG arrhythmia classification based on energy and entropy of the 4th level detail wavelet packet coefficients," *Submitted to Computers and Electrical Engineering, Elsevier.*

[61] J. Webster, *Medical instrumentation: application and design.* Wiley-India, 2009.

[62] MIT-BIH arrhythmia database. [Online]. Available: http://www.physionet.org/physiobank/database/mitdb/

[63] C. Thornton, "Separability is a learner's best friend," in *Proc. Citeseer 4th Neural Computation and Psychology Workshop: Connectionist Representations*, pp. 40–47, 1997.

[64] K. Fukunaga, *Introduction to statistical pattern recognition.* Academic Pr, 1990.

[65] M. Rahman, P. Bhattacharya, and B. Desai, "Similarity searching in image retrieval with statistical distance measures and supervised learning," *Pattern Recognition and Data Mining*, pp. 315–324, 2005.